

**AN *IN VITRO* INVESTIGATION OF  
FLUOROQUINOLONES ON GLYCAEMIC  
PHARMACOLOGICAL TARGETS**

A thesis submitted in fulfilment of the requirements for the degree of Master  
of Science (Pharmacy)

By Oyisa Katshaza

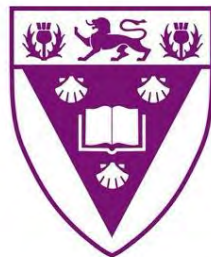
Faculty of pharmacy

Rhodes University

Makhanda

South Africa

February 2025



**RHODES UNIVERSITY**

*Where leaders learn*

---

## **Acknowledgements**

I would like to thank God and express my gratitude to my supervisor, Prof. N Sibiya, for his enduring patience, advice, assistance, and motivation to work hard and cultivate belief in myself when it was, at times, difficult.

Thank you to RUPG for providing me with the scholarship which provided me with the necessary resources to complete my studies.

. I would also like to thank my co-supervisor, Prof SD Khanye for his contribution to the success of this work. I want to thank my family for their ongoing support and for endowing me with the capacity to pursue this study.

I want to thank Praise Nhau, Mr Charles Arineitwe, Takudzwa Mugiya, Caroline Mwase, and Munyaradzi Chiwundura for their assistance in and out of the lab when I was struggling to find my footing.

Finally, I want to thank my friends, Okuku James Junior, Gideon Onah, and especially Praise Nhau for her support, understanding, patience and encouragement throughout this journey.

---

<b>Acknowledgements.....</b>	<b>ii</b>
<b>List Of Figures.....</b>	<b>vi</b>
<b>List Of Abbreviations .....</b>	<b>xi</b>
<b>Abstract.....</b>	<b>xiii</b>
<b>Chapter 1: Literature Review .....</b>	<b>15</b>
<b>1. Introduction .....</b>	<b>15</b>
1.1. Entry of Glucose .....	18
1.2. Glucose Metabolism and Its Physiological Use.....	19
1.2.1. Energy Production. ....	19
1.2.2. Glycogenesis and Glycogenolysis .....	20
1.2.3. Gluconeogenesis .....	22
1.3. Glucose Regulation and Role of Insulin .....	22
1.3.1. Insulin .....	24
1.3.2. Insulin Secretion .....	25
1.3.3. Insulin Signalling .....	28
1.3.4. Insulin Resistance .....	30
1.4. Diabetes Mellitus .....	30
1.4.1. Diabetes Mellitus Epidemiology.....	32
1.4.2. Type 2 Diabetes Mellitus Pathophysiology .....	33
1.4.3. Diabetes Mellitus and Infection .....	35
1.5. Cellular Targets for achieving glycaemic control.....	36
1.6. Conventional treatments and associated pharmacological targets.....	37
1.6.1. DPP-4.....	38
1.6.2. Phosphoinositide-3-Kinase (PI3K) .....	39
1.6.3. ATP-sensitive potassium channels .....	40
1.6.4. A-Glucosidase and Pancreatic Amylase .....	41

---

1.6.5. Peroxisome Proliferator-activated Receptor Gamma .....	42
1.7. Fluoroquinolones and Dysglycaemia.....	43
1.8. Justification for the study.....	48
1.9. Objectives of the Study.....	49
<b>Chapter 2: Materials and Methodology.....</b>	<b>51</b>
2.1. Materials and Equipment .....	51
2.1. Cell Culture.....	52
2.1.1. Skeletal Muscle Differentiation .....	53
2.1.2. Drug preparation for cell-based assay treatments.....	54
2.1.3. Glucometer Validation.....	55
2.2. Cell viability assay.....	57
2.3. Glucose Utilisation Assay.....	59
2.4. Glucose utilisation in the presence of PI3K inhibitor.....	60
2.5. In-Cell-Elisa.....	62
2.6. Compound Preparation .....	65
2.7. $\alpha$ -Amylase Assay .....	66
2.8. $\alpha$ -Glucosidase Inhibition Assay .....	68
2.9. In Silico Modelling .....	69
2.10. Calculations and Statistical Analysis .....	71
<b>Chapter 3: Results.....</b>	<b>72</b>
3.1. Cell Viability Assay.....	72
3.2.1. Glucose Uptake Assay .....	74
3.2.2. Media glucose in Wortmannin pretreated cells .....	77
3.3. In Cell Elisa Assay.....	81
3.3.2. Relative GLUT-4 Expression .....	83
3.3.3. AKT Expression.....	84
3.4. Non-cell Based Assays .....	86

---

---

3.4.1. $\alpha$ -Amylase Inhibition Assay .....	86
3.4.2. $\alpha$ -glucosidase Inhibition Assay .....	89
3.5. In Silico Docking .....	92
3.5.1. $\alpha$ -amylase .....	93
3.5.2. Phosphoinositide-3-Kinase .....	94
3.5.3. $\alpha$ -glucosidase .....	96
3.5.4. Insulin Receptor .....	98
<b>Chapter 4: Discussion .....</b>	<b>100</b>
<b>Conclusion.....</b>	<b>113</b>
<b>Study Limitations and Future Studies .....</b>	<b>114</b>
<b>APPENDICES.....</b>	<b>132</b>

---

## List Of Figures

<b>Figure 1.1:</b> 3D Structure of Insulin containing the alpha chains, containing 21 amino acids and the beta chain containing 30 amino acids. ....	24
<b>Figure 1.2:</b> Insulin secretion in beta cells. Glucose enters cells and triggers potassium channels. Calcium ions enter the cell. Vesicles containing insulin are exocytosed, releasing insulin into the bloodstream.....	27
<b>Figure 1.3:</b> Simplified Diagram of Insulin Signalling Pathway. Insulin binds to its receptor, causing conformational changes in the protein. Signal transduction leads to a cascade of phosphorylation events. Downstream glucose-controlling processes initiate [62].....	29
<b>Figure 1.4:</b> Chemical Structure of DPP-4 Inhibitor Alogliptin .....	39
<b>Figure 1.5:</b> Chemical Structure of PI3K inhibitor, Wortmannin .....	40
<b>Figure 1.6:</b> General chemical structure of Sulphonylureas.....	41
<b>Figure 1.7:</b> Chemical Structure of Acarbose .....	42
<b>Figure 1.8:</b> The general structure of thiazolidinediones .....	43
<b>Figure 1.9:</b> Pharmacophoric sites for fluoroquinolones. The key candidate sites potentially responsible for glycaemic effects are on carbons 1, 3, 4, and 7. [114].....	44
<b>Figure 1.10:</b> Structural similarity between aryl-quinazolinones and fluoroquinolones. Circled regions show quinolone backbone, a ketone in position 4 and a pyridine nitrogen [122] .....	46
<b>Figure 2.1:</b> Cell Culture procedure. Sterilise workspace; warm media to 37°C. Thaw cells; Seed cells in media; incubate at 37°C, 5% CO <sub>2</sub> . Monitor growth; replace media every 2–3 days. Check for contamination; maintain sterility. Subculture at 70–90% confluence using trypsin. Reseed cells at the desired density. Store cells in the freezer. [132].....	52
<b>Figure 2.2:</b> Regression Plot for Glucometer values vs standard.....	56
<b>Figure 2.3:</b> Conversion of Thiazolyl Tetrazolium Bromide to Formazan .....	57
<b>Figure 2.4:</b> MTT assay protocol – cells are seeded in a plate, MTT solution is introduced, incubated for 3-4 hours, reaction is stopped with DMSO, and absorbance is measured [138].....	58
<b>Figure 2.5:</b> Media Glucose Utilisation Assay Protocol – cells grown until confluence, fluoroquinolones introduced into wells and incubated for 24 hours, media glucose was measured subsequently [135].....	59
<b>Figure 2.6:</b> Wortmannin assay protocol – cells grown until confluence, cells treated with wortmannin and incubated for 24 hours, fluoroquinolones introduced into wells and incubated for 24 hours, media glucose is measured subsequently [149] .....	61

---

<b>Figure 2.7:</b> In-Cell Elisa protocol – cells grown until confluence, fluoroquinolones introduced into wells and incubated for 24 hours, cells are fixed and permeabilisation, after incubation and washing, primary antibody is introduced and wells incubated, after which secondary antibody is introduced and incubated. Resultant wells are then measured for protein expression.[146].....	63
<b>Figure 2.8:</b> 96 well-plates with each compound, primary antibody, positive and negative controls [147].....	64
<b>Figure 2.9:</b> Chemical reaction. 3,5-dinitrosalicylic acid + reducing sugar → 3-amino-5-nitrosalicylic acid and oxidised sugar [128] .....	66
<b>Figure 2.10:</b> Catalytic conversion of 4-nitrophenyl- $\alpha$ -D-glucoopyranoside to $\alpha$ -D-glucoopyranoside and p-nitrophenol [130] .....	68
<b>Figure 3.1:</b> Percentage viability in C2C12 and HepG-2 cells treated with fluoroquinolones (Ciprofloxacin, moxifloxacin, Lomefloxacin, and Gatifloxacin) at different concentrations (10, 25, 50, 75 and 100 $\mu$ g/ml). The data is presented as mean $\pm$ SD represented with error bars, (n = 3), and the asterisk (*) represents the compounds which meet the 80% threshold for cell viability, indicative of low toxicity.....	73
<b>Figure 3.2:</b> Media glucose concentrations in HepG-2 cells treated with fluoroquinolones (Ciprofloxacin, moxifloxacin, Lomefloxacin, and Gatifloxacin) at different concentrations of 12.5, 25, and 50 $\mu$ g/ml.). The data is presented as mean $\pm$ SD represented with error bars, (n = 3), and the asterisk (*) represents the statistical difference between the test compounds and the control at (p < 0.05) .....	75
<b>Figure 3.3:</b> Glucose uptake in C2C12 cells treated with fluoroquinolones (Ciprofloxacin, moxifloxacin, Lomefloxacin, and Gatifloxacin) at different concentrations of 12.5, 25, and 50 $\mu$ g/ml.). The data is presented as mean $\pm$ SD represented with error bars, (n = 3), and the asterisk (*) represents the statistical difference between the test compounds and the control at (p < 0.05) .....	76
<b>Figure 3.4:</b> Media glucose concentrations in C2C12 and HepG2 cells concurrently treated with wortmannin and Ciprofloxacin at different concentrations 12.5, 25, 50 $\mu$ g/ml. A-Control refers to the absolute control and W-Control refers to the wortmannin control. The data is presented as mean $\pm$ SD represented with error bars, (n = 3), and the asterisk (*) represents the statistical difference between the test compounds and the control at (p < 0.05).....	79
<b>Figure 3.5:</b> Media glucose concentrations in C2C12 and HepG2 cells concurrently treated with wortmannin and Moxifloxacin at different concentrations 12.5, 25, 50 $\mu$ g/ml. A-Control refers to the absolute control and W-Control refers to the wortmannin control. The data is presented as mean $\pm$	

---

---

SD represented with error bars, (n = 3), and the asterisk (\*) represents the statistical difference between the test compounds and the control at (p < 0.05).....80

**Figure 3.6:** Relative percentage expression of IL-6 in C2C12 and HepG-2 cells treated with fluoroquinolones (Moxifloxacin) at different concentrations 12.5, 25, and 50µg/ml. The data is presented as mean ± SD represented with error bars, (n = 3), and the asterisk (\*) represents the statistical difference between the test compounds and the control at (p < 0.05). .....81

**Figure 3.7:** Relative percentage expression of IL-6 in C2C12 and HepG-2 cells treated with fluoroquinolones (Ciprofloxacin) at different concentrations 12.5, 25, and 50µg/ml. The data is presented as mean ± SD represented with error bars, (n = 3), and the asterisk (\*) represents the statistical difference between the test compounds and the control at (p < 0.05). .....82

**Figure 3.8:** Relative percentage expression of GLUT-4 in C2C12 cells treated with fluoroquinolones (Ciprofloxacin and Moxifloxacin) at different concentrations 12.5, 25, and 50µg/ml. The data is presented as mean ± SD represented with error bars, (n = 3), and the asterisk (\*) represents the statistical difference between the test compounds and the control at (p < 0.05). .....83

**Figure 3.9:** Relative percentage expression of AKT in C2C12 and HepG-2 cells treated with fluoroquinolones (Moxifloxacin) at different concentrations 12.5, 25, and 50µg/ml. The cells presented as mean ± SD represented with error bars, (n = 3). The asterisk (\*) represents the statistical difference between the test compounds and the control at (p < 0.05). .....84

**Figure 3.10:** Relative percentage expression of AKT in C2C12 and HepG-2 cells treated with fluoroquinolones (ciprofloxacin) at different concentrations of 12.5, 25, and 50µg/ml . The cells presented as mean ± SD represented with error bars, (n = 3). The asterisks (\*) represents the statistical difference between the test compounds and the control at (p < 0.05). .....85

**Figure 3.11:** The inhibition of α-amylase activity by fluoroquinolones (Ciprofloxacin, moxifloxacin, Lomefloxacin, and Gatifloxacin) at different concentrations 10, 30, 50, and 75µg/ml. µg/ml). The results are represented in a clustered column. The control is set at 0%. Data are presented as mean ± standard deviation values. The error bars correspond to the standard errors of the means and asterisks (\*) indicate significant statistical differences relative to the control experiment (p-value ≤ 0.05). ....87

**Figure 3.12:** The inhibition of α-glucosidase activity by fluoroquinolones (Ciprofloxacin and Moxifloxacin, Lomefloxacin, and Gatifloxacin) at different concentrations, 10, 30, 50, and 75µg/ml. µg/ml). The results are represented in a clustered column. The Control is set at 0%. Data are presented as mean ± standard deviation values. The error bars correspond to the standard errors of the means and asterisks (\*) indicate significant statistical differences relative to the control experiment.....90

---

<b>Figure 3.13:</b> Ligand-Receptor complex between Ciprofloxacin and Alpha-amylase .....	93
<b>Figure 3.14:</b> Ligand-Receptor Complex between Ciprofloxacin and PI3K .....	94
<b>Figure 3.15:</b> Ligand-Receptor Complex between Moxifloxacin and PI3K .....	95
<b>Figure 3.16:</b> Ligand-Receptor Complex between Moxifloxacin and Alpha-glucosidase .....	96
<b>Figure 3.17:</b> Ligand-receptor complex between Ciprofloxacin and Insulin Receptor.....	98
<b>Figure 3.18:</b> Ligand-receptor complex between Moxifloxacin and Insulin Receptor.....	99

---

## List Of Tables

<b>Table 1.1:</b> Illustrates the varying types of fluoroquinolones, and their respective substituents that may potentially contribute to hypoglycaemia.....	46
<b>Table 2.1:</b> Summarised data for Glucometer validation .....	56
<b>Table 3.1:</b> The IC50 concentrations for the Fluoroquinolones and acarbose obtained from the alpha-amylase inhibitory assay .....	88
<b>Table 3.2:</b> The IC50 concentrations for the Fluoroquinolones and acarbose obtained from the alpha-glucosidase inhibitory assay. ....	91
<b>Table 3.3:</b> Docking profile of fluoroquinolones against alpha-amylase .....	93
<b>Table 3.4:</b> Docking profile of fluoroquinolones against PI3K.....	95
<b>Table 3.5:</b> Docking profile of fluoroquinolones against alpha-glucosidase.....	97
<b>Table 3.6:</b> Docking profile of fluoroquinolones against Insulin Receptor.....	99
<b>Table 4.1:</b> Suggested chemical derivatisation of ciprofloxacin envisaged to minimise toxicity .....	111

---

## List Of Abbreviations

Abs	absorbance
AGEs	advanced glycation end-products
AMPK	adenosine 5' monophosphate-activated protein kinase
ATP	adenosine triphosphate
cAMP	cyclic adenosine monophosphate
CO <sub>2</sub>	carbon dioxide
CNS	central nervous system
C2C12	Murine Myoblasts
CYP450	Cytochrome P450
DMEM	Dulbecco's Medium Essential Media
T2DM	Diabetes Mellitus
DNA	Deoxyribonucleic Acid
DPP-4	Dipeptidyl peptidase-4
ER	Endoplasmic reticulum
FADH <sub>2</sub>	Flavin adenine dinucleotide
GI	Gastrointestinal
GS	Glycogen Synthase
GIP	Glucose-dependent insulinotropic polypeptide
GLP-1	Glucagon-like peptide-1
GLUT4	Glucose transporter type 4
GSIS	Glucose-stimulated insulin secretion
GSK-3 $\beta$	Glycogen synthase kinase-3 beta
HBA1c	Glycosylated haemoglobin
HGP	Hepatic Glucose Production
HDL	High-density lipoprotein
HepG-2	Human hepatocellular carcinoma 2
HLA	Human leukocyte antigen
IC <sub>50</sub>	50% inhibitory concentration
IRS-1	Insulin receptor substrate-1
K <sup>+</sup>	Potassium ion
LDL	Low-density lipoprotein
min	minute

---

ml	millilitre
MEM	medium essential media
mmol/L	millimolar
mTOR,	mammalian target of rapamycin
MW	Molecular weight
Na <sup>+</sup>	sodium ion
NADH	Nicotinamide adenine dinucleotide
NADPH	Nicotinamide adenine dinucleotide phosphate
OGTT	oral glucose tolerance test
OH	hydroxyl/hydroxide
pH	potential of Hydrogen
PBS	Phosphate Buffer Saline
PI3K	Phosphoinositide 3-kinase
PDK-1	PIP-3-dependent protein kinase 1
PIP-3	Phosphatidylinositol-3,4,5-triphosphate
PEPCK	Phosphoenolpyruvate-carboxykinase
PPP	Pentose Phosphate Pathway
PPI	Protein Phosphatase I
PKA	Protein Kinase A
PPAR $\gamma$	Peroxisome proliferator-activated receptor- $\gamma$
RMSD	Root mean square deviation
RNA	Ribonucleic Acid
ROS	Reactive oxygen species
SGLT1	Sodium-glucose cotransporter 1
TZD	Thiazolidinediones
TCA	Tricarboxylic Acid
UDPG	Uridine diphosphate glucose
UTI	Urinary Tract Infection
VEGF	Vascular endothelial growth factor

---

# Abstract

## Background

In 2021, over 537 million adults worldwide (ages 20–79) had diabetes mellitus (T2DM), with numbers expected to rise to 643 million by 2030 and 783 million by 2045. T2DM makes up 90–95% of cases, primarily driven by obesity, sedentary lifestyles, and ageing. Oral antidiabetic treatments are effective initially but lose efficacy as beta cell failure progresses, making insulin therapy necessary to maintain normoglycemia. Additionally, these treatment options have numerous side effects such as gastrointestinal disturbances, hypoglycaemia, weight gain, diarrhoea, and abnormal liver function. A class of antibiotics, fluoroquinolones, has been shown to exert hypoglycaemia as a side effect. Fluoroquinolones show potential for diabetes treatment due to their cost-effective production, high oral absorption, and strong tissue penetration. Their dual oral and intravenous availability supports flexible treatment. This study aimed to explore the potential glucose-lowering properties of four fluoroquinolones. They were investigated for their potential inhibitory activity on carbohydrate-hydrolysing enzymes. and for effects on target cells (skeletal muscle and liver cells).

## Methodology

The selected fluoroquinolones for this study were Ciprofloxacin, Lomefloxacin, Moxifloxacin and Gatifloxacin. Cytotoxicity was assessed *in vitro* to determine the effects of fluoroquinolones on cell viability in skeletal muscle (C2C12) and hepatic (HepG-2) cell lines. Glucose utilisation was examined to evaluate the impact of fluoroquinolones on glucose metabolism in skeletal muscle and hepatic cell lines. The influence of fluoroquinolones on the expression of AKT and GLUT-4, key proteins involved in glucose metabolism and insulin signalling, was investigated in skeletal muscle and hepatic cell lines. Furthermore, the effect of fluoroquinolones on glucose utilisation was assessed in the presence of wortmannin, a PI3K inhibitor. The effect of fluoroquinolones on the expression of the inflammatory cytokine IL-6 was examined in skeletal muscle and hepatic cell lines. *In vitro* screening of fluoroquinolones was further conducted to assess their anti-diabetic potential through  $\alpha$ -amylase and  $\alpha$ -glucosidase inhibition. *In silico* studies were performed to predict interactions between selected fluoroquinolones and glycaemic targets, including phosphoinositide 3-kinase, the insulin receptor,  $\alpha$ -glucosidase, and  $\alpha$ -amylase.

## Results and discussion

Enzymatic inhibition assays revealed that fluoroquinolones exhibit promising anti-hyperglycaemic activity by strongly inhibiting  $\alpha$ -amylase and moderately inhibiting  $\alpha$ -glucosidase. The structural features of the fluoroquinolones observed using *in silico* docking, namely piperazine, carboxylate moieties and aromatic rings, contribute to this effect; these moieties share non-covalent interactions with the active sites of each selected target. All preliminary glucose utilisation assays showed enhanced glucose uptake upon treatment

---

with the selected fluoroquinolones. The cells also had minimal damage from the compounds, with moxifloxacin and ciprofloxacin notably demonstrating low cytotoxicity at 12.5–50 µg/ml. PI3K activation could have been essential for glucose utilisation, as confirmed by docking studies and In-cell ELISA. These findings suggest fluoroquinolones may serve as potential antidiabetic agents by promoting glucose uptake via PI3K-dependent pathways, warranting further investigation to optimise their efficacy as potential antidiabetic agents.

### **Conclusions**

The tested fluoroquinolones demonstrated anti-hyperglycaemic potentials in the different experimental models. Antihyperglycaemic potential could be linked to possible modulatory or inhibitory interactions with key protein targets that are involved in the pathogenesis and pathophysiology of diabetes. Reversible binding onto PI3K is the hypothesised mechanism by which fluoroquinolones induce glycaemic effects, notably the uptake of glucose through glucose transporters.

### **Keywords**

Type 2 Diabetes Mellitus (T2DM), Fluoroquinolones, Enzyme inhibitions, Insulin signalling, Glucose, Insulin

---

# Chapter 1: Literature Review

## 1. Introduction

South Africa has one of the highest diabetes rates in sub-Saharan Africa, with approximately 4.6 million adults affected in 2023 and a prevalence of 12.8% in the general population. Type 2 Diabetes (T2DM) is the most common form, largely linked to high obesity rates, especially among women, 40% of whom are obese. Around 50% of cases remain undiagnosed, leading to severe complications such as cardiovascular disease, kidney failure, and amputations. On a global scale, 1.6 million deaths in 2021 were attributed to Diabetes Mellitus, mainly due to complications like cardiovascular disease and kidney failure [73]. Global healthcare spending on diabetes reached \$966 billion in 2021, accounting for 9% of total health expenditures. The highest prevalence is found in the Western Pacific and Southeast Asia, while Africa has the lowest but also the highest proportion of undiagnosed cases (up to 60%) [74].

The current regimens available as treatment for diabetes require expansion and innovation. Treatments vary significantly in terms of their side effect profile, efficacy and cost. Metformin, the first-line therapy for T2DM, reduces blood glucose concentrations with a low risk of hypoglycaemia and demonstrates additional catalysed benefits, including weight neutrality and cardiovascular protection. Metformin therapy, however, often causes lactic acidosis and gastrointestinal side effects like nausea and diarrhoea, which can lead to discontinuation. Additionally, long-term use is associated with vitamin B12 deficiency, necessitating regular monitoring to prevent complications like anaemia and neuropathy, as evidenced by large-scale clinical trials and meta-analyses [167]. Moreover, challenges persist with 2<sup>nd</sup> and 3<sup>rd</sup>-line oral antidiabetic agents. For example, Sulphonylureas and thiazolidinediones were associated with adverse effects such as hypoglycaemia, weight gain, and cardiovascular risks, which limited their long-term use. Despite advancements, a substantial proportion of patients failed to achieve optimal glycaemic control, underscoring the need for personalised therapeutic approaches. Systematic reviews and meta-analyses highlighted variability in treatment responses, often attributed to genetic, environmental, and lifestyle factors. Additionally, the high cost of newer agents, such as GLP-1 agonists and SGLT-2 inhibitors, restricts their accessibility, particularly in low-resource settings [192].

---

Fluoroquinolones are a potential drug candidate, given their low cost of production and their reported clinical dysglycaemic effects. The mechanisms by which these dysglycaemic effects arise, however, are under-researched. A hypothesised effect is the accumulation of the compound in pancreatic cells, causing beta-cell vacuolation and endoplasmic reticulum dilation, disrupting insulin production, leading to hyperglycaemia [118]. Conversely, *in-vitro* studies reveal fluoroquinolones enhance insulin secretion via K<sup>+</sup>ATP channel blockage, but only at elevated glucose levels, suggesting potential antidiabetic properties without inappropriate insulin release. [116]

This study is dedicated to the *in vitro* and *in silico* exploration of standard fluoroquinolones to assess their impact on therapeutic targets relevant to diabetes mellitus (T2DM) and to uncover their potential antidiabetic properties. This exploration, in part, aims to overcome the limitations associated with current T2DM therapies, offering the possibility of enhanced treatment options. Given the substantial global burden of T2DM, it is imperative to investigate promising compounds to broaden the therapeutic arsenal available to patients. Additionally, fluoroquinolones can be systematically evaluated to establish correlations between their enzyme-inhibitory or activating effects and specific structural features, thereby identifying pharmacophoric units with potential antidiabetic activity. Such investigations may pave the way for the development of more precise and effective therapeutic strategies for T2DM.

---

## Background

Glucose metabolism is a collection of complex biochemical processes and pathways that drive glucose utilisation and storage. Glucose is obtained from dietary carbohydrates, which vary in their degrees of polymerisation and digestibility. Monosaccharides, disaccharides, and polysaccharides are typical sources of glucose. Once digested, these carbohydrates undergo catabolism into simpler monomeric units, the most useful of which are glucose, lactose, and fructose [1].

Glucose is an essential nutrient that provides energy to sustain the physiological health of most cells and tissues. When broken down through cellular respiration, glucose yields ATP, pyruvate, and other molecules that maintain the cell's health through nutrient replenishment. Additionally, the central nervous system relies on glucose for major metabolic fuel. Glucose and its requisite metabolism and regulation matter as an area of investigation for health and general optimisation of well-being.

The endocrine system drives glucose regulation through the secretion of hormones, which promote the storage and release of glucose. Pancreatic hormones glucagon and insulin function antagonistically to regulate blood glucose concentrations [2]. Post-prandial states of excess glucose concentrations are termed hyperglycaemic, and the converse, where blood glucose concentrations are below a healthy threshold, is termed hypoglycaemia. Hypoglycaemia has a more serious pathology than its counterpart, afflicting most untreated patients with coma. Euglycaemic physiological conditions are where blood glucose concentration is under 7 mmol/L or 126.11 mg/dl. Under fasted conditions, blood glucose concentration ranges from 3.9-5.8 mmol/L or 70.26-104.49 mg/dl [3].

Insulin secretion is triggered in hyperglycaemic conditions, lowering serum glucose concentrations. Glucagon is conversely secreted in hypoglycaemic conditions to increase glucose concentrations. Both these hormones are secreted by the islets of Langerhans, a cluster of cells located in the pancreas; namely, alpha cells that secrete glucagon and beta cells that secrete insulin [4]. Insulin possesses anabolic properties that promote glucose storage and conversion into glycogen. Conversely, the catabolic effects of glucagon promote the breakdown of these metabolic stores and the reconversion of lipids, proteins, and macromolecules back into glucose [5]. Regulation of glucose metabolism can be influenced by various factors, including but not limited to diet, exercise, age, genetics, and treatment. The treatments that will be investigated in this study will be fluoroquinolones.

---

## 1.1.Entry of Glucose

Glucose enters mammalian cells through transmembrane proteins, integral channel proteins which transport glucose from the extracellular space into the cell. The expression of these transporters mediates the rate of glucose entry. Sodium-glucose-linked transporters (SGLTs) and facilitated diffusion glucose transporters (GLUTs) are the general groupings of glucose transmembrane proteins, differing by location, function, and structure [6].

SGLTs rely on a preformed sodium concentration gradient driven by the movement of sodium ions out of cells through sodium-potassium ATPase. The ions accumulate and drive the symport of glucose and sodium. Cells with high SGLT expression line the lumen of the small intestine, where they take up glucose from food sources, and the renal tubules, where they facilitate nephron glucose reabsorption [7].

GLUTs, however, rely on facilitated diffusion, a passive process by which molecules traverse the cell membrane through channels or carrier proteins along concentration gradients. There are three classes of GLUTs, i.e., classes I, II, and III, divided according to their amino acid similarity, function, and anatomical sites of expression. Class I, consisting of GLUT1 to GLUT4, is found in blood-tissue barriers, adipocytes, muscles, neurons, testis, liver, pancreas, and small intestine. In this study, GLUT4 is of primary interest, given its relationship to the target sites previously listed, and their connection to T2DM pathophysiology and pharmacology [8].

Although GLUT2 is present in renal and neuronal cells, its most significant expression occurs in pancreatic beta cells and hepatocytes, where it plays a critical role in glucose uptake and sensing. It has a low affinity to glucose ( $K_m=17$  mmol/L) in contrast to the other members of the glucose transport genus [8]. The protein interacts with intracellular glucose-converting enzymes, e.g. Glucokinase, to register concentrations of glucose to promote a concentration equilibrium between the extracellular and intracellular space. In the fasting state, glucose-6-phosphatase in the cellular endoplasmic reticulum hydrolyses glucose-6-phosphate to glucose and phosphates. The glucose then exits the cell through GLUT2 to re-equilibrate external and intracellular concentrations of glucose, achieving homeostatic balance [9]. GLUT2, therefore, contributes significantly to blood glucose homeostasis. GLUT4 plays a similar role in gatekeeping the entry and exit of glucose in key target tissues [10].

---

## 1.2. Glucose Metabolism and Its Physiological Use

Before glucose can perform its various physiological functions, it is converted, stored, broken down, and polymerised into products appropriate for their specific cellular environment. The processes by which glucose undergoes these changes matter for researchers to understand the destination for glucose and its subsequent physiological uses. The major uses of glucose are related to how it contributes to ATP production, how it is stored as glycogen, and how it is produced through gluconeogenesis.

### 1.2.1. Energy Production.

Multiple physiological processes require energy as a catalyst. The biological currency for energy in the body is Adenosine 5'-triphosphate (ATP), a purine nucleotide found in all human cells. The energy released upon dephosphorylation is stored in the high-energy phosphate bonds of the molecule [11]. ATP facilitates the movement of important nutrients and minerals against a concentration gradient through active transport. ATP participates in intracellular metabolic reactions often by coordinating with kinases to advance steps in complex biochemical pathways such as insulin signalling, glycolysis [12], etc. Finally, ATP can be found to play an important role in sustaining physiological processes which are integral to health, muscle contraction, cardiac and platelet function, and neurotransmission, among others [13]. Given this important role, understanding glucose as a biochemical precursor to the production of ATP is necessary to evaluate the role of glucose metabolism in maintaining overall physiological health.

One molecule of glucose can approximately yield 36 molecules of ATP, as a product of aerobic cellular respiration [14]. This process has three stages, all of which produce ATP, which is later shunted to perform the functions listed above. The first stage is glycolysis, a 10-step biochemical pathway in which one glucose molecule is converted to 2 pyruvate molecules. The process commences when glucose enters the cell through glucose transporters and interacts with hexokinase or glucokinase to produce glucose-6-phosphate. During the first four steps, also known as the pay-off phase, glucose undergoes several metabolic steps to accumulate energy that facilitates the cleaving of the molecule into two molecules of glyceraldehyde-3-phosphate, energy arising from ATP-related kinase activity [15]. During the rest of the 10 steps, Glyceraldehyde-3-phosphate is further broken down into pyruvate with NADH as a by-product. Pyruvate is then transported into the mitochondria, where it undergoes oxidative decarboxylation to produce acetyl coenzyme-A (acetyl-CoA). Acetyl-CoA then enters a complex series of reactions, collectively known as the Krebs Cycle, ultimately to produce carbon dioxide (CO<sub>2</sub>). The by-products of the Krebs Cycle, NADH with H<sup>+</sup> and FADH<sub>2</sub>, are then used

---

---

in the mitochondrial membrane as drivers of the Electron Transport Chain; the process by which energy from NADH with  $H^+$  and  $FADH_2$ , cytochrome electron carriers and ATP synthase produces more ATP [16].

Lastly, various steps of these pathways produce precursor molecules which mediate ancillary biochemical processes that are important for cell metabolism, typically through the synthesis of endogenous nutrients and building blocks of inner cellular machinery. For example, glucose-6-phosphate – the first metabolic intermediate of glucose from glycolysis – is converted into 6-phosphogluconolactone by the enzyme glucose-6-phosphate dehydrogenase in the first step of the pentose phosphate pathway (PPP) [17]. This pathway is important for producing precursors for nucleotide, pyridoxine, and amino acid synthesis. These molecules are integral for ensuring that cells have the requisite material for building RNA and DNA. Additionally, PPP promotes redox homeostasis, assists in preventing oxidative stress, and maintains carbon homeostasis.

### 1.2.2. Glycogenesis and Glycogenolysis

Glycogen is a storage-branched polymer of glucose, most commonly located within hepatocytes. Glycogen is produced through glycogenesis, typically in the liver and muscles. When physiological glucose concentrations are above equilibrium or during a postprandial glucose surge – hyperglycaemia – glucose is converted into glycogen to regulate and decrease serum glucose concentrations. Glucose is converted into glucose-6-phosphate by glucokinase or hexokinase [18]. The phosphate group located on the 6<sup>th</sup> carbon is then transferred to the 1<sup>st</sup> carbon atom on the glucose molecule by the enzyme phosphoglucomutase in the presence of magnesium ions and glucose-1,6-bisphosphate, yielding glucose-1-phosphate as a first intermediate in glycogen synthesis [19]. The intermediate subsequently reacts irreversibly with uridine triphosphate by the enzyme uridine diphosphate-glucose pyrophosphorylase, producing uridine diphosphate glucose (UDPG). This is the final version of glucose, which is polymerised to pre-existing glycogen [20]. Polymerisation follows an alternating branch sequence due to the interchange of glycogen synthase and branching enzyme [21]. Glycogen synthase forms  $\alpha 1 \rightarrow 4$  bonds between approximately 10 or more glucose residues until the branching enzyme cleaves a terminal region roughly consisting of 6 or more residues and builds an  $\alpha 1 \rightarrow 6$  glycosidic bond, forming a new side chain on which polymerisation continues [22]. This process continues until the complex macromolecule glycogen has stored sufficient amounts of excess glucose. All these effects are downstream from insulin secretion. Insulin increases glycogen synthesis via the activation of glycogen synthase (GS). GS responds to the net downstream dephosphorylation processes

---

---

triggered by Protein Phosphatase I (PPI). Insulin activates PPI, which heightens the enzyme's substrate-specific activity on glycogen, accelerating glycogenesis by activating glycogen synthase. Additionally, PPI attenuates the dephosphorylation of both phosphorylase and phosphorylase kinase, the key glycogenolytic enzymes which would otherwise be active under hypoglycaemic conditions [23]. The resultant effect is the production of glycogen, which goes on to store glucose and thereby lower serum concentrations back to the physiological baseline.

In hypoglycaemic conditions, however, the hormone glucagon is secreted. Glucagon promotes hepatic glucose production (HGP) through promoting gluconeogenesis and glycogenolysis and through inhibiting glycogenesis. It therefore binds onto the glucagon receptor, a G-protein coupled receptor that, through a series of activations of protein subunits, activates adenylate cyclase, converting ATP into cyclic AMP (cAMP) [24]. cAMP is a second messenger which activates various other proteins that go on to promote physiological changes. The target of interest is protein kinase A (PKA), as the active form of the enzyme inactivates glycogen synthase (GS) [25]. Cyclic adenosine monophosphate binds to PKA, thereby activating it. Attenuated GS activity results in less glycogen buildup, allowing for lengthened glucose circulation. Protein Kinase A additionally phosphorylates phosphorylase kinase, which subsequently phosphorylates glycogen phosphorylase. Phosphorylated glycogen phosphorylase is the activated enzyme principally responsible for glycogen breakdown [26].

This breakdown follows two biochemical pathways: The first involves the dual action of glycogen phosphorylase with debranching enzyme, and the second pathway revolves around the breakdown in lysosomes by  $\alpha$ -glucosidase. Glycogen phosphorylase is the rate-limiting enzyme for the breakdown of glycogen. The enzyme cleaves the terminal glucose residue connected to a glycogen branch, breaking the 1,4 glycosidic bonds [27]. Conversely, the debranching enzyme cleaves  $\alpha$  1,6 glycosidic bonds and transfers a branch to the end of the polymer. Glycogen phosphorylase subsequently further breaks down the branch. Additionally, the glucose residues are phosphorylated to the carbon atom in position one, yielding glucose-1-phosphate [28]. Phosphoglucomutase converts glucose-1-phosphate to glucose-6-phosphate, a primary intermediate in glycolysis. In gluconeogenic organs such as the liver, kidney, and intestines, glucose-6-phosphate needs to be dephosphorylated to glucose with the aid of the enzyme glucose-6-phosphatase so that it can undergo transport from the endoplasmic reticulum (ER) to the interstitial and extracellular space as free molecules of glucose. However, the glucose-6-phosphate remaining in the cell subsequently enters glycolysis, where it undergoes the remainder of the enzymatic conversions to various intermediates and is consequently converted to pyruvate.

---

Pyruvate then acts as a critical metabolic intermediate for further biochemical pathways, including the Krebs, alanine, and Cori cycle, along with fatty acid synthesis [29].

### **1.2.3. Gluconeogenesis**

Gluconeogenesis is the process by which glucose is formed intracellularly, typically in the liver and kidneys, in response to low physiological glucose concentrations. Non-carbohydrate sources such as lactate, amino acids and glycerol are converted to glucose, which is then transported into the systemic circulation and ultimately skeletal, neuronal, and hepatic cells [30]. Glucagon stimulates gluconeogenesis in the manner described in the prior paragraph. The pathway itself is the biochemical reverse of glycolysis. Pyruvate is carboxylated into oxaloacetate, which is converted into a glycolytic intermediate known as phosphoenolpyruvate by the enzyme phosphoenolpyruvate-carboxykinase (PEPCK) [31]. PEPCK is the rate-limiting enzyme for this process, the transcription of which is influenced by available concentrations and ratios of glucagon and insulin [32]. The series of enzymatic reactions occurs to yield a molecule of glucose-6-phosphate, which then enters the smooth endoplasmic reticulum (ER) for dephosphorylation by glucose-6-phosphatase. The resultant glucose molecule exits the smooth ER through transmembrane protein T2, traverses the cytosol and ultimately exits the cell through GLUT-2 [33]. Blood glucose concentrations, therefore, increase to compensate for the pre-existing deficit. This reaction is stimulated by high concentrations of acetyl-CoA, which is via beta-oxidation of hepatic fatty acids. Conversely, high concentrations of ADP and glucose prevent this process. Ultimately, gluconeogenesis works in tandem with glycogenolysis to promote hepatic glucose production (HGP) to maintain normoglycemic concentrations [34].

### **1.3. Glucose Regulation and Role of Insulin**

Optimal glucose utilisation and storage are homeostatic. The endocrine system, composed of various glands and secretory ducts, secretes hormones that bind to target sites to initiate various biochemical pathways that alter physiological states for lengthened periods. The system of interest is located in the pancreas, which is divided into an exocrine and endocrine region. The exocrine portion is composed of acinar and duct tissue, and the endocrine portion consists of the islets of Langerhans [35]. These clusters of cells are primarily responsible for hormone secretion that controls glucose homeostasis, i.e. Glucagon and Insulin. Glucose regulation is vital for preventing pathological complications arising from a paucity of or an excess of serum glucose concentration [36]. An excess of glucose can harm organs, blood vessels, and nerves, resulting in pathological complications such as kidney failure,

---

---

cardiovascular disease, and vision loss [37]. Blood glucose concentrations below a healthy baseline can lead to pathologies affecting the brain, leading to disorientation, light-headedness, seizures, and in extreme situations, coma and death [37]. Moreover, glucose regulation assists with metabolic functions by providing the carbon skeletons and metabolic intermediates for intracellular processes such as lipid synthesis where glucose provides acetyl-CoA, a precursor for fatty acid synthesis, amino acid synthesis, where glucose provides the carbon skeletons for the synthesis of non-essential amino acids through transamination reactions, and finally, nucleotide synthesis where glycolytic intermediates are shunted into the pentose phosphate pathway which yields ribose-5-phosphate, a building block for nucleotides and nucleic acids [38]. Energy balance and metabolic homeostasis are maintained by glucose control, which guarantees that metabolic pathways, including glycolysis, gluconeogenesis, and glycogenesis, operate at their best. Therefore, how glucose is regulated matters significantly for investigating the degree to which it can be manipulated, degraded upon the onset of disorders, and alleviated by treatment.

---

### 1.3.1. Insulin

Insulin is a dipeptide hormone secreted by the beta cells located in the pancreatic islets of Langerhans which contains 51 amino acids arranged in an  $\alpha$  chain and a  $\beta$  chain linked by disulphide bridges [39]. The hormone binds primarily to the insulin receptor, triggering the insulin signalling cascade that initiates a physiological regulation of blood glucose concentrations from high to equilibrium concentrations. The various biochemical processes implicated are glycogen synthesis, glycogenolysis, glucose uptake, and insulinotropic gene expression of metabolic enzymes [40]. The hormone is initially synthesized as pre-proinsulin. Pre-proinsulin enters the endoplasmic reticulum where it interacts with enzyme protein disulphide isomerase along with selective proteolytic enzymes to form proinsulin [41]. Afterwards, proinsulin is translocated from the endoplasmic to the Golgi apparatus. Proinsulin then is processed and packaged into granules, where it is hydrolysed from the long single-chain protein into insulin and a residual connecting segment called C-peptide [42]. The resultant insulin is then stored in immature secretory vesicles, which migrate from the cytoplasm to the cell membrane, i.e. exocytosis upon electrochemical stimulation. The figure below shows the 3D structure of insulin.

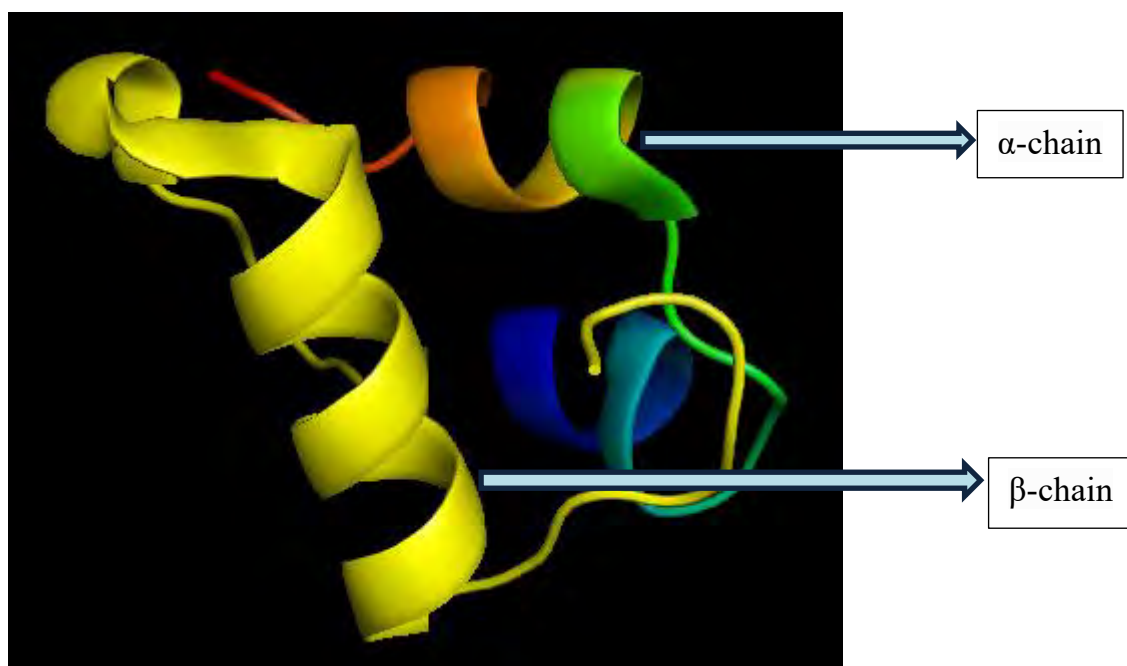


**Figure 1.1:** 3D Structure of Insulin containing the alpha chains, containing 21 amino acids and the beta chain containing 30 amino acids.

---

### 1.3.2. Insulin Secretion

Insulin secretion in response to a glucose spike is termed Glucose-Stimulated Insulin Secretion (GSIS). Insulin released from beta cells enters the portal vein in oscillatory pulses postprandially. Insulin secretion is biphasic, with release following two biochemical pathways: the triggering pathway and the amplifying pathway, the former being a rapid phase and the latter a less intense but more sustained release [43]. The rate-limiting step of glucose metabolism is catalysed by hexokinase IV or glucokinase, enzymes which convert intracellular glucose into glucose-6-phosphate, which is further broken down by endogenous enzymes into pyruvate in Glycolysis [44].

Following the conversion of glucose to glucose 6-phosphate, ATP is produced by glycolysis or glucose oxidation, raising the ATP/ADP ratio in the cytoplasm, which subsequently causes the ATP-sensitive potassium channels ( $K^+$ ATP) to close and voltage-gated  $Ca^{2+}$  channels to open [45]. An intracellular influx of calcium ions ultimately triggers vesicular bodies containing insulin to migrate and fuse with the cell membrane, releasing insulin particles through exocytosis from the cells [46].

Intracellular concentrations of glucose are converted and metabolised further in the Krebs cycle (TCA cycle) into products of cellular respiration, i.e., water, carbon dioxide and adenosine triphosphate (ATP). ATP is the by-product of both the Krebs Cycle and Glycolysis. ATP binds onto membrane-bound potassium channels, facilitating an efflux of positively charged potassium ions, causing membrane depolarisation [47]. The consequent electrochemical potential generated triggers voltage-gated calcium channels, allowing for the entry of calcium ions into the cell. The intracellular ion spike during the triggering phase initiates exocytosis of insulin located in secretory granules in vesicles, and tetrameric complexes of proteins. Insulin secreted in this pathway accounts for a smaller proportion of overall insulin [48].

The amplifying pathway contributes to the rest of insulin secretion, typically through sustained and slow insulin release during the post-absorptive meal. The mechanisms behind insulin release are independent of potassium channel stimulation. 60-70% of the total insulin secreted postprandially originates from this pathway [49]. The amplifying pathway facilitates the recruitment and translocation of insulin granules from storage pools to the plasma membrane, where they are exocytosed. This process is reliant on the presence of certain metabolic intermediates and regulators of intracellular processes, such as the Tricarboxylic acid cycle (TCA cycle). Isocitrate, NADPH, Glutamate, ATP, and Glutathione, to mention a few, are examples of positive regulators which enhance insulin secretion postprandially [50].

---

---

Concurrently, glucagon secretion is suppressed by elevations in glucose and insulin. Additionally, increased concentrations of somatostatin and islet amyloid polypeptide suppress glucagon secretion [51]. Cytokines produced by adipocytes also contribute to insulin secretion. Adipocytes store lipids and also manufacture and secrete a variety of hormones known as adipokines, which can have a significant impact on energy and metabolism. Adiponectin, for example, functions as an insulin sensitiser, and its downregulation has been associated with obesity-linked insulin resistance [52].

Once insulin is secreted, it courses through the blood and eventually leads to insulin receptors located on the surfaces of hepatic, cardiac, adipose and skeletal cells where signal transduction commences. The receptor is a heterotetrameric glycoprotein of two extracellular  $\alpha$ -subunits with binding sites on their surfaces and two  $\beta$ -transmembrane subunits linked by a disulphide bridge [53]. Insulin binds to  $\alpha$ -subunits, triggering a series of conformational changes that lead to the phosphorylation of insulin receptor substrates that go on to activate protein kinases and phosphatases. The result is increased expression of the glucose transporter, GLUT-4, increased glucose uptake and utilisation into cells, the formation of glycogen, protein, and fat, and, lastly, decreased glycogenolysis and gluconeogenesis, all of which led to decreased blood glucose concentrations [54].

A variety of factors control the extent and duration of GSIS. These factors range in their duration of activity and the stage of insulin's pathway of development. Beta cell mass and differentiation correlated highly with the extent of insulin secretion [55]. Endogenous biomolecules such as amino acids, fatty acids, acetylcholine, glucose-dependent insulinotropic polypeptide (GIP), and glucagon-like peptide (GLP) additionally function as insulinotropic compounds that promote additional release of insulin from secretory stores [56]. Glucose metabolism, however, is the primary determinant of insulin secretion. Therefore, the important area of interest is how pharmacological interventions influence glucose metabolism to alter insulin secretion. Figure 1.2 shows the simplified diagram of insulin secretion in beta cells upon glucose stimulation.

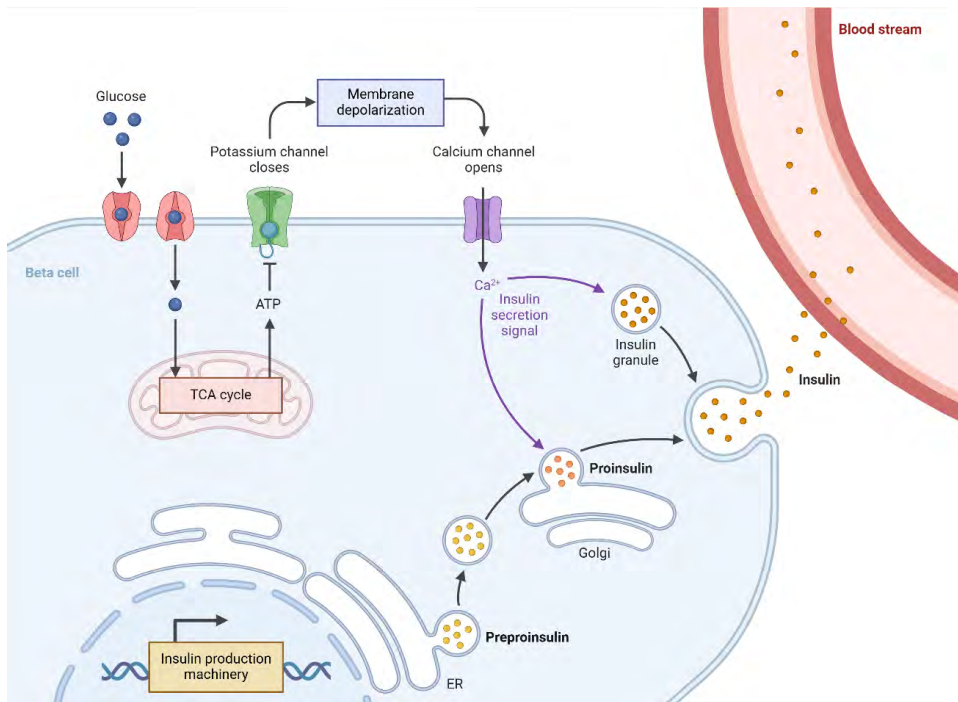


**Figure 1.2:** Insulin secretion in beta cells. Glucose enters cells and triggers potassium channels. Calcium ions enter the cell. Vesicles containing insulin are exocytosed, releasing insulin into the bloodstream.

---

### 1.3.3. Insulin Signalling

Insulin signalling involves a complex network of activation of tyrosine and serine/threonine phosphorylation events, which are downstream from insulin signal transduction. Insulin binds to its receptor, and the subsequent conformational changes initiate a cascade of kinase activation reactions which collectively result in glucose regulation [57]. The insulin receptor (IR) is a transmembrane glycoprotein critical for regulating glucose homeostasis and metabolism. The receptor is heterotetrameric and is composed of two extracellular  $\alpha$ -subunits and two transmembrane  $\beta$ -subunits linked by disulfide bonds. The  $\alpha$ -subunits contain the insulin-binding site, while the  $\beta$ -subunits possess tyrosine kinase activity. Insulin binding to the  $\alpha$ -subunits induces a conformational change, activating the  $\beta$ -subunits' kinase domain.

The first reaction is cross-autophosphorylation of tyrosine residues on the beta subunits. The phosphorylated tyrosine residue acts as an attachment point for insulin receptor substrate-1 (IRS-1) [58]. The IRS-1 proteins are then also phosphorylated and act as attachment points for phosphoinositol-3-kinase (PI3K). The active site of this kinase then migrates near the inner surface of the cell membrane, where it phosphorylates phosphatidylinositol-4,5-diphosphate (PIP-2), converting the protein to phosphatidylinositol-3,4,5-triphosphate (PIP-3), where the third carbon is phosphorylated. PIP-3 migrates across the cell membrane, where it reaches and activates PIP-3-dependent protein kinase (PDK-1) [59]. PDK-1 then goes on to activate protein kinase B, a non-membrane-bound protein that activates enzymes which catalyse glucose conversion to glycogen and facilitate translocation of GLUT-4 from the cytoplasm to the cell membrane [60]. The result is an increased expression of the glucose transporter, GLUT-4, located on adipose and skeletal muscle cells, increasing glucose transport into cells, increasing glucose utilisation, formation of glycogen, protein, and fat and decreased glycogenolysis and gluconeogenesis, all of which led to decreased blood glucose concentrations. The extent of these various processes is proportional to the insulin secretion rate. The increased expression of these metabolic intermediates has downstream effects on the rate and extent of physiological glucose utilisation [61]. Figure 1.3. shows the simplified steps behind insulin signalling.

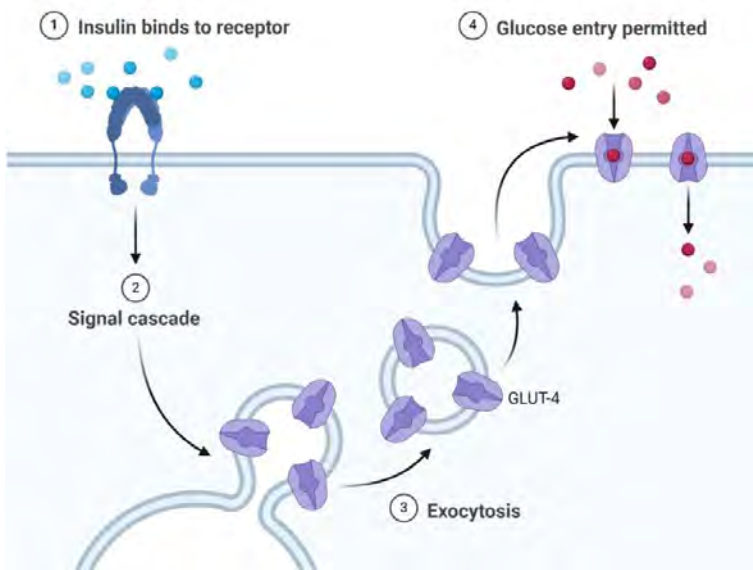


**Figure 1.3:** Simplified Diagram of Insulin Signalling Pathway. Insulin binds to its receptor, causing conformational changes in the protein. Signal transduction leads to a cascade of phosphorylation events. Downstream glucose-controlling processes initiate [62].

---

### 1.3.4. Insulin Resistance

Insulin resistance refers to impaired physiological sensitivity to insulin-mediated glucose control, typically through receptor downregulation resulting from persistent hyperinsulinemia [63]. Target cells are unresponsive to insulin and therefore lose their ability to stabilise glucose concentrations. The sites on which such defects are observed are primarily in skeletal muscle cells and adipocytes. Under normal physiological conditions, insulin inhibits gluconeogenesis, decreasing hepatic glucose production. In converse conditions, namely insulin resistance, the failure of insulin to sufficiently bind to target receptors leads to uncontrolled hepatic glucose production. Similarly, skeletal muscle cells fail to take in glucose from glucose transporters, given that this downstream process requires GLUT4 translocation, which is inhibited during insulin resistance [64]. Moreover, metabolic syndrome, a disorder often occurring concurrently with obesity and insulin resistance, correlates strongly with an increase in dyslipidaemia, physiologically marked by low HDL-C, elevated LDL-C and serum triglycerides [65]. Often, these lipids are metabolised by hormone-sensitive lipase, an enzyme responding to insulin signalling in adipose tissue. Insulin resistance, therefore, leads to an increase in circulating free fatty acids, worsening insulin resistance by decreasing skeletal cell sensitivity to glucose and activating inflammatory pathways. Inflammation and obesity importantly have a mutually reinforcing effect on insulin resistance, creating a vicious cycle. For instance, excess growth and circulation of adipose tissue may deplete the local oxygen supply for cells, triggering cellular stress pathways that promote the release of cytokines and the deployment of immune cells [66].

### 1.4. Diabetes Mellitus

Diabetes mellitus is a chronic metabolic disorder characterised by a lack of or defect in homeostatic control of blood glucose concentrations. If left untreated, the disorder typically results in serious complications such as end-stage nephropathy, gangrenous foot, and blindness [67]. The disorder is classified according to its aetiology, with Type 1 being immune-mediated or idiopathic, and Type 2 being acquired and lifestyle dependent. The hallmark clinical manifestations of diabetes mellitus include polyuria (excessive urination), resulting from osmotic diuresis induced by urinary glucose excretion; polydipsia (excessive thirst), triggered by hypothalamic osmoreceptor activation in response to fluid loss; and polyphagia (increased hunger), arising from cellular energy deprivation despite systemic hyperglycaemia due to impaired glucose uptake [187]. Moreover, patients may experience unintentional weight loss due to accelerated lipolysis and proteolysis as insulin deficiency forces alternative metabolic pathways to compensate for disrupted glucose homeostasis. They may

---

---

also experience persistent fatigue and muscular weakness resulting from disrupted ATP synthesis. Finally, patients can experience blurred vision that develops from osmotic lens distortion. These symptoms collectively underscore the metabolic derangements caused by either insulin deficiency or resistance [187].

Aside from symptom manifestation, a cardinal sign of diabetes is chronic hyperglycaemia 2, with the following diagnostic signs: A fasting serum glucose concentration of greater than 126 mg/dL (7.0 mmol/L), classic symptoms of hyperglycaemia along with random plasma glucose greater than 200 mg/dL (11.1 mmol/L), a 2-hour serum glucose concentration higher than 200 mg/dL (11.1 mmol/L) following a standard 75 g oral glucose load (oral glucose tolerance test - OGTT), or glycated haemoglobin (HbA1C) greater than 6.5% [68]. HbA1C values reflect the average blood glucose concentrations over a 2-3-month period, representing the average half-life of glycosylated haemoglobin in erythrocytes [69].

Beyond primary causes, insulin resistance often results from adverse drug events after long-term use of atenolol, prednisone, and/or hydrochlorothiazide, or it can be a secondary effect of conditions such as pheochromocytoma and Cushing's syndrome [70]. Importantly, there are numerous sites of resistance throughout the endocrine system, such as decreased insulin receptor function, decreased binding affinity of insulin to the receptor, and downregulation of glucose transporter expression and translocation from intracellular vesicles to the cell membrane.

Glucose homeostatic disruptions are attributed to abnormalities in insulin production and/or reduced sensitivity of target sites to insulin. T2DM, also known as non-insulin-dependent diabetes mellitus, is a complex disorder; patient variation in the signs and symptoms makes it considerably harder to have homogeneous treatment regimens. This form of diabetes is the most common, affecting adults with obesity and a diet generally high in the glycaemic index. Patients may vary in symptom manifestation; some have more resistance or more beta-cell deficiency, with abnormalities ranging from mild to severe. Patients experiencing beta cell failure may eventually need exogenous insulin therapy. The general observation, however, for T2DM is peripheral tissue resistance [71]. Furthermore, intermediate steps involved in insulin signalling may be disrupted. For example, endocrine dysfunction may include premature phosphorylation of insulin receptor substrates (IRS-1), precluding stimulation by the transmembrane beta subunit of the insulin receptor. Finally, whilst all these processes can individually contribute to insulin resistance, they often present in tandem with one another, complicating the pathophysiology of the disorder. Current treatment goals include symptom reduction, which in turn

---

---

lowers the risk of macrovascular disease complications and mortality. Clinical indicators of progress include stable plasma glucose and HbA1C concentrations. The understanding of various pathophysiological processes at play provides insights into the potential pharmacological targets for treatment. For example, failure to produce insulin endogenously may be treated with exogenous insulin supplementation [72].

#### **1.4.1. Diabetes Mellitus Epidemiology**

T2DM accounts for over 90% of cases, while Type 1 diabetes and gestational diabetes contribute to the remaining incidences [73]. This disease is a global public health issue with a significant impact on morbidity, mortality, and healthcare costs. The global prevalence of diabetes has surged in recent decades, largely due to population growth, ageing, urbanisation, and lifestyle changes. According to the International Diabetes Federation (IDF), an estimated 537 million adults aged 20–79 years have been living with diabetes (type 1 or type 2) from as early as 2021. This estimate is projected to reach 643 million by 2030 and 783 million by 2045. Prevalence is also a function of geography, where regions which adopt sedentary lifestyles correlated with obesity have a significantly higher incidence of diabetes. The highest rates are observed in the Middle East, North Africa, and Southeast Asia, where urbanisation and lifestyle shifts have escalated risk factors, allowing for less labour-intensive work and more consumption of fatty and high glycaemic foods. Low- and middle-income countries bear the brunt of the diabetes epidemic, with over 75% of people with diabetes living in these regions [74]. In contrast, high-income countries often have better access to healthcare and early detection programs, reducing the burden of complications.

Risk factors for diabetes can be categorised into modifiable and non-modifiable, the central differentiator being the capacity to prevent and control the pre-existing condition. Modifiable risk factors for diabetes include obesity, physical inactivity through living a sedentary lifestyle, unhealthy diets, and smoking. Non-modifiable factors such as genetics, ethnicity, and family history also play critical roles. Indigenous populations, South Asians, and African descendants have a higher genetic predisposition to diabetes. Genetic susceptibility arises from the expression of particular gene variants that code for insulinotropic peptides and intermediates. Variants in genes that code for peroxisome proliferator-activated gamma (PPAR) and insulin receptor substrate 1 (IRS1) influence the body's response to insulin, increasing insulin resistance in tissues like muscle and liver. Finally, the TCF7L2, KCNJ11, and HHEX genes are linked to reduced pancreatic beta-cell function and lower insulin production [75]. Diabetes prevalence increases with age, with the highest rates observed in individuals

---

---

over 65 years. However, T2DM is increasingly being diagnosed in younger populations due to rising obesity rates and sedentary behaviours. Although men and women are affected relatively equally, men may have a slightly higher prevalence of undiagnosed diabetes [76].

#### **1.4.2. Type 2 Diabetes Mellitus Pathophysiology**

Initially, pancreatic  $\beta$ -cells compensate for the excess glucose circulating in the blood and the declining efficacy of insulin by secreting additional amounts of insulin over an extended duration, resulting in hyperinsulinemia. However, prolonged insulin resistance, hyperglycaemia, and increased lipid circulation ultimately lead to  $\beta$ -cell exhaustion and a decline in insulin secretion. Furthermore, impaired incretin hormone function, particularly reduced glucagon-like peptide 1 (GLP-1) activity, disrupts glucose homeostasis. Inadequate insulin signalling in peripheral tissues such as skeletal muscles and fat impairs glucose uptake, resulting in greater circulating glucose concentrations. Chronic high blood glucose concentrations then damage blood vessels, nerves, and organs over time. Inflammatory processes also play a role, as adipose tissue secretes pro-inflammatory cytokines that exacerbate insulin resistance [77]. Additionally, changes in gut microbiota and increased concentrations of fatty acids may further disrupt insulin sensitivity [78].

The accumulation of free fatty acids, VLDL, LDL, and a consistent intake of high-glucose foods places a strain on the body's ability to maintain homeostatic glucose concentrations [79]. Excess lipids and free fatty acids, for example, lead to an increased generation of reactive oxygen species, which are markers responsible for cellular apoptosis (programmed cell death) [80]. Elevated triglycerides contribute to inflammation, a process involving the release of leukocytes, macrophages, and other immune cells. This inflammatory state also results in the overproduction of reactive oxygen species, which outpace pre-existing antioxidant mechanisms that would otherwise safeguard insulin signalling [81]. Furthermore, oxidative stress inhibits the mobilisation of calcium ions from the endoplasmic reticulum, promotes the presence of pro-apoptotic signals, and increases proinsulin mRNA degradation, all of which hinder downstream effects that prevent insulin release [82]. Ultimately, these effects lay the groundwork for the complications of T2DM.

While more common in type 1 diabetes, diabetic ketoacidosis DKA can occur in T2DM during severe insulin deficiency or metabolic stress (e.g., infection, trauma). Insulin deficiency leads to uncontrolled lipolysis, releasing free fatty acids that are metabolised into ketone bodies ( $\beta$ -hydroxybutyrate, acetoacetate). The accumulation of ketones overwhelms the body's buffering capacity, causing

---

metabolic acidosis, severe dehydration, and electrolyte imbalances. Without prompt treatment, DKA progresses to coma, multi-organ failure, and death [188].

Regarding the kidneys, chronic hyperglycaemia damages glomerular hyperfiltration, AGE deposition, and promotes renal inflammation. These changes thicken the glomerular basement membrane, promote mesangial expansion, and eventually lead to glomerulosclerosis. Proteinuria develops as the filtration barrier deteriorates, followed by a progressive decline in glomerular filtration rate (GFR) [189]. End-stage renal disease (ESRD) likely ensues, necessitating dialysis or kidney transplantation for survival. Diabetic retinopathy (DR) is an additional progressive microvascular complication of diabetes mellitus, characterised by retinal damage resulting from chronic hyperglycaemia-induced endothelial dysfunction. The pathogenesis is driven by three interrelated mechanisms: vascular endothelial growth factor (VEGF) overexpression, pericyte loss, and capillary occlusion, which collectively contribute to microvascular dysfunction [190]. Persistent hyperglycaemia promotes oxidative stress and the accumulation of advanced glycation end-products (AGEs), leading to pericyte apoptosis and subsequent destabilisation of retinal capillaries. This loss of pericytes, coupled with basement membrane thickening and endothelial cell injury, results in increased vascular permeability and the formation of microaneurysms [190]. The subsequent retinopathy results in irreversible vision loss and blindness, all of which is downstream from persistent hyperglycaemia.

Finally, another common complication of T2DM is Peripheral arterial disease (PAD) and neuropathy, both of which impair blood flow and sensation in the extremities. Minor injuries go unnoticed due to sensory loss, while poor perfusion delays healing, promoting infection and tissue necrosis. Dry gangrene (coagulative necrosis) or wet gangrene (bacterial infection with liquefactive necrosis) may develop. Without intervention, gangrene leads to systemic sepsis and necessitates limb amputation to prevent fatal complications [191].

Untreated T2DM results in severe complications through chronic hyperglycaemia, oxidative stress, and microvascular/macrovascular damage. Each complication follows a progressive course, culminating in organ failure, disability, or death. Early glycaemic control, regular screening, and multidisciplinary management are essential to mitigate these devastating outcomes.

---

### 1.4.3. Diabetes Mellitus and Infection

Diabetes Mellitus and infection are co-reinforcing, where patients with infections are more likely to experience glucose homeostatic disruptions and where diabetic patients are at greater risk of infection. Inflammation and stress may undergird this connection, given that both underlying conditions predispose patients to the cardinal symptoms of each illness. Interleukin-6 (IL-6) is a pro-inflammatory cytokine that plays a critical role in immune regulation and inflammation. IL-6 is linked to diabetes, as elevated levels contribute to insulin resistance and chronic low-grade inflammation, which are hallmarks of T2DM [184]. Dysregulated IL-6 expression is a key biomarker for inflammation and disease progression. Additionally, prolonged hyperglycaemia impairs the function of white blood cells, which are responsible for fighting infections, resulting in a weakened immune system that predisposes people to higher chances of developing more severe disease symptoms and signs upon infection [83]. Additionally, poor circulation, particularly in the extremities such as hands and feet due to diabetic complications, can slow down and, in some instances, obstruct the flow of immune cells to the sites of infection, disrupting diapedesis and chemotactic function during inflammation [84]. Impaired migration of immune cells to the site of infection poses a greater risk of microbial organisms replicating and spreading to a greater extent and duration. Wounds, therefore, receive less circulation and healing is slowed. Hyperglycaemia produces an external environment conducive to microbial growth. Glucose provides nutrition to bacteria and fungi, allowing for greater growth; *Escherichia coli*, *Staphylococcus saprophyticus* and *Candida* species prefer glucose as an energy source. Diabetes patients may also experience higher concentrations of glucose in bodily fluids like urine, which provides a rich nutrient source for microorganisms. This explains why diabetic patients are estimated to have a 1.5-to-4-fold increase in the chances of developing severe infection [85]. Diabetic patients, therefore, are at heightened risk of developing urinary tract infections (UTIs) and skin and foot infections.

Infections and their corresponding symptoms and treatments, conversely, can predispose patients to diabetes. Infections predispose patients to diabetes by triggering immune responses, which can lead to systemic inflammation, impairing pancreatic function. Patients with predisposing factors like obesity, genetics, or prediabetes are more vulnerable to these effects. Infection can also contribute to insulin resistance. Acute infections often activate the stress response, leading to elevated cortisol, adrenaline, and glucagon concentrations, all of which lead to increased glucose concentrations [86]. Prediabetic, obese and genetically susceptible individuals are at greater risk of experiencing a compounded effect, consequently, thus hastening the onset of chronic hyperglycaemia. Infections such as HIV, hepatitis,

---

---

and COVID-19 can directly or indirectly damage pancreatic beta cells and alter their function, resulting in impaired insulin production. Finally, the treatments for infections themselves can inadvertently interfere with glucose homeostasis, resulting in hyperglycaemia [185]. Corticosteroids and protease inhibitors, for example, can trigger hyperglycaemia and suppress the immune system, making the body more susceptible to infections, including bacterial, viral, and fungal infections [87].

Therefore, antimicrobial regimens that promote glucose homeostasis may pose a useful dual effect, i.e. treating both infection and dysglycaemia and preventing complications consequently. Additionally, antimicrobial agents with effects on glucose metabolism require additional research into the precise mechanisms by which glucose homeostasis is altered. This may empower researchers with knowledge on how these drugs can be repurposed so that their current adverse effects can be co-opted and purposefully directed into disease treatment.

### **1.5. Cellular Targets for achieving glycaemic control**

Target tissues of interest are skeletal and hepatic tissue. The morphology of these cells contributes significantly to their capacity to conduct effective glucose utilisation. The presence of glucose-sensitive channel proteins, glycolytic enzymes, and insulin-responsive genes accounts for the glucose metabolic properties of these cells [88].

Furthermore, this capacity is modulated by intracellular insulin signalling, a process by which various biochemical pathways are triggered to increase the storage and decrease the production of glucose. Glucose uptake is the process of glucose entering target cells from the extracellular space into the cytoplasm through glucose transporters [89]. Moreover, these cells differ in their physiology and therefore utilise glucose to perform different functions. Skeletal muscle cells, for example, are contractile and therefore require energy from ATP (a resultant product of glucose catabolism) to perform muscle contractions. Additionally, cell nutrition and growth are dependent on the dietary consumption of glucose-containing foods. In this study, skeletal Muscle Cells (C2C12) were selected for experimental purposes. Skeletal cells undergo myogenesis, a process by which immature or embryonic skeletal cells change their nucleation and morphology to yield contractile muscle cells. These embryonic cells, i.e. murine myoblasts, are initially mesenchymal mononucleated cells with a fusiform morphology. Upon experimentation, controlled nutrient depletion of myoblasts can trigger morphological change. The primary nutrient for C2C12 cells is foetal bovine serum (FBS), typically in 10% concentration dissolved in Dulbecco's medium essential media [92]. HepG-2 cells are *in vitro*

---

---

alternatives to human functional hepatocytes. They possess a similar morphology to epithelial cells and can thus serve as a proxy for determining the cytoprotective, anti-insulin-resistant, and antioxidant properties of compounds that would otherwise be administered to human cells [90]. They differ, however, in the expression of cytochrome P450 enzymes and xenobiotic receptors that may be present in human liver cells and therefore may not yield similar pharmacodynamic profiles in drug-receptor interactions and drug-drug interactions. Nevertheless, these cells are promising for their replication and storage capacity for persistent experimentation [91]. HepG-2 was also selected in this study to investigate the effect of fluoroquinolones on glucose metabolism, these cells are also cultured under similar conditions to those of C2C12 culturing.

### **1.6. Conventional treatments and associated pharmacological targets**

Conventional antidiabetic regimens prevent diabetes complications by stabilising serum glucose concentrations. The standard mechanisms by which this is achieved are through enhancing sensitivity to insulin, uptake of glucose into target organs, prevention of digestion of polysaccharides, hepatic gluconeogenesis, and promotion of insulin secretion [93]. In the instances where patients are responsive to insulin but fail to secrete sufficient amounts endogenously, the administration of exogenous insulin subcutaneously is the common treatment regimen. Insulin regimens differ in their duration of action and potency to treat postprandial glucose surges, and for maintaining long-term plasma glucose concentrations. Glargine and detemir insulin, for example, are long-acting insulins, which sustain baseline concentrations of glucose in the blood [94]. Aspart and Lispro insulin, on the other hand, are the short-acting insulins that treat postprandial hyperglycaemia. For T2DM, the conventionally prescribed first-line oral anti-diabetic treatment is metformin, a biguanide which activates adenosine 5' monophosphate-activated protein kinase (AMPK) in the liver, and promotes glucose uptake, prevents gluconeogenesis and glycogenolysis [95]. Moreover, metformin improves insulin sensitivity in the liver and peripheral tissues by enhancing tyrosine kinase activity. Lastly, metformin lowers triglyceride and LDL-C concentrations, which prevents lipid-induced diabetic complications [96]. These various qualities of the drug explain why it is often recommended as the treatment of choice for T2DM. Patient reports indicate that they prefer the treatment because of its effectiveness, affordability, and tolerable side effects. Metformin reduces HbA1c concentrations by 1.5–2% and can be used alone or combined with other therapies for uncontrolled diabetes [97]. Its ability to promote weight loss makes it particularly beneficial for obese diabetic patients.

---

Therapeutic targets are microscopic sites in the body where treatments act to alleviate or control disease. They tend to be receptors, enzymes, and glucose transporters that modulate plasma glucose concentrations. The basic principle is that a drug will bind to a receptor, activating or inactivating a cascade of events modulating glucose homeostasis. Additionally, drugs can interfere with the processes of glucose uptake or absorption from the gastrointestinal tract into the systemic circulation, thereby preventing surges in glucose concentrations. Therefore, a broad area of interest is the discovery of new targets on which novel drug candidates may exert therapeutic effects. Below, we will describe conventional glycaemic pharmacological targets.

### **1.6.1. DPP-4**

The Dipeptidyl peptidase-4 (DPP-4) enzyme is responsible for inactivating endogenous insulinotropic peptides. Glucagon-like peptide (GLP-1) and glucose-dependent insulinotropic polypeptide GIP are incretins which stimulate insulin secretion upon detecting elevated blood glucose concentrations. DPP-4 inhibition prolongs the residence time of these hormones, allowing for pronounced and extended glucose-dependent insulin secretion and prevention of hyperglycaemia [98]. Sitagliptin, Saxagliptin and vildagliptin are blockers of DPP-4. Once DPP-4 is blocked, incretins inhibit glucagon release, extend the action of insulin, and promote additional insulin release. DPP-4 inhibitors, therefore, are often prescribed as monotherapy or in combination with metformin, insulin secretagogues or thiazolidinediones [99]. The adverse effects of these treatments include nausea, vomiting, upper respiratory tract infections and cardiac failure. DPP-4 inhibitors share structural motifs like amino acid-like cores, heterocyclic rings, and hydrophobic groups, enabling effective enzyme binding. They differ in specific functional groups (e.g., a cyano group in Vildagliptin and a trifluorophenyl in Sitagliptin) and pharmacokinetics. While all enhance incretin activity, structure variations influence potency, duration, and metabolic pathways, tailoring them for diverse patient needs.

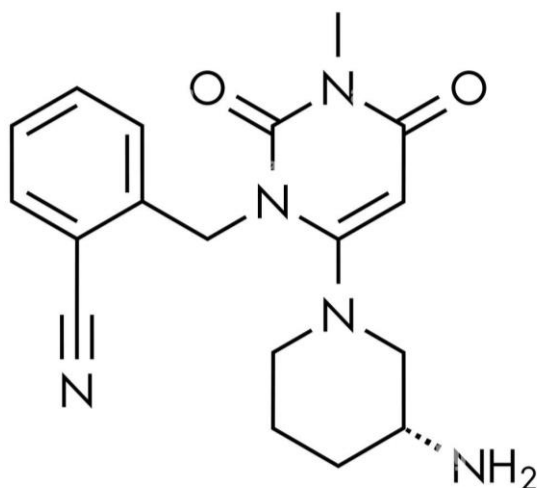


**Figure 1.4:** Chemical Structure of DPP-4 Inhibitor Alogliptin

### 1.6.2. Phosphoinositide-3-Kinase (PI3K)

Phosphoinositide 3-kinase (PI3K) plays a central role in insulin signalling. The activated pathways downstream of PI3K stimulation are crucial for serum glucose reduction. Insulin first binds to its receptor, activating tyrosine kinase. The conformational changes of this kinase facilitate autophosphorylation and recruitment of insulin receptor substrates (IRS) [100]. These phosphorylated IRS proteins serve as docking sites for the regulatory subunit of PI3K, which goes on to activate PI3K. Activated PI3K initiates a series of phosphorylation reactions and activation of kinases, including AKT (protein kinase B) and phosphoinositide-dependent kinase-1 (PDK1). AKT activation is a pivotal step in insulin signalling. Downstream effects of AKT activation include regulating glucose transporter translocation to the plasma membrane and enhancing glucose uptake in insulin-responsive tissues like muscle and adipose [101]. Finally, PI3K signalling also influences glycogen synthesis, lipogenesis, and cell growth by modulating pathways like mTOR and GSK-3 $\beta$ . Dysregulation of PI3K activity is associated with insulin resistance, a hallmark of metabolic disorders such as T2DM. Thus, PI3K serves as a critical node in insulin-mediated metabolic homeostasis. Drugs that bind to PI3K interfere with insulin signalling, leading to a decline in glucose control. High concentrations of glucose, therefore, persist, triggering the further secretion of insulin to combat the subsequent rise. PI3K, therefore, is instrumental for assessing if novel compounds utilise the insulin signalling pathway. In other words, if a compound can influence insulin signalling in the presence of a PI3K inhibitor such as Wortmannin,

---

it can indicate that the compound is utilising an alternative signalling pathway to bring about an increase or decrease in insulin release [102].

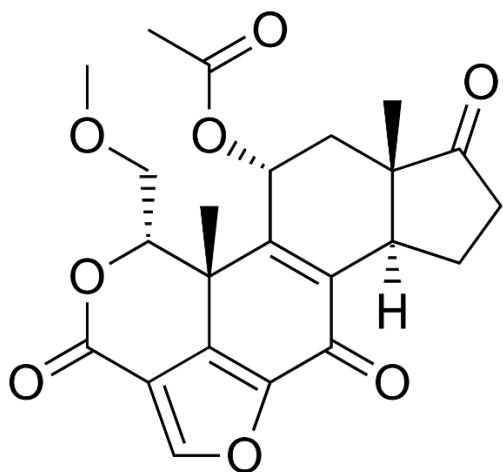


**Figure 1.5:** Chemical Structure of PI3K inhibitor, Wortmannin

### 1.6.3. ATP-sensitive potassium channels

ATP-sensitive potassium channels represent the collection of transmembrane proteins responsible for the efflux of potassium ions against a concentration gradient. These channels are composed of Kir6.2 (inward-rectifier potassium channel) and SUR1 (Sulphonylureas receptor 1) subunits. The change in ATP/ADP ratio – a subsequent result of ATP production from glycolysis – is the initial step that catalyses the closure of these transport proteins, typically in pancreatic beta cells. Once stimulated, the subsequent depolarisation caused by K-ATP channels causes a change in the electrochemical gradient within the cell, leading to the activation of voltage-gated calcium channels, leading to a calcium ion influx [103]. The cytosolic concentration of calcium ions therefore increases, importantly promoting the exocytosis of insulin-containing vesicles, thereby releasing insulin into the bloodstream. This migration of insulin is a function of the extent and duration of the external stimuli, i.e. the postprandial glucose surge [104]. The subsequent insulin secretion leads to greater binding of insulin to its respective receptors, initiating signal transduction, transmission and ultimately the initiation of metabolic processes, all of which contribute to lowering serum concentrations of glucose to a homeostatic baseline, i.e. 3.5-5.2 mmol/L. Beta cells are located within a general cluster of pancreatic cells known as the islets of Langerhans. Drugs targeting potassium channels include sulphonylureas (e.g., glibenclamide) and meglitinides (e.g., repaglinide), which close potassium channels in beta cells,

---

promoting insulin release for T2DM patients. Conversely, diazoxide opens potassium channels, inhibiting insulin secretion, and can be used for hyperinsulinism. These drugs modulate insulin release by directly influencing beta cell membrane potential.

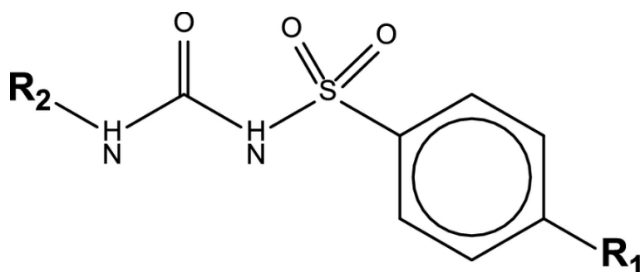


**Figure 1.6:** General chemical structure of Sulphonylureas

#### 1.6.4. A-Glucosidase and Pancreatic Amylase

A-glucosidase is an enzyme responsible for the enzymatic breakdown of complex polymer sugars (disaccharides) to simpler monomeric units (glucose), facilitating their absorption into the systemic circulation. The enzyme is located on columnar epithelial membranes on the brush border of the small intestine. The enzyme catalyses the breakdown of alpha-1,4-glycosidic bonds to release glucose. Its catalytic domain features a ( $\beta/\alpha$ )<sub>8</sub>-barrel structure which houses the active site with key residues like aspartic and glutamic acid for hydrolysis. Additional domains, such as beta-sandwich structure – a protein structure made up of two antiparallel beta sheets – aid in substrate recognition. The enzyme often forms dimers or tetramers stabilised by non-covalent interactions and may undergo N-linked glycosylation for stability. Its structure is critical for understanding its mechanism and designing inhibitors, particularly for diabetes management, where inhibitors slow carbohydrate digestion to control blood glucose levels. A-glucosidase inhibition delays intestinal absorption of monosaccharides in the lumen, hence preventing a postprandial glucose surge. Acarbose and miglitol are carbohydrate analogues that inhibit the enzyme and are primarily indicated for Diabetes Mellitus type 2, which is not well controlled by first-line anti-diabetic agents [105].

Pancreatic amylase catalyses the cleaving of a-D-1,4 glycosidic linkages in starch, glycogen and various oligosaccharides, releasing  $\alpha$ -anomers such as  $\alpha$ -D-glucopyranose and  $\alpha$ -D-fructofuranose. The enzyme is important in carbohydrate metabolism for breaking down alpha-1,4-glycosidic bonds in starch and glycogen. It typically adopts a ( $\beta/\alpha$ )<sub>8</sub>-barrel fold (TIM barrel) in its catalytic domain, with conserved aspartic and glutamic acid residues in the active site for hydrolysis. The enzyme often

---

functions as a single polypeptide chain but may form oligomers in some organisms. Its structure enables substrate specificity and efficient catalysis, making it a target for industrial and therapeutic applications, such as diabetes management. Moreover, pancreatic amylase ( $\alpha$ -amylase) is also inhibited by treatments that inhibit  $\alpha$ -glucosidase. Pancreatic amylase inhibition, therefore, prevents

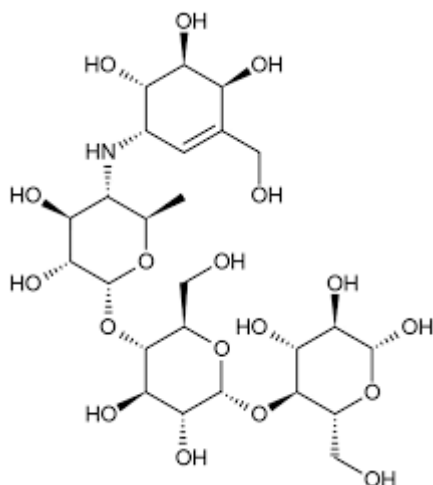


**Figure 1.7:** Chemical Structure of Acarbose

the formation of monosaccharides such as glucose, thereby decreasing postprandial glucose concentrations. Alpha-glucosidase inhibitors such as acarbose and Miglitol also block alpha-amylase. The drugs are metabolised by intestinal bacteria and are notorious for their gastrointestinal disturbances, including flatulence, stomach cramps and diarrhoea [107].

### 1.6.5. Peroxisome Proliferator-activated Receptor Gamma

Insulin-responsive genes are responsible for proteins and kinases that sensitise target cells to insulin and control adipogenesis. Peroxisome proliferator-activated receptor gamma, a type of nuclear receptor, regulates the translation of these genes [108]. Once acted on, this receptor initiates a cascade of events which go on to sensitise tissues to insulin, promoting glucose uptake into hepatic, skeletal and adipose tissue. Furthermore, receptor activation also leads to decreases in fasting and postprandial glucose concentrations and prevents hepatic gluconeogenesis. Thiazolidinediones are a class of insulin sensitisers which primarily function as agonists on PPAR $\gamma$  receptors [109]. Pioglitazone, for example, is indicated for type 2 diabetes as monotherapy or in combination with metformin or insulin secretagogues. The adverse effects of this treatment include, but are not limited to, oedema, cardiac failure, angina, and weight gain. These side effects often discourage the consistent use of these therapies, rendering treatment outcomes unsuccessful for diabetic patients [110]. Conventional

---

therapies, therefore, may not always be suitable for patients who exhibit adverse events. Moreover, patients chronically administering anti-diabetic treatments may experience tolerance as time goes by, rendering the treatment ineffective. Long-term use of pioglitazone, for example, has been associated with increased cancer risk, and patients failing first- or second-line therapy often have to adopt dual or polypharmaceutical regimens, placing them at higher risk for developing severe side effects. Substitutions from classic anti-diabetic regimens may therefore be necessary for these patients. The most basic structure of thiazolidinediones consists of a five-membered heterocyclic ring containing three carbon atoms, nitrogen and sulphur, known as a thiazolidine ring, with a 2,4-dione substitution. Here's a breakdown of the structure. 2,4-Dione Substitution refers to the presence of two ketone (C=O) groups at the 2nd and 4th positions of the thiazolidine ring.

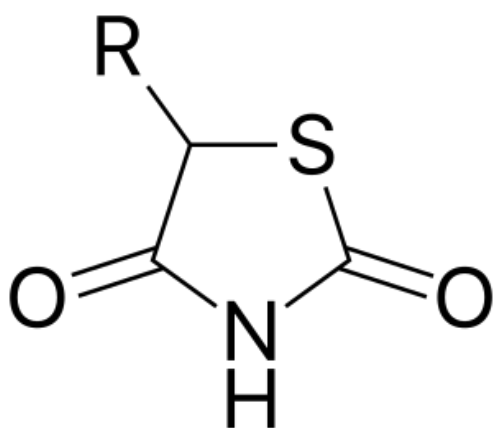


**Figure 1.8:** The general structure of thiazolidinediones

### 1.7. Fluoroquinolones and Dysglycaemia

Fluoroquinolones are synthetic fluorinated analogues of nalidixic acid; more specifically, an N-alkylated-3-carboxypyrid-4-one ring fused with another aromatic ring. There are more than 20 quinolones used clinically, with most varying in their pharmacokinetic profile and their binding affinity to targets [111]. Quinolone and fluoroquinolones work by passively diffusing into a cell and interfering with the synthesis of bacterial DNA by inhibiting DNA gyrase and topoisomerase IV. Inhibition of topoisomerase IV results in disrupting the separation of duplicate chromosomal DNA into daughter cells during mitosis. The binding onto DNA gyrase inhibits the relaxation of positively supercoiled DNA, a step needed for transcription and replication [112]. These drugs, upon administration of the appropriate dose, exhibit bactericidal effects. They are broad-spectrum and typically kill Gram-

positive and Gram-negative bacteria. These antimicrobials are stratified according to generations, with each varying concerning its structural modifications and the bacteria covered. The structural modifications influence the potency, selectivity and pharmacokinetic profile of the drug, all of which can expand its spectrum of activity and its bactericidal effects against known bacteria. These modifications include the addition of substituents on the pyridine nitrogen on positions 1, the 6th, 7th and 8th carbon, and changes to the absolute configuration of substituents on chiral carbons [113]. Fluoroquinolones treat various bacterial infections, including upper and lower respiratory infections, and some skin, bone, soft tissue infections, urinary tract infections, as well as community-acquired pneumonia. The Diagram below shows the basic quinolone backbone and the various sites on which bonding can occur. The diagram below shows the basic fluoroquinolone backbone and its corresponding sites for potential derivatisation.

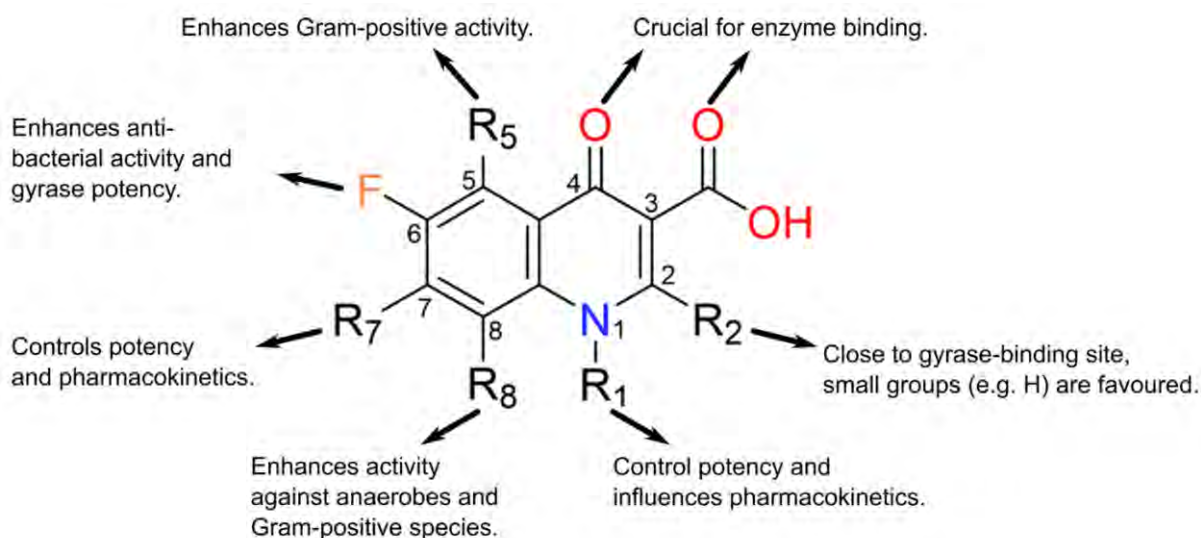


**Figure 1.9:** Pharmacophoric sites for fluoroquinolones. The key candidate sites potentially responsible for glycaemic effects are on carbons 1, 3, 4, and 7. [114]

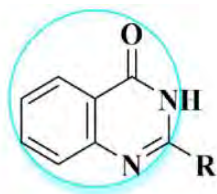
Beyond their traditional use, these antimicrobials have exhibited effects on blood glucose concentrations. Gatifloxacin and moxifloxacin, for example, have been linked to hypoglycaemia due to their hypothesised effect on ATP-dependent potassium channels in beta cells [186]. This is analogous to the triggering pathway of GSIS, with the depolarisation inside the cell causing an influx of calcium ions, which trigger exocytosis of insulin from granules located inside vesicles. The Kir6.2 subunit of the potassium channel is theorised to be the precise source from which potassium channel

---

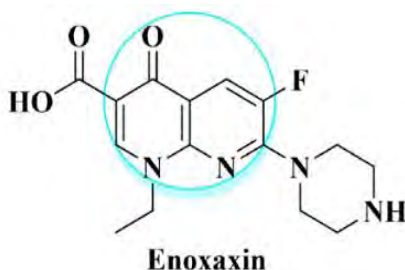
closure is initiated [115]. These ATP-sensitive channels sense acute metabolic stress such as hyperglycaemia and hypoglycaemia, assisting in homeostatic regulation of glucose. Clinical and laboratory studies have reported that fluoroquinolones affect glucose homeostasis [116]. The extent to which disturbance in glucose homeostasis depends upon the fluoroquinolone of choice. Moreover, these compounds are linked to hyperglycaemia and hypoglycaemia through mechanisms that are still incompletely researched.

A hypothesised mechanism for how fluoroquinolones cause hypoglycaemia is the induction of insulin release, especially for gatifloxacin, which has a 3-to-4-fold probability of inducing hypoglycaemia over standard antimicrobial regimens such as macrolides and cephalosporins [117]. Hyperglycaemia, however, is hypothesised to be caused by dysregulated vacuolation of pancreatic beta cells, thereby impairing insulin release. Vacuolation is a process by which vacuoles (membrane-bound structures) within the cytoplasm of a cell are formed [118]. This morphological change in cells can be a sign of cell injury and can independently lead to cell death by disrupting key cellular processes, inducing organelle dysfunction, and activating stress and death pathways [119].

Additionally, molecular docking studies have shown the potential inhibitory effects of fluoroquinolones on  $\alpha$ -glucosidase [122]. This is theorised to be because of structural similarity in the pharmacophoric units of  $\alpha$ -glucosidase inhibitors and fluoroquinolones, i.e., a ketone in position 4 and a pyridine nitrogen. Moreover, fluoroquinolones may cause hypoglycaemia through the cytochrome P450 (CYP450) system [120]. This system underlies drug-drug interactions, more specifically in this context, interactions between fluoroquinolones and conventional anti-diabetic treatments. The CYP450 system is a complex collection of endogenous hepatic enzymes responsible for the metabolism of xenobiotics, typically through induction or inhibition. Fluoroquinolones inhibit CYP enzymes, thereby increasing plasma concentrations of concurrently administered anti-diabetic regimens, e.g. Sulphonylureas such as glibenclamide, and heightening the risk of hypoglycaemia [121]. Figure 1.10 circles around the structural similarity between a known inhibitor of  $\alpha$ -glucosidase and a fluoroquinolone



2-Arylquinazolin-4(3H)-ones <sup>[32]</sup>  
 $\alpha$ -Glucosidase Inhibitors



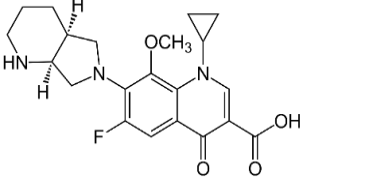
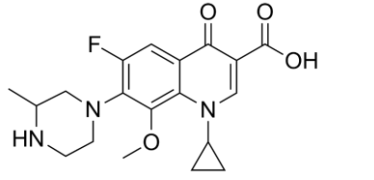
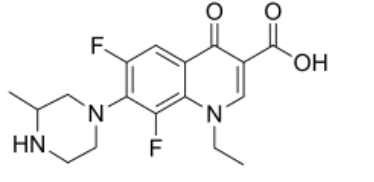
Enoxacin

**Figure 1.10:** Structural similarity between aryl-quinazolinones and fluoroquinolones. Circled regions show quinolone backbone, a ketone in position 4 and a pyridine nitrogen [122]

The current methods by which glycaemic aberrations are discovered are through observing side effects in patients being treated for bacterial infections. Case reports have shown that patients on fluoroquinolone regimens develop dysglycaemia. Tosufloxacin in Japan, for example, was found to correlate with hypoglycaemia even in non-diabetic patients [123]. Moxifloxacin, temafloxacin, gatifloxacin and levofloxacin have been associated with glycaemic aberrations; these are higher-generation fluoroquinolones implicated with hypoglycaemia from strongest to weakest. Their strength is related to the relative affinity the drug has to islet beta cells. Higher affinity allows for more saturation in beta cells [124]. The substituents on the fluoroquinolone structure can be correlated to hypoglycaemic effects. What has yet to be demonstrated is any causal connection between the specific generation of fluoroquinolone and the type of dysglycaemia event. Table 1.1. shows the type of fluoroquinolone selected for experimentation and their respective moieties of interest.

**Table 1.1:** Illustrates the varying types of fluoroquinolones, and their respective substituents that may potentially contribute to hypoglycaemia.

Fluoroquinolone	Moieties of interest	Structure
Ciprofloxacin	Cyclopropyl ring on N1 Piperazine ring on position 7	

Moxifloxacin	Methyl-ether on carbon 8. Heterocyclic indole ring on carbon 7	 <p>The structure of Moxifloxacin features a central quinolone core. It has a methyl ether group (-OCH<sub>3</sub>) at position 8, a fluorine atom at position 6, and a cyclopropylmethyl group at position 7. The piperazine ring is attached to the quinolone core at position 7.</p>
Gatifloxacin	Methyl Ether on carbon 8. 3-methyl on piperazine ring	 <p>The structure of Gatifloxacin features a central quinolone core. It has a methyl ether group (-OCH<sub>3</sub>) at position 8, a fluorine atom at position 6, and a cyclopropylmethyl group at position 7. The piperazine ring is attached to the quinolone core at position 7, with a methyl group on the nitrogen at position 3.</p>
Lomefloxacin	Methyl on N5 on piperazine ring. Ethyl Group on N1	 <p>The structure of Lomefloxacin features a central quinolone core. It has a fluorine atom at position 6, a cyclopropylmethyl group at position 7, and an ethyl group on the nitrogen at position 1 of the piperazine ring. The piperazine ring is attached to the quinolone core at position 7.</p>

---

## 1.8. Justification for the study

Fluoroquinolones may present a promising opportunity to expand on diabetic treatment regimens. They are relatively cheap to produce altogether. Another notable feature of fluoroquinolones is their favourable pharmacokinetics. They are well absorbed orally, allowing for convenient dosing, and achieve high tissue penetration, ensuring effective treatment of systemic infections. They possess excellent tissue penetrative properties with 60 to 90% bioavailability and moderate to long elimination half-lives [125]. The availability of both oral and intravenous formulations enables a seamless transition between inpatient and outpatient care. The practical application of this research is expansive. Here are several potential uses: Firstly, in instances where we discover a detrimental effect of the antibiotics on glycaemic control targets, we can enrich our knowledge on contraindications for diabetic patients, improving the practice of pharmacists and health practitioners. Fluoroquinolones could have their mechanisms of action behind their glycaemic effects elucidated. Patients on Sulphonylureas can be advised against concurrently taking moxifloxacin due to the potentially additive hypoglycaemic effects on ATP-dependent potassium channels. Secondly, in instances where we discover an antidiabetic effect of the fluoroquinolones, we can assess if the effect is significant enough to justify repurposing it, possibly through chemical structural modifications. Thirdly, it can be investigated for dual mechanisms of action for diabetic patients with bacterial infections, treating both illnesses simultaneously and eliminating the need for polypharmacy for chronic illnesses.

### **Aim:**

This study aimed to investigate the glucose-controlling effects of fluoroquinolone against key glycaemic targets *in vitro*.

---

## 1.9.Objectives of the Study

### Cell-based Assays

- 1) Perform *in vitro* cytotoxicity assay to evaluate the impact of fluoroquinolones on cell viability in:
  - a) Skeletal muscle (C2C12) cell lines
  - b) Hepatic (HepG-2) cell lines
- 2) Investigate glucose utilisation to assess how fluoroquinolones may influence glucose metabolism in:
  - a) Skeletal muscle (C2C12) cell lines
  - b) Hepatic (HepG-2) cell lines
- 3) Investigate the effect of fluoroquinolones on glucose utilisation in the presence of PI3-K inhibitor (Wortmannin) in:
  - a) Skeletal muscle (C2C12) cell lines
  - b) Hepatic (HepG-2) cell lines
- 4) Investigate the effect of fluoroquinolones on the expression of the key proteins, AKT and GLUT-4 that are involved in glucose metabolism and insulin signalling:
  - a) Skeletal muscle (C2C12) cell lines
  - b) Hepatic (HepG-2) cell lines
- 5) Investigate the effect of the expression of inflammatory cytokine IL-6 in:
  - a) Skeletal muscle (C2C12) cell lines
  - b) Hepatic (HepG-2) cell lines

### Non-cell-based Assays

- 6) *In vitro* screening of novel fluoroquinolones to determine their antidiabetic activity on the following enzymes:
    - a)  $\alpha$ -amylase.
    - b)  $\alpha$ -glucosidase.
  - 7) *In silico* studies to predict the interaction of selected fluoroquinolones against glycaemic targets' potential interactions on:
    - a) Phosphoinositide 3-kinase
    - b) Insulin Receptor
-

---

c)  $\alpha$ -Glucosidase

d)  $\alpha$ -Amylase

---

## Chapter 2: Materials and Methodology

### 2.1. Materials and Equipment

$\alpha$ -Amylase,  $\alpha$ -glucosidase, distilled or deionized water, Paraformaldehyde, Phosphate Buffered Saline (PBS), Disodium hydrogen phosphate ( $\text{Na}_2\text{HPO}_4$ ), acarbose, *p*-nitrophenyl phosphate (PNP), Sodium carbonate ( $\text{Na}_2\text{CO}_3$ ), hydrochloric acid (HCl), dimethyl sulfoxide (DMSO), methanol ( $\text{CH}_3\text{OH}$ ), Starch, Dimethyl Sulfoxide (DMSO), Ciprofloxacin, Moxifloxacin, Lomefloxacin, Gatifloxacin, Potassium dihydrogen phosphate ( $\text{KH}_2\text{PO}_4$ ), sodium chloride (NaCl), potassium chloride (KCl), sodium hydroxide (NaOH) Triton X-100, Tween-20 skim milk were purchased from Sigma-Aldrich Chemical Corporation (Johannesburg, South Africa). Dulbecco's modified Eagle's medium (DMEM), minimum essential medium eagle (MEM), foetal bovine serum (FBS), and Ciprofloxacin were purchased from Sigma-Aldrich (Johannesburg, South Africa). C2C12 and HepG-2 cell lines were sourced from Dr Ngcobo at the University of KwaZulu-Natal (Durban, South Africa). All other chemicals and reagents were of analytical grade.

UV-VIS Spectrophotometer (UVmini-1240)(AC 220 – 240~ 50/60Hz 160VA; SHIMADZU CORPORATION, made in China), CO<sub>2</sub> Incubator (FSOH4)(220/240V 50Hz, 0.5kW; Labcon (pty) ltd 15 Achtenberg street Chamdor Krugersdorp Transvaal), Spectramax M3 multi-mode microplate reader (100 – 240V~3.5A 50 – 60Hz; manufactured in China, designed in California, USA), BV1000 vortex mixer (230VAC 50Hz, 0.75amps; Benchmark Scientific Inc. PO BOX 709, Edison, NJ 08818, USA; made in Taiwan), Accu-Check Performa glucometer and contour plus test stripes, inverted microscope BS-2092,200-240V 50/60HZ,0.8A Lasec,(BIO38RAD)TC20; Automated cell counter(508BR09575, 30W, made in Singapore); Centrifuge,166145,1-14, Made in Germany(SIGMA); hotplate stirrer (H3760-HSE)(230V, 60Hz; (Lasec Laboratories) Benchmark Scientific Inc. PO BOX 709, Edison, NJ 08818, USA), and Labtech Ecobath model 207 40 Litre reciprocal shaking bath 230V~50Hz,1600W.2

## 2.1. Cell Culture

Cell culturing and sub-culturing involve preparing an aseptic environment and cell growth medium. This creates the correct cultural environment conducive to growth but sufficiently sterile to prevent contamination. To ensure sterility, proper hood regulations and autoclaving were followed. All media, supplements, and reagents were sterilised to prevent microbial growth. Cells were checked microscopically daily to ensure they were healthy and growing as expected. To culture the skeletal (C2C12) muscle and hepatocarcinoma (HepG-2) cell lines, their respective media (DMEM and MEM) were supplemented with 10% foetal bovine serum (FBS), (1%) L-glutamine, and 1% penicillin-streptomycin to ensure nutrition and sterility [131] The frozen cell lines were then transferred into cell culture flasks for growth and incubated at 37 °C until reaching confluency. The confluent cells were washed three times with pre-warmed phosphate buffer solution (PBS) before being trypsinised with 1 ml of trypsin (for detachment from the bottom of the flask) and serially diluted into new flasks for subculturing. The diagram below illustrates the mammalian cell culture protocol.

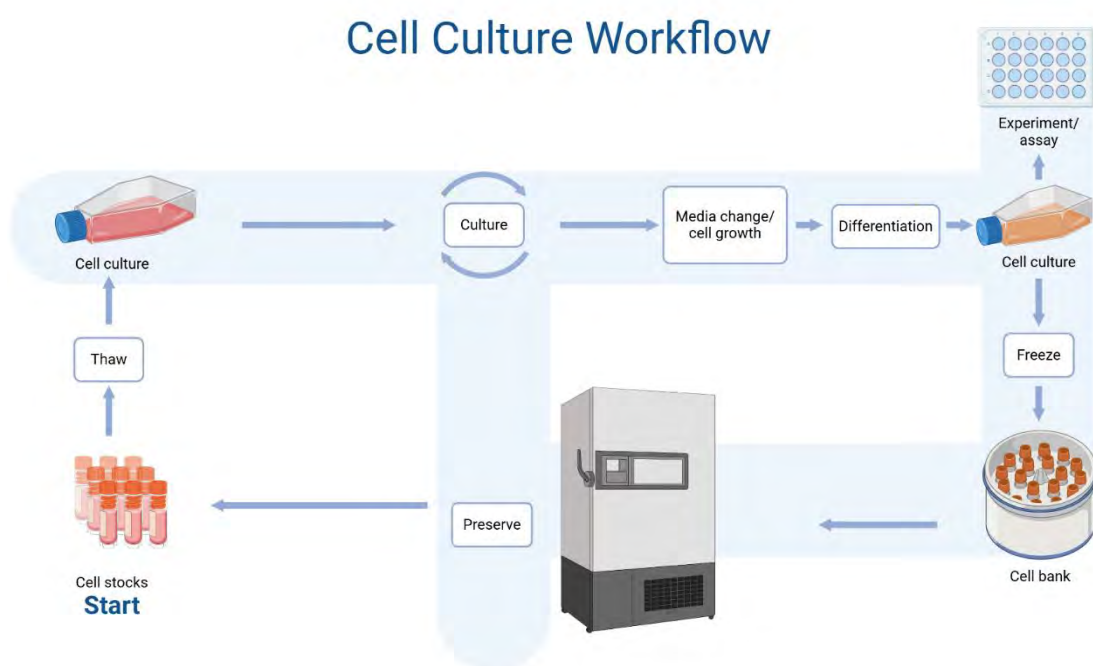


**Figure 2.1:** Cell Culture procedure. Sterilise workspace; warm media to 37°C. Thaw cells; Seed cells in media; incubate at 37°C, 5% CO<sub>2</sub>. Monitor growth; replace media every 2–3 days. Check for contamination; maintain sterility. Subculture at 70–90% confluency using trypsin. Reseed cells at the desired density. Store cells in the freezer. [132]

---

### 2.1.1. Skeletal Muscle Differentiation

Skeletal muscle differentiation in C2C12 cells, a murine myoblast cell line, is widely used to investigate how contractile cells respond to external stimuli, be it environmental stressors or chemical compounds. When cultured under high-serum conditions, namely the 10% FBS-supplemented DMEM, C2C12 cells proliferate as myoblasts. Upon serum withdrawal (switching to low-serum differentiation medium), i.e. from 10% to 2% of FBS, the nutrient shift signals cells to exit the proliferative phase and initiate the myogenic differentiation program, where they exit the cell cycle, align, and begin the differentiation process, eventually fusing to form multinucleated myotubes, mimicking skeletal muscle fibres [133].

Furthermore, nutrient deprivation triggers the activation of myogenic regulatory factors (MRFs) like MyoD and myogenin, which are drivers of myogenesis and modulate the gene expression of constitutive muscle proteins [134]. Differentiation was therefore achieved through switch cells from 10% to 2% FBS, and the media was replaced daily for 4 days. Differentiation was confirmed by visual inspection using a light optical microscope. Undifferentiated C2C12 cells are small, round, and mononucleated. Differentiated cells fuse to form multinucleated myotubes, which are elongated, tube-like structures.

---

### 2.1.2. Drug preparation for cell-based assay treatments

A stock solution of Lomefloxacin, Ciprofloxacin, Gatifloxacin and Moxifloxacin with a concentration of 1000 µg/ml was prepared by weighing out 0.01 g of each compound and dissolving it in 1 ml of dimethyl sulfoxide DMSO, and it was then made up to 10 ml with the required medium essential media (MEM). These stock solutions were diluted further to make the desired concentrations (10, 30, 50 and 75 µg/ml) using the  $C1V1 = C2V2$  formula. For each assay, the desired concentrations were freshly prepared using the relevant tissue culture media.

NovoLog<sup>®</sup> insulin (100 units per ml) was prepared as the positive controls for the media glucose utilisation assay. 1 unit of insulin is equal to 6 nmol. The target concentration for the control was 0.05 units/ml or 1.75µg/ml, therefore, 5µL of insulin was pipetted into 10 ml of medium essential media to yield the target concentration. The solution was mixed thoroughly using the Vortex mixer to ensure complete dissolution and uniformity. The solution was filtered using a 0.22 µm membrane filter to ensure sterility. The resultant solution was stored at 2°C to 8°C [136]. The treated cells were compared to insulin for their capacity to induce media glucose utilisation.

---

### 2.1.3. Glucometer Validation

For the glucose utilisation assays, we made use of the Accu-Chek Performa glucometer. The quality of the results for glucose uptake, therefore, is contingent upon the accuracy and precision of this device. To prevent significant confounds in the results, the use of a glucometer for media glucose reading was assessed and validated for quality control. Standards of known concentration were the independent variable, and their readings upon measurement with a glucometer were the dependent variable. The standard in this case was the media in which the cells were cultured. The volume, concentration, and amount of glucose in each container are known and detailed in the package description for MEM and DMEM, i.e., 1g/L of glucose. Five serial dilutions were performed to yield 5 data points representing the X values. Each solution stored in 10 ml plastic tubes was then tested for its glucose concentration using the glucometer. The resultant concentrations were the 5 data points representing the Y values. A regression plot was constructed to obtain the regression coefficient and to determine the linearity strength of the two variables, namely the concentrations of the standard and the measured values.

Table 2.1 and Figure 2.2 below show the resultant data from the method verification test. The regression coefficient was found to be 0.99. A regression coefficient close to 1 indicates a strong positive linear relationship between the known standard concentrations and values obtained from the glucometer. Formally, it means that a one-unit increase in the independent variable is associated with approximately a one-unit increase in the dependent variable, holding other variables constant. This implies a near-proportional relationship, suggesting the independent variable is a significant predictor of the dependent variable in the model. The Shapiro-Wilk test was used to assess whether the dataset followed a normal distribution. The P-value of 0.697 indicated no significant deviation from normality, meaning the data were consistent with a normal distribution. The standard error of 0.162 indicates significant precision concerning the values obtained for the theoretical and measured concentrations. This indicates that the glucometer readings are statistically consistent with theoretical glucose concentrations, supporting the use of the glucometer to estimate media glucose utilisation assays.

### Glucometer Validation Protocol

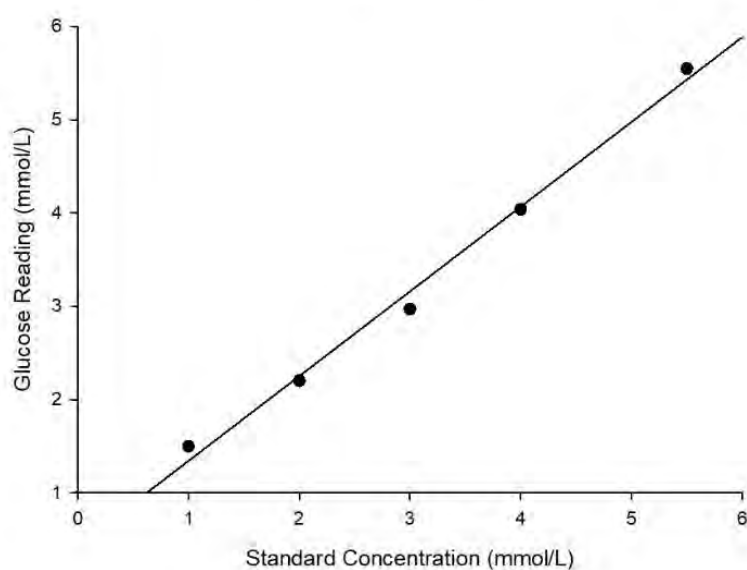


**Figure 2.2:** Regression Plot for Glucometer values vs standard

**Table 2.1:** Summarised data for Glucometer validation

X values (mmol/L)	Y values (mmol/L)	Statistical Parameters
5.5	5.3	$Y(X) = (0.99X) + 0.434$
4	4.7	Regression Coefficient: 0.99
3	2.9	Normality Passed (P = 0.697)
2	2.2	Standard Error= 0.162
1	1.5	N=5

---

## 2.2. Cell viability assay

### Principle

Thiazolyl tetrazolium bromide is a yellow dye which can be metabolised by mitochondrial dehydrogenases to produce a purple-blue product called formazan, which can be detected colorimetrically. The reduction of the tetrazolium salt, 3-(4,5-dimethylthiazol-2-yl)-2,5-diphenyltetrazolium bromide (MTT), to purple formazan crystals by metabolically active cells is what indicates cell viability. This reduction occurs primarily in the mitochondria via NADPH-dependent oxidoreductase enzymes. The MTT assay was particularly valuable for drug screening, enabling the evaluation of the cytotoxic effects of fluoroquinolones. MTT can be used to quantify metabolically active cells, thus an important tool to determine the cytotoxicity of various compounds [137]. Formazan is solubilised using DMSO, yielding a purple-blue solution. Thiazolyl tetrazolium bromide is highly photosensitive, and therefore, the procedure was performed under limited light exposure in a laminar flow hood. The diagram below shows the catalytic conversion of Thiazolyl Tetrazolium Bromide to Formazan.

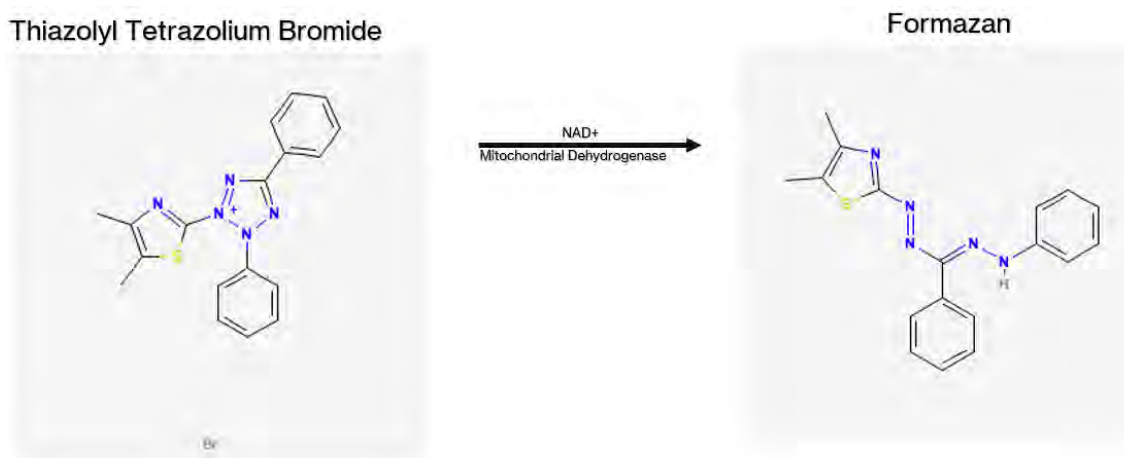


**Figure 2.3:** Conversion of Thiazolyl Tetrazolium Bromide to Formazan

### Experiment

The MTT assay was performed to evaluate the effects of selected fluoroquinolones—ciprofloxacin, moxifloxacin, lomefloxacin, and gatifloxacin in C2C12 and HepG-2 cells. The cells were seeded at a density ranging from  $(4.55 \times 10^4)$  cells/ml to  $(4.15 \times 10^4)$  cells/ml and cultured until

---

they reached approximately 80% confluence. The cells were then exposed to varying concentrations (10, 25, 50, 75 and 100 µg/ml) of each drug for 24 hours.

Following treatment, 200 µL of MTT solution (5 mg/ml), prepared in 10% PBS and 90% FBS-free media, was added to each well. The plates were incubated for 3 hours at 37°C in the dark to allow formazan crystal formation. The solution was carefully discarded, and 100 µL of DMSO was added to each well to solubilise the crystals. After 10 minutes of incubation, the absorbance was measured using a spectrophotometer at a wavelength of 560 nm (540–570 nm also works) to quantify cell viability. This protocol ensured consistent and reliable assessment of drug-induced cytotoxicity. The controls were wells that did not contain any fluoroquinolones. The cytotoxic properties of fluoroquinolones were calculated using the following equation: The diagram below shows the simplified protocol for the MTT assay.

$$\text{Percentage Cell Viability} = \left( \frac{\text{Absorbance of treated wells}}{\text{Absorbance of control}} \right) \times 100$$

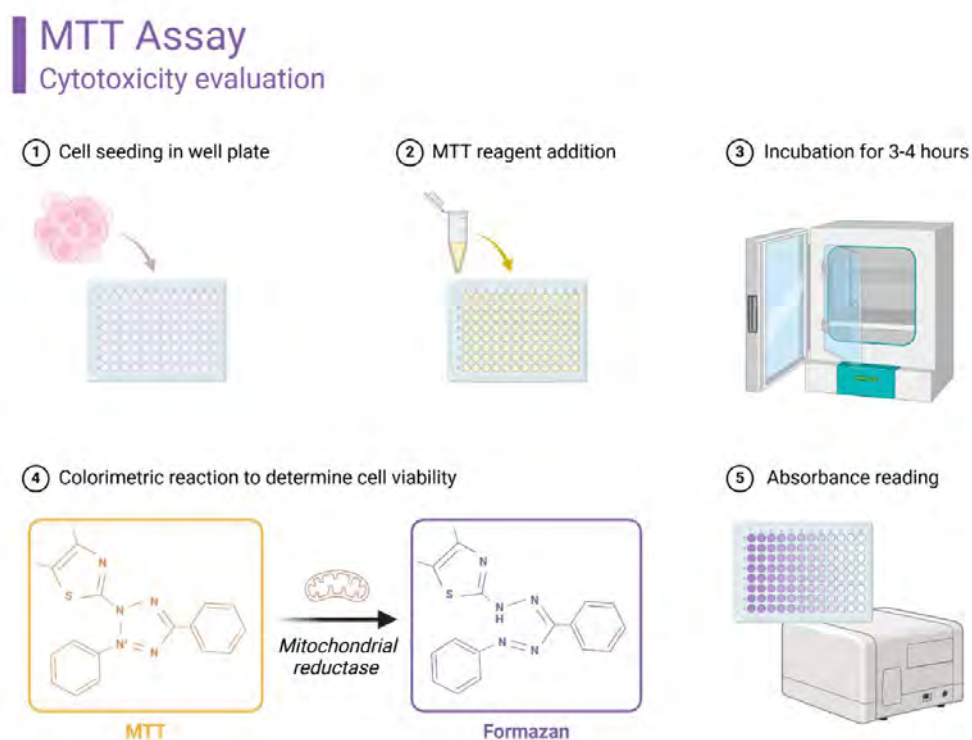


**Figure 2.4:** MTT assay protocol – cells are seeded in a plate, MTT solution is introduced, incubated for 3-4 hours, reaction is stopped with DMSO, and absorbance is measured [138]

---

### 2.3. Glucose Utilisation Assay

The glucose uptake was determined by measuring the concentration of glucose present in the medium after 24 hours. The HepG-2 cells and the differentiated C2C12 myoblasts fused into multinucleated myotubes in a 24-well plate were used. The old, cultured medium was removed, and the cells were washed three times with 200  $\mu$ L of phosphate buffer saline (PBS), after which the cells in wells were exposed to 200  $\mu$ L of fluoroquinolone (12.5, 25 and 50  $\mu$ g/ml) in medium supplemented with 10% FBS and 1% penicillin-streptomycin. Media glucose concentration was measured before incubation to serve as Time 0 (T0), then the cells were incubated in a 5% CO<sub>2</sub> environment at 37°C for 24 hours. Following the same procedure, 200  $\mu$ L of the medium was added to the cells as a control. After incubating for 24 hours, the glucose concentration in the medium was measured using an Accu-Chek Performa glucometer. The assay was performed in triplicate. The negative controls were wells which contained cells and media but no compounds to subtract the background extent of glucose utilisation of cells. The positive controls were wells which contained cells treated with 0.05 units/ml of insulin. The diagram below illustrates the steps involved in the media glucose uptake assay.

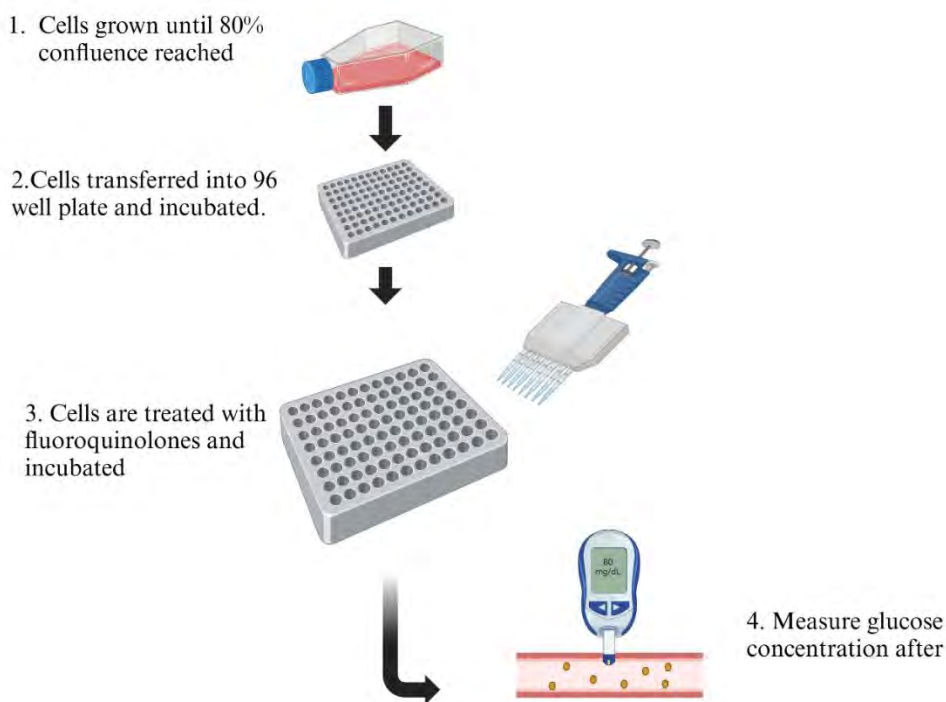


**Figure 2.5:** Media Glucose Utilisation Assay Protocol – cells grown until confluence, fluoroquinolones introduced into wells and incubated for 24 hours, media glucose was measured subsequently [135]

---

---

Moxifloxacin and ciprofloxacin were selected for further investigation based on their demonstrated superiority in glucose-lowering effects, higher cell viability, and lower cytotoxicity compared to gatifloxacin and lomefloxacin. Experimental findings revealed that moxifloxacin and ciprofloxacin consistently exhibited favourable metabolic and non-cytotoxic profiles, distinguishing them as more promising candidates. In contrast, gatifloxacin and lomefloxacin not only produced redundant and replicated data but also showed higher cytotoxicity, reducing their therapeutic appeal. Given the economic constraints associated with laboratory resources, it was deemed impractical to pursue all four compounds. Consequently, the decision to focus on moxifloxacin and ciprofloxacin was driven by their enhanced efficacy and safety, as well as the need to allocate resources efficiently. This retrospective justification underscores the rationale for prioritising these compounds, ensuring that research efforts were directed toward those with the greatest potential for therapeutic application.

#### **2.4. Glucose utilisation in the presence of PI3K inhibitor**

Wortmannin inhibits Phosphoinositide-3-Kinase (PI3K), an intermediate enzyme that facilitates the biochemical pathways downstream from insulin receptor activation. Blocking this enzyme, therefore, interferes with insulin signal transduction and its consequent insulin release.

Enhanced glucose uptake that occurs in cells treated with wortmannin must exploit an alternative pathway to reduce media glucose concentrations relative to untreated cells. Cell membranes feature a baseline amount of glucose transporters that allow for glucose entry. This explains why wortmannin does not block all glucose uptake [148]. The measure of interest in this assay, therefore, concerns media glucose concentrations after treatment with wortmannin. Ciprofloxacin and Moxifloxacin, due to their pronounced effect on enhancing glucose uptake, were further investigated to determine their impact on glucose uptake in the presence of the PI3K inhibitor wortmannin.

The aim was to evaluate whether these compounds utilise the insulin signalling pathway or an alternative mechanism. C2C12 and HepG2 cells were plated in 24-well plates and pre-treated with Wortmannin (25nM) for 24 hours before fluoroquinolone (ciprofloxacin and moxifloxacin) exposure (12.5, 25, and 50 µg/ml). After fluoroquinolone exposure, the media glucose concentrations were measured using the glucometer. Control groups included cells maintained in medium alone or 25 nM wortmannin, without treatments with fluoroquinolones. The diagram below summarises the steps in the wortmannin assay protocol.

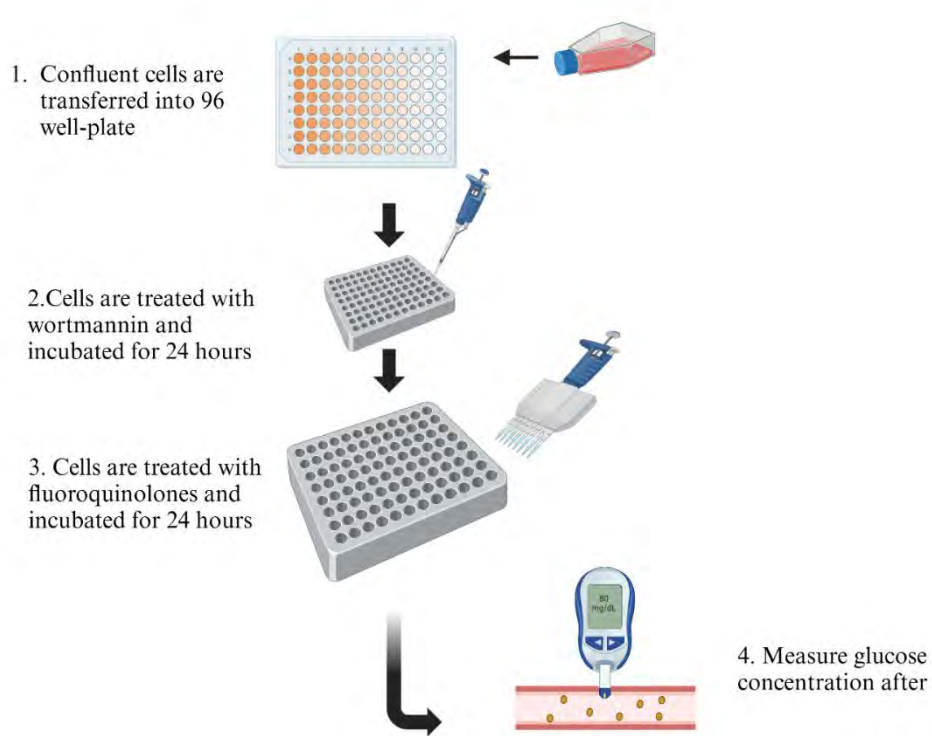


**Figure 2.6:** Wortmannin assay protocol – cells grown until confluence, cells treated with wortmannin and incubated for 24 hours, fluoroquinolones introduced into wells and incubated for 24 hours, media glucose is measured subsequently [149]

---

## 2.5. In-Cell-Elisa

### Principle

In-Cell-Elisa refers to an immunohistochemical process of quantifying the presence of proteins or translational modifications on target proteins within target cells. It combines the specificity of immunoassays with the ability to analyse proteins in their cellular context, making it ideal for studying signalling pathways, protein expression, and drug responses. The process exploits the adaptive immunological response of antibodies binding to antigens [145]. Proteins of interest represent antigens on which primary antibodies bind. Secondary antibodies bind to primary antibodies and are the proxy molecules for the analytes of interest; in other words, the general measure of the secondary antibodies that bind to the primary antibodies indicates by extension the concentration of the analyte, i.e. the protein of interest.

### Experiment

C2C12 and HepG-2 at an optimal density between  $4.09 \times 10^4$  and  $4.15 \times 10^4$  cells per well were seeded in a 96-well plate and allowed to adhere overnight (incubated for 24 hours). Subsequently, the cells were treated with 100  $\mu$ l of the different concentrations of Ciprofloxacin and Moxifloxacin (12.5, 25, and 50  $\mu$ g/ml) and incubated overnight.

The in-cell ELISA Assays were conducted in C2C12 and HepG-2 cells to investigate the expression of Akt, IL-6 and GLUT-4 for C2C12, exclusively. Cells were treated with varying concentrations of fluoroquinolones (12.5, 25, 50  $\mu$ g/ml) in DMEM for C2C12 and MEM for HepG-2 and incubated at 37°C for 24 hours. After incubation, the medium was aspirated, and cells were fixed by adding 100  $\mu$ L of 8% paraformaldehyde to each well, followed by a 15-minute incubation at room temperature on a microplate shaker set at 300 rpm. The paraformaldehyde was aspirated, and each well was washed four times with 200  $\mu$ L of PBS. Permeabilisation was performed by adding 200  $\mu$ L of permeabilisation buffer (0.1% Triton X-100 in PBS) to each well, and plates were incubated for 30 minutes at room temperature while shaking at 300 rpm. After permeabilisation, blocking was carried out by adding 200  $\mu$ L of blocking buffer (1% BSA in PBS) to each well, and plates were incubated at room temperature for 2 hours while shaking. The blocking buffer was aspirated, and 100  $\mu$ L of primary antibody (GLUT4, AKT, or IL-6; diluted 1:5000 in incubation buffer) was added to each well, followed by overnight incubation at 4°C. The primary antibody was aspirated, and plates were washed three times

---

---

with 250  $\mu\text{L}$  of wash buffer (0.1% Tween-20 in PBS). Next, 100  $\mu\text{L}$  of secondary antibody (anti-rabbit IgG, HRP-conjugated) was added to each well, and plates were incubated at room temperature for 2 hours while shaking. After secondary antibody incubation, plates were washed four times with 250  $\mu\text{L}$  of wash buffer, and 100  $\mu\text{L}$  of HRP substrate (0.05 mg/ml TMB in citrate buffer) was added to each well. Plates were incubated for 30 minutes while shaking at 300 rpm, and the reaction was stopped by adding 100  $\mu\text{L}$  of 0.1M HCl to each well. Absorbance was measured at 450 nm using a spectrophotometer. All assays were performed in triplicate and repeated twice to ensure reproducibility. The diagram below shows the simplified steps for the In-Cell ELISA protocol.

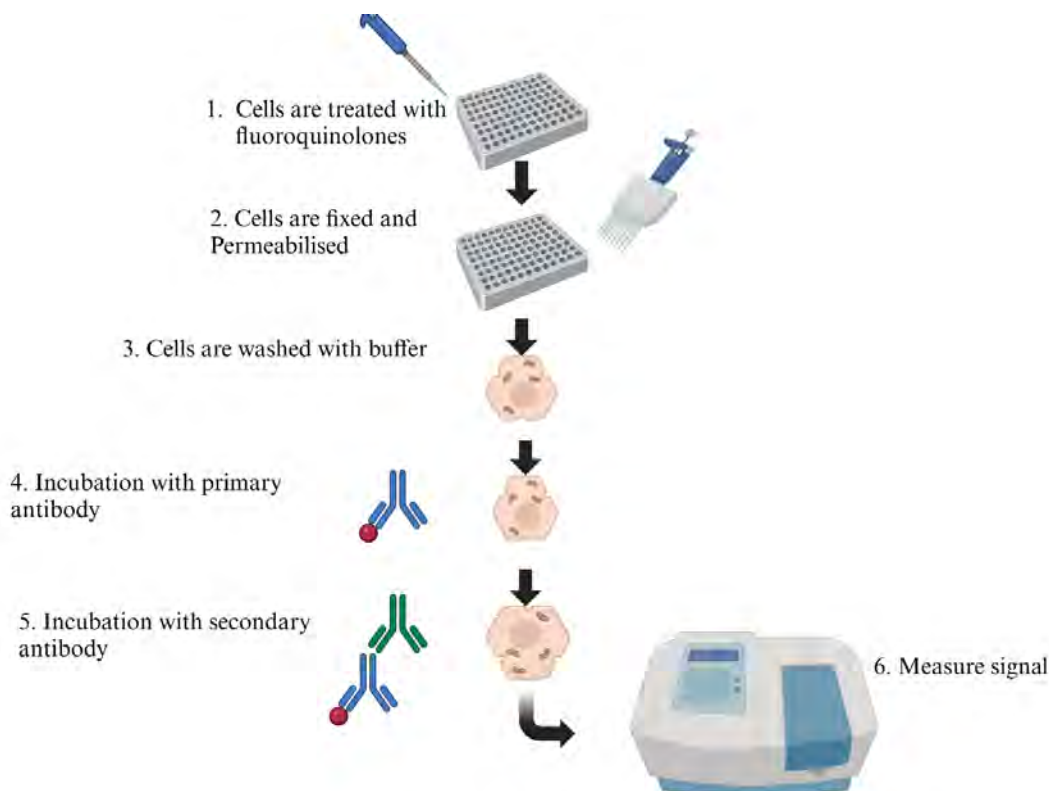


**Figure 2.7:** In-Cell Elisa protocol – cells grown until confluence, fluoroquinolones introduced into wells and incubated for 24 hours, cells are fixed and permeabilisation, after incubation and washing, primary antibody is introduced and wells incubated, after which secondary antibody is introduced and incubated. Resultant wells are then measured for protein expression.[146]

The experiment had positive and negative controls. The negative control sample did not express the target proteins of interest for detection, enabling the ability to rule out non-specific binding and false positives. The negative control contained media and fluoroquinolones, but no cells existed. The positive controls contained cells but no fluoroquinolones, to confirm if there is background expression of the target proteins of interest. The 96 well plates were carefully annotated for which cells had primary antibodies and fluoroquinolones, along with their respective concentrations Figure 2.8. shows a colour-coded illustration of the well-plate treatment design.

The relative expression of each protein was calculated as follows:

$$\text{Relative percentage expression} = \left( \frac{\text{Average absorbance of treated wells}}{\text{Average absorbance of control}} \right) \times 100$$



**Figure 2.8:** 96 well-plates with each compound, primary antibody, positive and negative controls [147]

---

## Non-Cell-Based Assays

### 2.6. Compound Preparation

The four selected fluoroquinolones—ciprofloxacin, moxifloxacin, gatifloxacin, and lomefloxacin—were sourced from Sigma-Aldrich. For *in vitro* testing, stock solutions of each compound were prepared by accurately weighing 0.01 g of each fluoroquinolone using a Precisa analytical balance and dissolving it in 1 ml of dimethyl sulfoxide (DMSO) and 1 ml of phosphate buffer (pH 6.8) to achieve a stock concentration of 1000 µg/ml. These stock solutions were aliquoted into sterile, 15 ml centrifuge tubes to prevent degradation and stored at -20°C to maintain stability and prevent microbial contamination, with care taken to avoid repeated freeze-thaw cycles.

Prior to each assay, the stock solutions were thawed and diluted to the desired working concentrations (10, 30, 50, and 75 µg/ml) using the appropriate buffer (e.g., phosphate buffer or cell culture media) and the  $C_1V_1 = C_2V_2$  formula to ensure accuracy. Fresh working solutions were prepared for each experiment to avoid degradation or loss of activity. All preparations and handling were conducted under proper aseptic techniques to prevent contamination. This protocol ensured the stability, accuracy, and reproducibility of fluoroquinolone concentrations for *in vitro* testing.

---

## 2.7. $\alpha$ -Amylase Assay

### Principle

This assay was performed using the 3,5-dinitrosalicylic acid (DNSA) method [127]. The  $\alpha$ -amylase activity is measured using a colourimetric method with DNSA reagent.  $\alpha$ -amylase breaks down starch into simpler sugars, i.e. maltose. Once released from starch, maltose is measured by the reduction of 3,5-dinitrosalicylic acid. Maltose reduces the pale-yellow alkaline DNS to orange-red, as illustrated in the chemical reaction below. This intensity change in colour is proportional to the concentration of maltose present in the sample. The hemiacetalic reducing groups of the resultant catalytic fragments of starch, i.e. maltose and other reducing sugars, are needed for the reduction process. The consequent nitroaminosalicylic acid concentration corresponds to the enzymatic activity of amylase. Therefore, the presence of an  $\alpha$ -amylase inhibitor decreases the liberation of maltose, leading to a decrease in the reduction of DNS and absorbance detected and measured at a wavelength of 540 nm, where orange/red hues are observed on the electromagnetic spectrum.

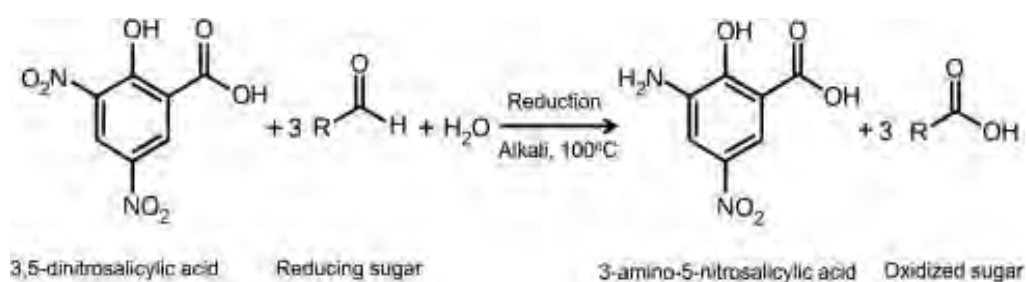


**Figure 2.9** Chemical reaction. 3,5-dinitrosalicylic acid + reducing sugar  $\rightarrow$  3-amino-5-nitrosalicylic acid and oxidised sugar [128]

---

## Experiment

In a test tube, 200  $\mu\text{L}$  of  $\alpha$ -amylase (1 U/ml) in phosphate buffer solution (0.02 M at pH 6.8) was mixed with selected fluoroquinolones (200  $\mu\text{L}$ ) at concentrations of 10, 30, 50, and 75  $\mu\text{g}/\text{ml}$  and incubated at 37  $^{\circ}\text{C}$  for 10 min. The starch solution (200  $\mu\text{L}$  at 1%w/v) was added to each tube and incubated for 10 min. The reaction was terminated by the addition of 500  $\mu\text{L}$  DNSA reagent (6 g of sodium potassium tartrate tetrahydrate in 4.0 ml of 2 M NaOH and 10 ml of 96 mM of 3,5-dinitrosalicylic acid solution) and boiled for 5 minutes in a water bath at 85  $^{\circ}\text{C}$ . Cells containing only the phosphate buffer were used as a negative control, and wells containing acarbose (and no fluoroquinolones) constituted the positive control. The mixture was cooled to ambient temperature and diluted with 5 ml of distilled water, after which the absorbance was measured using the Ivymen microplate reader (2100-C). The assay was performed in triplicate. Acarbose was used as the positive control. The  $\alpha$ -amylase inhibitory activity was expressed as percentage inhibition and calculated using the equation below: The percentage  $\alpha$ -amylase inhibition was plotted against the concentration, and the IC50 values were obtained from the graph using SigmaPlot.

$$\text{Inhibition of } \alpha\text{-amylase activity (\%)} = \left( \frac{\text{Absorbance of control} - \text{absorbance of compound}}{\text{Absorbance of control}} \right) \times 100$$

---

## 2.8. $\alpha$ -Glucosidase Inhibition Assay

### Principle

The  $\alpha$ -glucosidase inhibitory activity was determined using the Sigma Aldrich protocol [129].  $\alpha$ -glucosidase catalyses the 4-nitrophenyl- $\alpha$ -D-glucopyranoside (PNPG) conversion to  $\alpha$ -D-glucopyranoside and p-nitrophenol (PNP) at pH 6.8 under 37 °C. The yellow colour of PNP is measured spectrophotometrically at 405 nm. The presence of an  $\alpha$ -glucosidase inhibitor thus prevents the conversion of PNPG to PNP, resulting in a lower concentration of PNP. This intensity change in colour is proportional to the concentration of PNP in the sample.

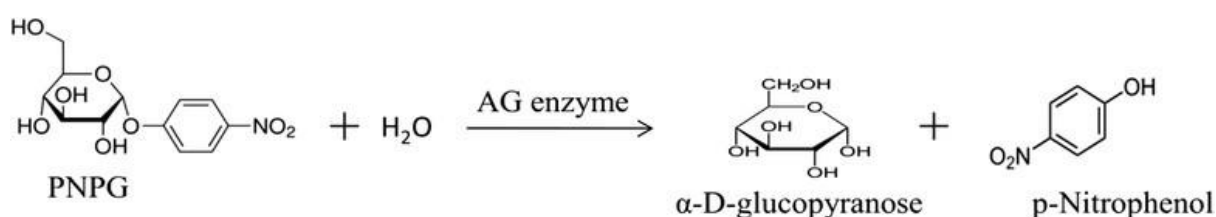
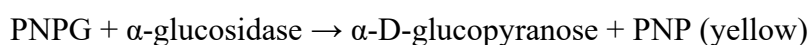


**Figure 2.10:** Catalytic conversion of 4-nitrophenyl- $\alpha$ -D-glucopyranoside to  $\alpha$ -D-glucopyranoside and p-nitrophenol [130]



### Experiment

To perform this assay, 100  $\mu$ L of fluoroquinolone derivatives of concentrations 10, 20, 30, 50 and 75  $\mu$ g/ml were diluted with 100  $\mu$ L of 0.1 M potassium phosphate buffer (pH 6.8) containing  $\alpha$ -glucosidase solution (1.0 IU/ml) and was incubated in a 96-well plate at 37 °C for 10 min. After pre-incubation, 5 mM *p*-nitrophenyl- $\alpha$ -glucopyranoside solution (100  $\mu$ L) in 0.1 M potassium phosphate buffer (pH 6.8) was added to each well at timed intervals. The reaction mixtures were incubated at 37 °C for 60 min. The reaction was stopped by adding 0.1 M NaCO<sub>3</sub> (125  $\mu$ L). The absorbance values were then measured at 405 nm using the Ivymen microplate reader (2100-C). Acarbose was used as the positive control. The phosphate buffer was used as a blank. The  $\alpha$ -glucosidase inhibitory activity was determined as a percentage of inhibition, calculated as follows:

$$\text{Inhibition of } \alpha\text{-glucosidase activity (\%)} = \left( \frac{\text{Absorbance of control} - \text{absorbance of compound}}{\text{Absorbance of control}} \right) \times 100$$

---

## 2.9. In Silico Modelling

Molecular docking is an important computational technique in structural biology and computer-aided drug design. The primary objective of molecular docking is to evaluate the feasible binding geometries of various protein-ligand complexes of known three-dimensional structures. The 3D crystal structure of various glycaemic targets was downloaded from the Protein Data Bank (PDB) (<https://www.rcsb.org/>). Each target protein and ligand has its corresponding PDB code; for the proteins, Phosphoinositide-3-Kinase: 5JHB,  $\alpha$ -glucosidase: 3WY1,  $\alpha$ -amylase: 1B2Y, and insulin receptor: 1P14. Moxifloxacin, Ciprofloxacin, Lomefloxacin, and Gatifloxacin were downloaded as structural data files (SDF) from the protein data bank and then converted using OpenBabel Software-2.4.2 into protein format with partial charge and atom type format (PDBQT) for AutoDockTools-1.5.7 (ADT). The raw PDB document was modified in Autodock tools by removing water molecules and adding electrostatic charges and polar hydrogens to prepare it for docking. The grid box dimension within which receptor-ligand complexes were fixed at 60x60x60 Å. ADT was used to perform docking 50 simulations per receptor-ligand interaction. For ADT, the uploaded PDB documents are internally converted into grid parameter files (GPF) and docking parameter files (DPF) to produce docking log files (DLG), which detail the properties of the simulated drug-receptor complexes [139].

The requisite parameters extracted from the DLG files to evaluate the success of the protein-ligand complex are the free binding energies, root mean squared deviations (RMSD) and the inhibition constants. The free binding energy is the change in Gibbs free energy ( $\Delta G$ ) when two molecules, such as a protein and ligand or DNA and RNA, bind to form a stable complex. It is a thermodynamic measure of the interaction strength, combining enthalpic (bonding interactions) and entropy. Negative or lower free energies indicate a spontaneous and favourable binding conformation and generally signify stronger, more specific binding, aiding in the identification of high-affinity compounds for therapeutic targets [140].

The Root Mean Squared Deviation (RMSD) is a statistical measure used to quantify the average deviation between predicted or observed values and their reference points. For small molecules (ligands) binding to receptor targets, the measure can be used to compare the structures of ligands in different binding modes or to evaluate the accuracy of docking predictions. The measure is mathematically expressed as follows:

---

$$RMSD = \sqrt{\frac{\sum_{i=1}^n (\vec{x}_{1,i} - \vec{x}_{2,i})^2}{n}}$$

N is the number of data points.  $\vec{x}_{1,i}$  is the i-th measurement, and  $\vec{x}_{2,i}$  is its corresponding prediction. RMSD is commonly applied to compare three-dimensional molecular structures, such as proteins or nucleic acids, to assess their similarity. A lower RMSD indicates higher structural similarity or alignment accuracy, making it a critical metric for validating computational models [141].

The inhibition constant, also known as  $K_i$ , is a value that quantifies the strength of an inhibitor in blocking the activity of an enzyme. A lower  $\Delta G$  corresponds to a lower  $K_i$ , which indicates a more favourable interaction between the ligand and the target. The parameter was obtained from the binding energy ( $\Delta G$ ) using the formula:  $K_i = \exp(\Delta G/RT)$ , where R is the universal gas constant ( $1.985 \times 10^{-3} \text{ kcal mol}^{-1} \text{ K}^{-1}$ ) and T is the temperature (298.15 K). A lower  $K_i$  suggests the ligand can effectively inhibit the target at lower concentrations, making it a potentially more potent drug candidate [142].

The docking simulations are then ranked for their respective clusters that yield optimal binding. The binding energy of each cluster is the mean binding energy of all the conformations. Therefore, the highest ranked clusters will be the selected ones for the results, as they not only display the likely binding conformation of the ligand and the receptor but also provide the corresponding data that indicates if these complexes would likely obtain under physiological conditions [143].

The binding residues and different bonds involved in the interactions of the resulting docked complexes were evaluated and visualised using Ligplot, Proteinplus and Cluspro. The resultant protein-protein complexes were visualised using Pymol and Protein-Plus. Complexes were converted into a PDB format that is compatible with the visualisation software. The software not only provides key visual recognition of the various binding regions but also characterises the nature of the interactions themselves. Interactions range from strong covalent bonding, which are irreversible chemical bonds, to weak dispersion forces, which permit temporary binding. Additionally, the amino acids and peptide groups identified can be characterised by their involvement in general binding onto important receptors physiologically and their role in signal transduction pathways [144].

---

## 2.10. Calculations and Statistical Analysis

The half-maximal inhibitory concentration (IC<sub>50</sub>) measures a substance's effectiveness in inhibiting a specific biological or biochemical function. This quantitative measure indicates how much of a drug or inhibitor is needed to inhibit a given process by half. To calculate IC<sub>50</sub>, the percentage inhibitions obtained for each enzyme inhibitory study were analysed by linear regression analysis using SigmaPlot. IC<sub>50</sub> values were calculated for  $\alpha$ -glucosidase and  $\alpha$ -amylase. The data were expressed as three replicates' mean  $\pm$  standard deviation (SD). Analysis was performed using Excel Office 365. One-way analysis of variance (ANOVA) was used to assess the statistical significance of the differences between the means and the controls of the experiments. Statistical analysis conducted from the absorbance/fluorescence readings before normalisation obtained for each experiment was determined using SigmaPlot. The Bonferroni T test for significance between the test compounds and the control was followed by the statistical analysis. The asterisks represent the groups which have a statistically significant difference (at  $p < 0.05$ ) from the control [150].

---

## Chapter 3: Results

### 3.1. Cell Viability Assay

Figure 3.1. illustrates the cell viability of fluoroquinolones in differentiated C2C12 and HepG-2 cells. Lomefloxacin, Ciprofloxacin, Moxifloxacin, and Gatifloxacin were investigated at various concentrations compared to an untreated control sample. Ciprofloxacin exhibited the highest cell viability, with 99.6% at the lowest concentration (12.5 µg/ml) and 74.4% at the highest concentration (100 µg/ml) in C2C12 cells.

In contrast, Moxifloxacin showed greater variability in activity between 12.5 µg/ml and 100 µg/ml, displaying clear dose-dependent toxicity, where higher concentrations were more cytotoxic. Gatifloxacin demonstrated the lowest average percentage activity, with even low concentrations (12.5 µg/ml) exhibiting greater cytotoxicity than high concentrations of both Ciprofloxacin and Lomefloxacin.

Similar to results in C2C12 cells, Ciprofloxacin maintained the low cytotoxic profile, albeit with a slightly lower average percentage activity. Gatifloxacin showed the highest cytotoxicity, with only 23% activity at 100 µg/ml, indicating significant disruption of HepG-2 cell metabolic function. Lomefloxacin and Moxifloxacin exhibited intermediate effects, with Lomefloxacin closely resembling Ciprofloxacin's activity, while Moxifloxacin displayed high variability across concentrations, similar to gatifloxacin.

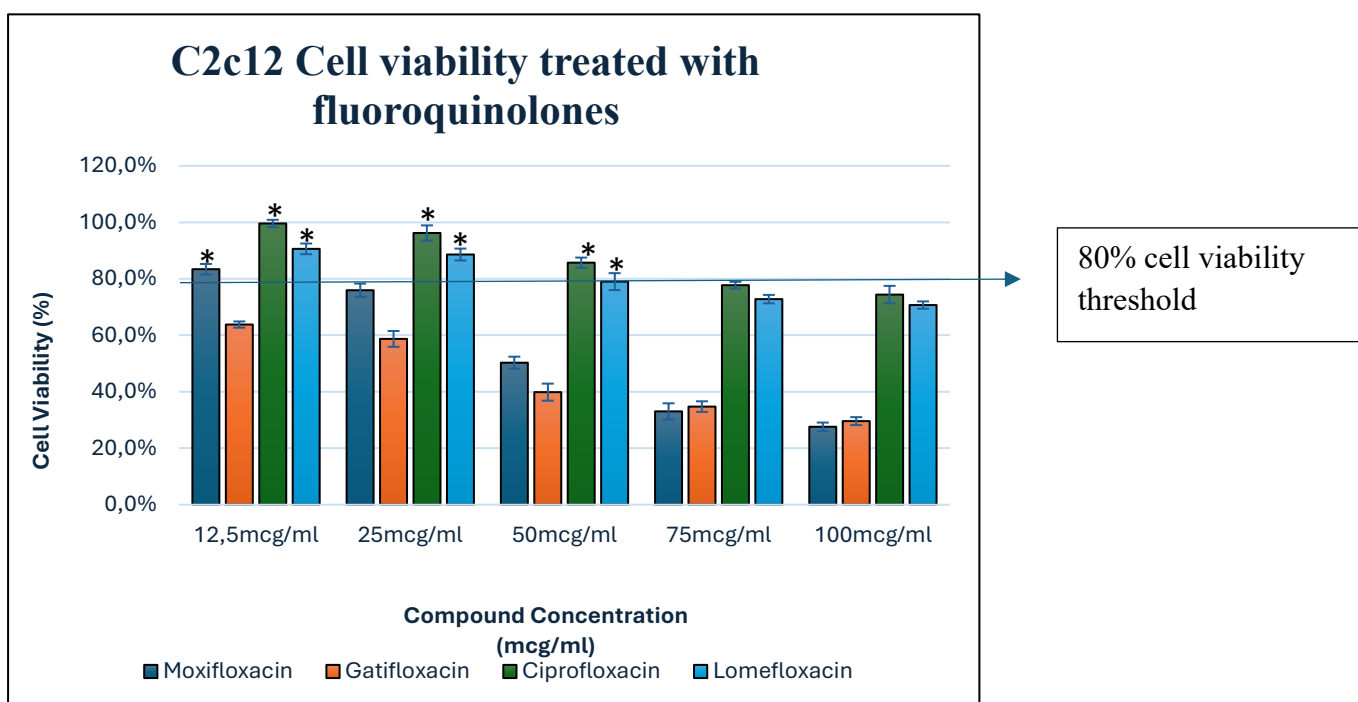
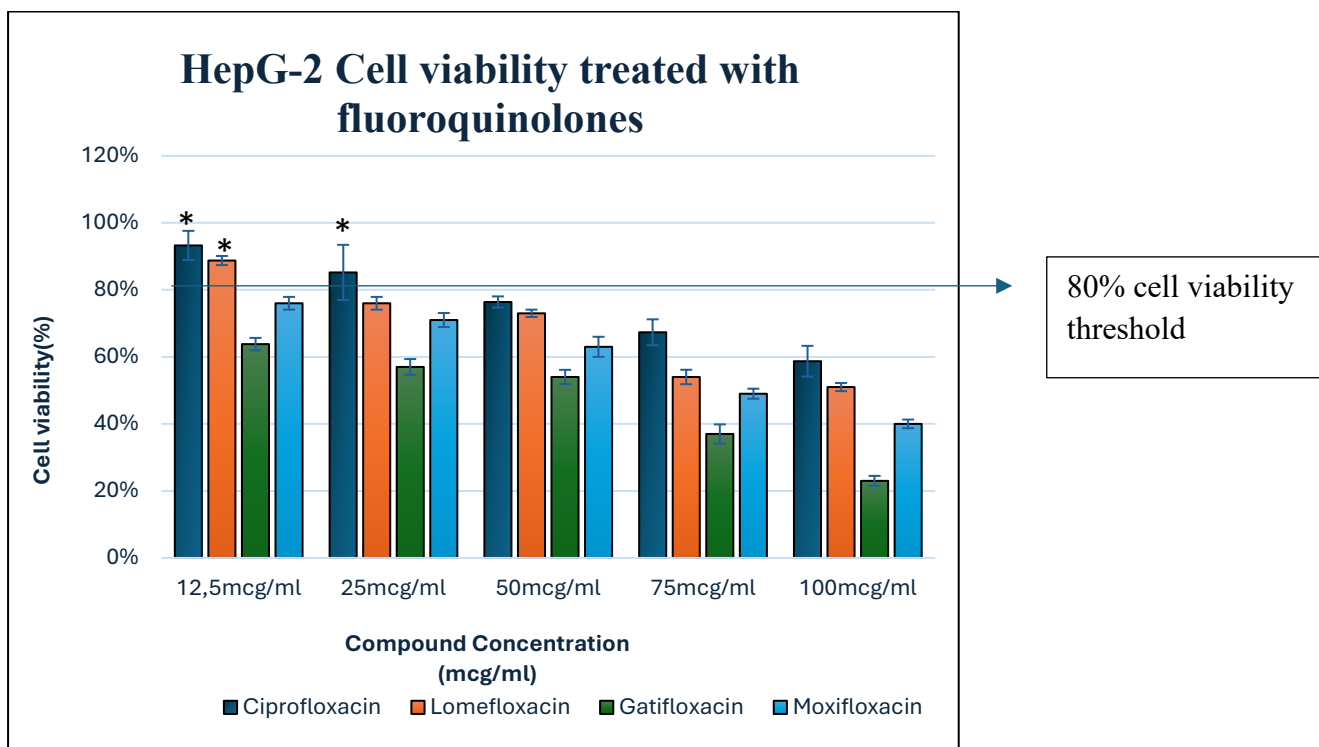


**Figure 3.1:**Percentage viability in C2C12 and HepG-2 cells treated with fluoroquinolones (Ciprofloxacin, moxifloxacin, Lomefloxacin, and Gatifloxacin) at different concentrations (10, 25, 50, 75 and 100 µg/ml). The data is presented as mean ± SD represented with error bars, (n = 3), and the asterisk (\*) represents the compounds which meet the 80% threshold for cell viability, indicative of low toxicity.

---

### 3.2.1. Glucose Uptake Assay

The media glucose concentrations following exposure of C2C12 and HepG-2 cell lines to fluoroquinolones at concentrations of 12.5, 25, and 50 µg/ml for 24 hours are presented in Figure 3.3. Treated cells were compared to positive (insulin) and negative controls (cells and media only). The baseline glucose concentration in medium essential media (MEM) without insulin or fluoroquinolones was 2.88 mmol/L, reflecting the inherent glucose uptake capacity of HepG-2 cells.

Ciprofloxacin demonstrated a linear, dose-dependent reduction in media glucose, indicating enhanced glucose uptake by HepG-2 cells at higher concentrations. At 50 µg/ml, Ciprofloxacin reduced media glucose by 93%, lowering glucose more than the positive control, insulin (1.75 µg/ml or 0.05 units/ml). Similarly, Gatifloxacin exhibited a dose-dependent decrease in media glucose, with significant media glucose reduction at 50 µg/ml compared to insulin. However, the difference in glucose concentrations between successive doses appeared stochastic, with only a 0.1997 mmol/L reduction between 12.5 µg/ml and 25 µg/ml, and a sharper decline of 0.8 mmol/L at 50 µg/ml, suggesting that effective doses of Gatifloxacin may begin at higher concentrations than those of Ciprofloxacin.

Moxifloxacin and Lomefloxacin showed inconclusive linearity in its glucose-lowering effect, indicating reduced responsiveness of HepG-2 cells within the same concentration range compared to Gatifloxacin and Ciprofloxacin. While Moxifloxacin lowered media glucose concentrations relative to the control, it did not surpass the effect of insulin at any concentration. In differentiated myotubes, Ciprofloxacin also exhibited a glucose-lowering effect, though weaker than insulin. A sharper decline was observed between 12.5 µg/ml and 25 µg/ml than between 25 µg/ml and 50 µg/ml, suggesting that lower doses may suffice to elicit this effect.

## HepG-2 Cells

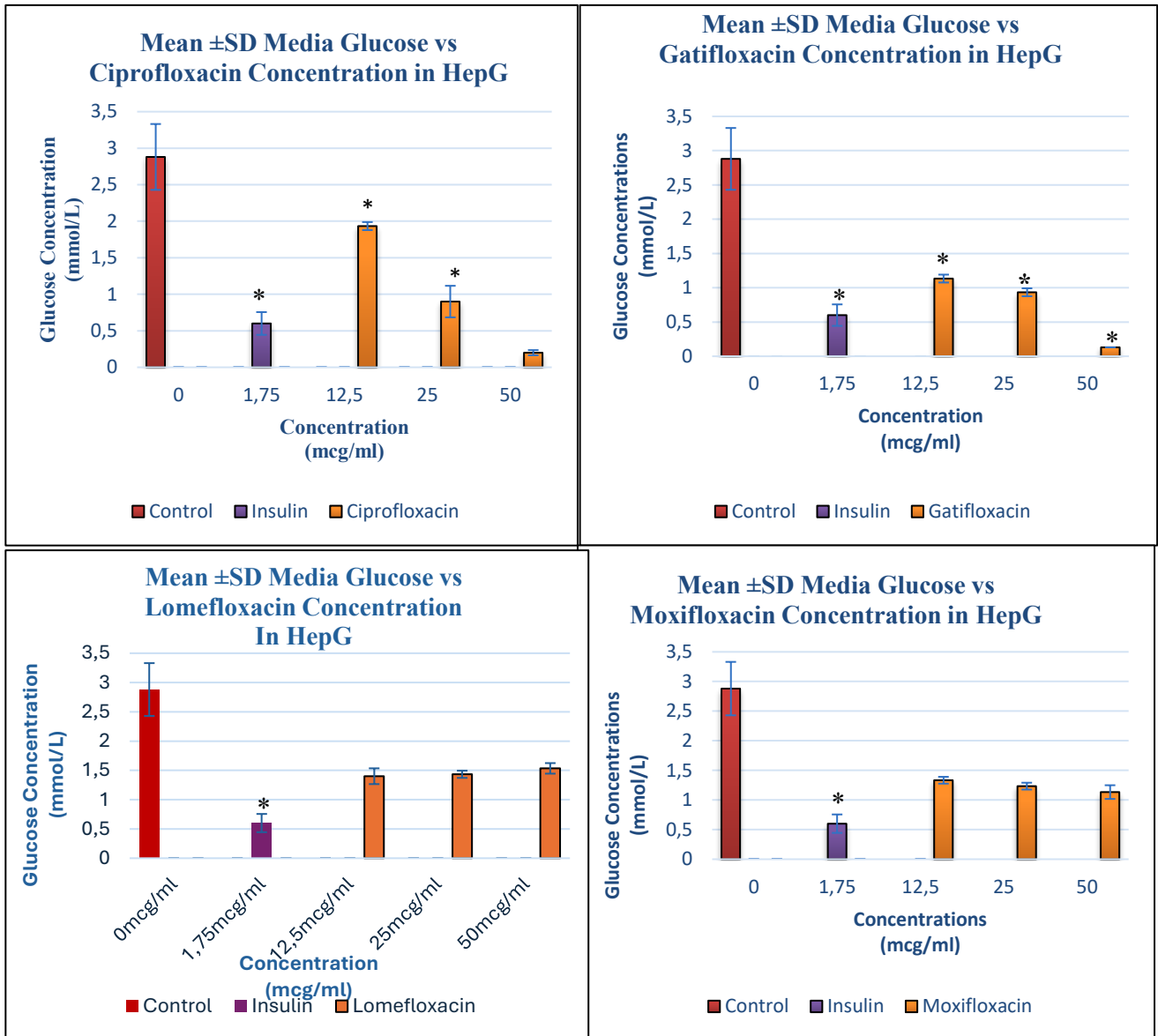


**Figure 3.2:** Media glucose concentrations in HepG-2 cells treated with fluoroquinolones (Ciprofloxacin, moxifloxacin, Lomefloxacin, and Gatifloxacin) at different concentrations of 12.5, 25, and 50  $\mu\text{g/ml}$ . The data is presented as mean  $\pm$  SD represented with error bars, (n = 3), and the asterisk (\*) represents the statistical difference between the test compounds and the control at (p < 0.05)

## C2C12 Cells

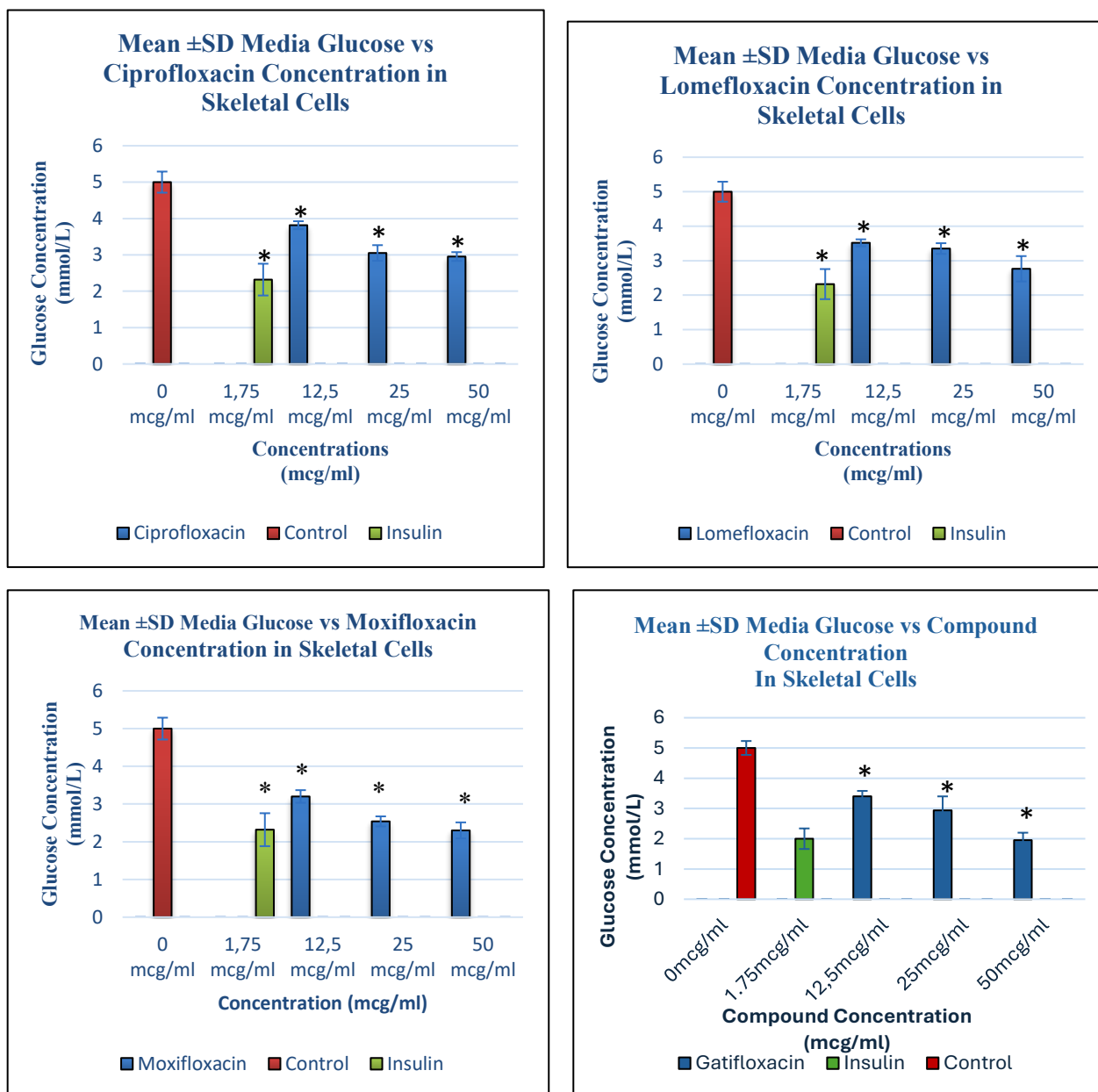


**Figure 3.3:** Glucose uptake in C2C12 cells treated with fluoroquinolones (Ciprofloxacin, moxifloxacin, Lomefloxacin, and Gatifloxacin) at different concentrations of 12.5, 25, and 50  $\mu\text{g/ml}$ . The data is presented as mean  $\pm$  SD represented with error bars, ( $n = 3$ ), and the asterisk (\*) represents the statistical difference between the test compounds and the control at ( $p < 0.05$ )

---

### 3.2.2. Media glucose in Wortmannin pretreated cells

Given the established data demonstrating the capacity of ciprofloxacin and moxifloxacin to promote glucose uptake in a concentration-dependent manner, further investigations were conducted to determine whether these compounds utilise the insulin signalling pathway, which is dependent on PI3K activation. To assess this, wortmannin, a known PI3K inhibitor, was employed to block the insulin signalling pathway. The rationale behind this approach is that any observed increase in glucose uptake in the presence of wortmannin would suggest the involvement of an alternative pathway mediating glucose regulation, independent of PI3K signalling. This experimental design allows for the elucidation of potential mechanisms by which ciprofloxacin and moxifloxacin influence glucose metabolism, particularly in the context of PI3K inhibition.

Figures 3.4 and 3.5 depict the effect of fluoroquinolones (12.5, 25, and 50 µg/ml) on media glucose concentration in HepG-2 and C2C12 cells pretreated with 25 nM wortmannin. The experimental design included two control groups: a wortmannin control, where cells were treated exclusively with 25 nM wortmannin, and an absolute control, consisting of cells untreated with either wortmannin or fluoroquinolones, with measurements taken after 24 hours. The remaining wells were exposed to wortmannin in combination with either moxifloxacin or ciprofloxacin. Across all cell lines, wortmannin significantly reduced glucose uptake compared to the absolute control, as evidenced by slightly higher media glucose concentrations. This result confirms that wortmannin effectively disrupts normal glucose uptake mechanisms that are active in untreated cells.

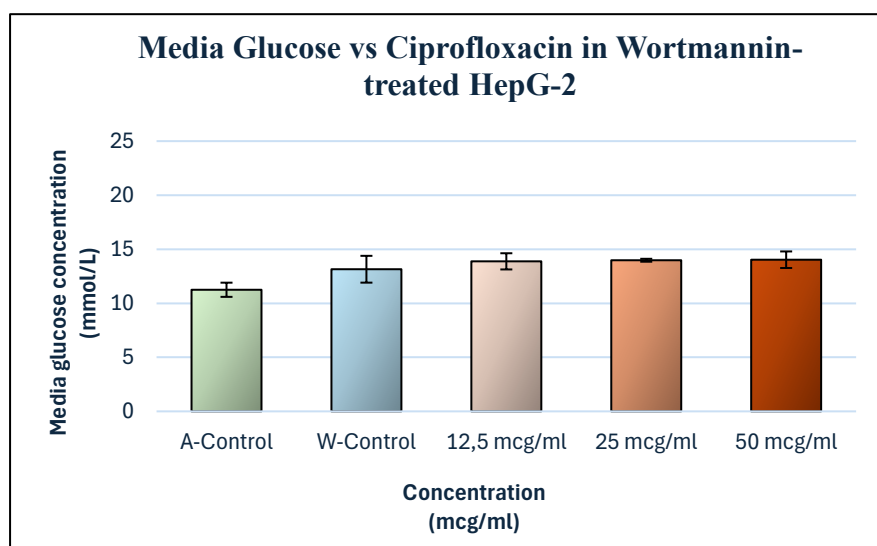
Notably, in HepG-2 cells, neither moxifloxacin nor ciprofloxacin elicited statistically significant changes in glucose uptake across the tested concentrations by comparison to the absolute control group and Wortmannin control group. In contrast, C2C12 cells displayed statistically significant reductions in media glucose concentrations in response to both fluoroquinolones, indicating enhanced glucose uptake. Across both cell lines, media glucose concentrations in most treatment groups exposed to ciprofloxacin and moxifloxacin were higher than those of the absolute control, except for moxifloxacin at 50 µg/ml in C2C12 cells. At this concentration, a marked decline in media glucose concentration was observed, signifying a pronounced increase in glucose uptake. These findings suggest that, at lower concentrations, fluoroquinolones potentiate the inhibitory effects of wortmannin on glucose uptake. However, beyond a specific concentration threshold, fluoroquinolones appear to counteract the PI3K-inhibitory action of wortmannin, thereby promoting glucose uptake. This biphasic response

---

---

underscores a concentration-dependent interplay between fluoroquinolones and wortmannin in modulating glucose metabolism, highlighting distinct regulatory mechanisms in HepG2 and C2C12 cells.

Figure 3.4 further depicts the media glucose utilisation in HepG2 and C2C12 cells treated with wortmannin and ciprofloxacin. In HepG2 cells, no statistically significant differences in mean glucose concentrations were observed between ciprofloxacin-treated groups across all concentrations and the wortmannin control, indicating inconclusive effects of ciprofloxacin on glucose utilisation in this cell line. Additionally, media glucose concentrations remained unchanged regardless of ciprofloxacin concentration. In contrast, C2C12 cells exhibited a dose-dependent response, with increasing ciprofloxacin concentrations leading to reduced media glucose concentrations. However, none of the concentrations lowered glucose levels below those of either control, underscoring the dominant inhibitory effect of wortmannin on glucose uptake.



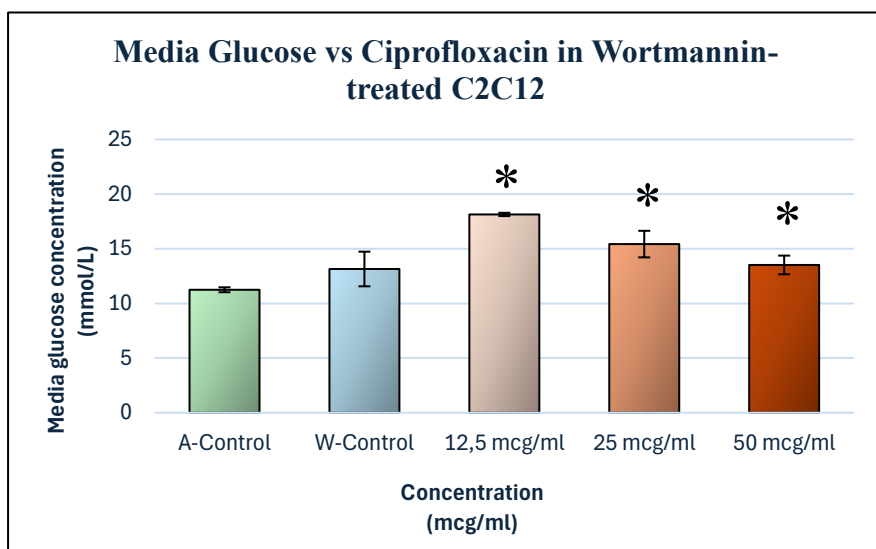


**Figure 3.4:** Media glucose concentrations in C2C12 and HepG2 cells concurrently treated with wortmannin and Ciprofloxacin at different concentrations 12.5, 25, 50  $\mu\text{g/ml}$ . A-Control refers to the absolute control and W-Control refers to the wortmannin control. The data is presented as mean  $\pm$  SD represented with error bars, ( $n = 3$ ), and the asterisk (\*) represents the statistical difference between the test compounds and the control at ( $p < 0.05$ ).

Figure 3.5 presents the media glucose utilisation in HepG2 and C2C12 cells treated with wortmannin and moxifloxacin. Similar to ciprofloxacin, moxifloxacin did not reduce mean glucose concentrations in HepG2 cells. The media glucose concentration, however, was significantly higher than the Wortmannin control, suggesting compounding effects with wortmannin. In C2C12 cells, however, moxifloxacin demonstrated a linear, concentration-dependent reduction in media glucose concentrations, albeit mostly still higher than the controls. At 50 µg/ml, moxifloxacin reduced media glucose levels below those of the wortmannin control, effectively reversing the inhibition of glucose uptake caused by wortmannin.

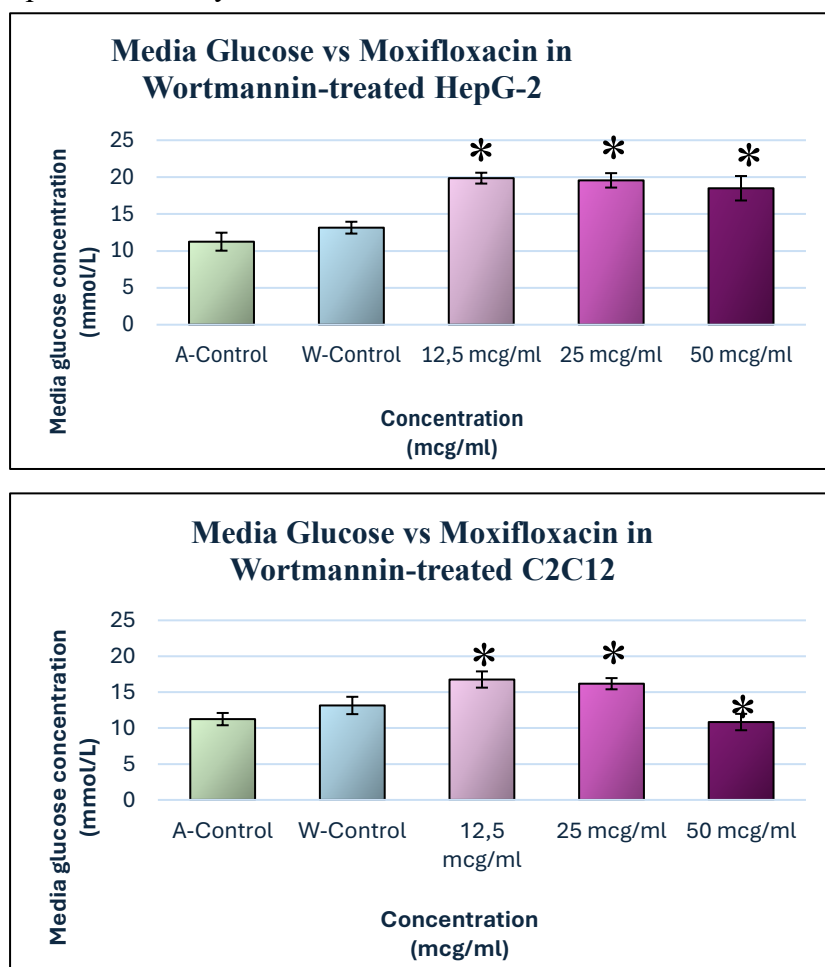


**Figure 3.5:** Media glucose concentrations in C2C12 and HepG2 cells concurrently treated with wortmannin and Moxifloxacin at different concentrations 12.5, 25, 50 µg/ml. A-Control refers to the absolute control and W-Control refers to the wortmannin control. The data is presented as mean ± SD represented with error bars, (n = 3), and the asterisk (\*) represents the statistical difference between the test compounds and the control at (p < 0.05).

### 3.3. In Cell Elisa Assay

#### 3.3.1. Relative IL-6 Expression

Figures 3.6 to 3.7 present the relative percentage of IL-6 expression in C2C12 and HepG2 cells following treatment with fluoroquinolones, namely moxifloxacin and ciprofloxacin, at concentrations of 12.5, 25, and 50  $\mu\text{g/ml}$ . In HepG2 cells, moxifloxacin treatment at 12.5 and 25  $\mu\text{g/ml}$ , as well as in C2C12 cells at 25 and 50  $\mu\text{g/ml}$ , resulted in negligible increase in IL-6 expression, with no statistically significant differences observed compared to the control ( $p > 0.05$ ). However, at 50  $\mu\text{g/ml}$  in HepG2 cells, moxifloxacin significantly increased IL-6 expression relative to the control, whereas at 12.5  $\mu\text{g/ml}$  in C2C12 cells, it reduced IL-6 expression.

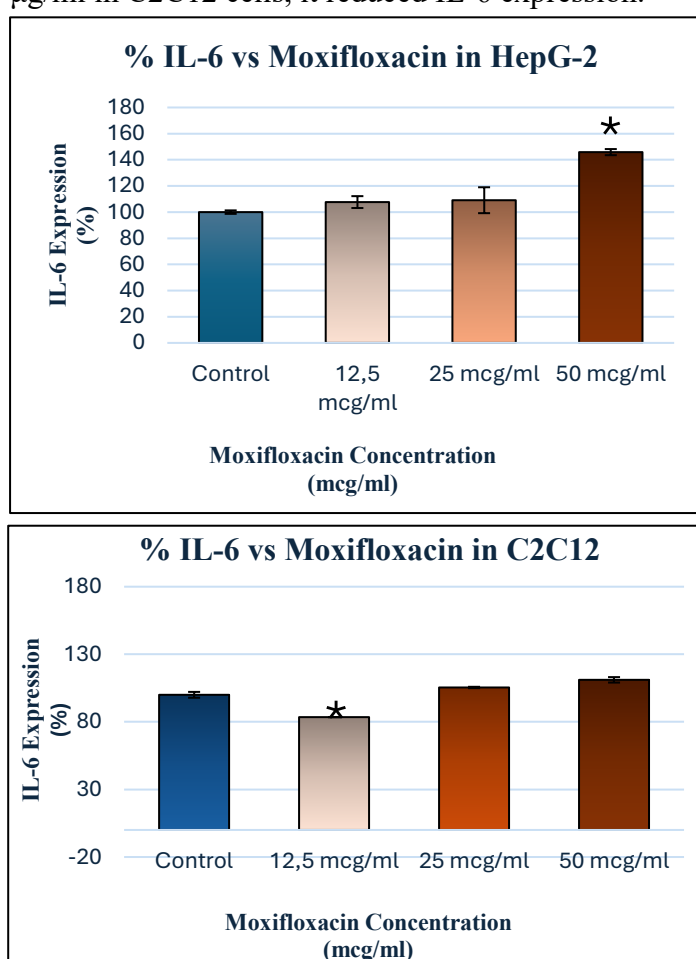


**Figure 3.6:** Relative percentage expression of IL-6 in C2C12 and HepG-2 cells treated with fluoroquinolones (Moxifloxacin) at different concentrations 12.5, 25, and 50 $\mu\text{g/ml}$ . The data is presented as mean  $\pm$  SD represented with error bars, ( $n = 3$ ), and the asterisk (\*) represents the statistical difference between the test compounds and the control at ( $p < 0.05$ ).

In HepG2 cells, ciprofloxacin treatment demonstrated inconclusive linearity in IL-6 expression, with minimal variability observed across successive samples within each concentration. In contrast, ciprofloxacin treatment in C2C12 cells exhibited a dose-dependent increase in IL-6 expression, though the levels did not exceed those of the control. Notably, at 12.5  $\mu\text{g}/\text{ml}$ , ciprofloxacin induced significantly lower IL-6 expression compared to the control in both HepG2 and C2C12 cells. These findings suggest an IL-6 lowering effect from moxifloxacin and ciprofloxacin in lower concentrations until higher concentrations gradually lose this effect and match the untreated controls.

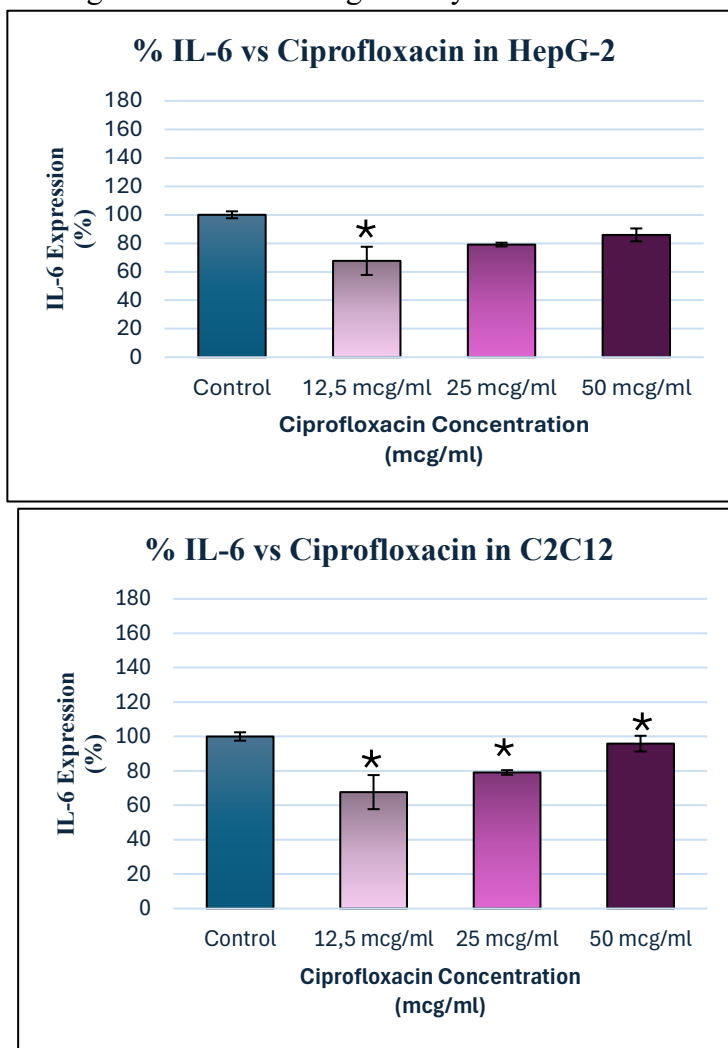


**Figure 3.7:** Relative percentage expression of IL-6 in C2C12 and HepG-2 cells treated with fluoroquinolones (Ciprofloxacin) at different concentrations 12.5, 25, and 50 $\mu\text{g}/\text{ml}$ . The data is presented as mean  $\pm$  SD represented with error bars, ( $n = 3$ ), and the asterisk (\*) represents the statistical difference between the test compounds and the control at ( $p < 0.05$ ).

### 3.3.2. Relative GLUT-4 Expression

Figure 3.8 depicts the relative percentage expression of GLUT-4 in C2C12 and HepG2 cells following treatment with fluoroquinolones, specifically moxifloxacin and ciprofloxacin, at concentrations of 12.5, 25, and 50 µg/ml. In skeletal muscle cells (C2C12), treatment with both moxifloxacin and ciprofloxacin at 50 µg/ml resulted in statistically significant differences in mean GLUT-4 expression compared to the control, with both compounds inducing a pronounced increase in GLUT-4 expression that substantially exceeded control levels. However, at lower concentrations (12.5 and 25 µg/ml), the effects of ciprofloxacin and moxifloxacin on GLUT-4 expression exhibited inconclusive linearity and minimal deviation from the control, suggesting a lack of response below a threshold.

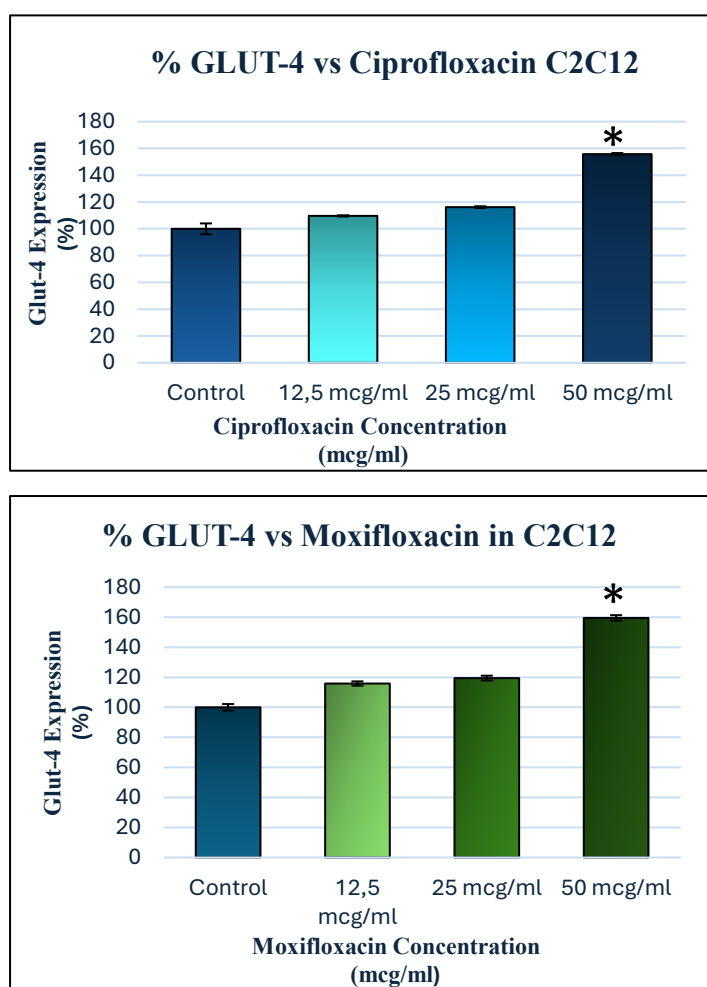


**Figure 3.8:** Relative percentage expression of GLUT-4 in C2C12 cells treated with fluoroquinolones (Ciprofloxacin and Moxifloxacin) at different concentrations 12.5, 25, and 50µg/ml. The data is presented as mean ± SD represented with error bars, (n = 3), and the asterisk (\*) represents the statistical difference between the test compounds and the control at (p < 0.05).

### 3.3.3. AKT Expression

Figures 3.9 to 3.10 illustrate the percentage expressed of AKT in C2C12 and HepG2 cells after treatment with fluoroquinolones (moxifloxacin and ciprofloxacin) at varying concentrations of 12.5, 25, and 50 µg/ml. Figure 3.9 shows greater AKT expression in HepG-2 cells than for C2C12 compared to their respective controls whose wells did not contain moxifloxacin. At 12.5µg/ml and 25µg/ml Moxifloxacin shows no effect on % AKT expression relative to the control in C2C12 cells until at 50 µg/ml where we observe a statistically significant increase in AKT expression. In HepG-2 cells, all concentrations moxifloxacin increased AKT expressions albeit slightly. The AKT expression increases linearly with moxifloxacin concentration in HepG-2, indicating a dose-dependent correlation.

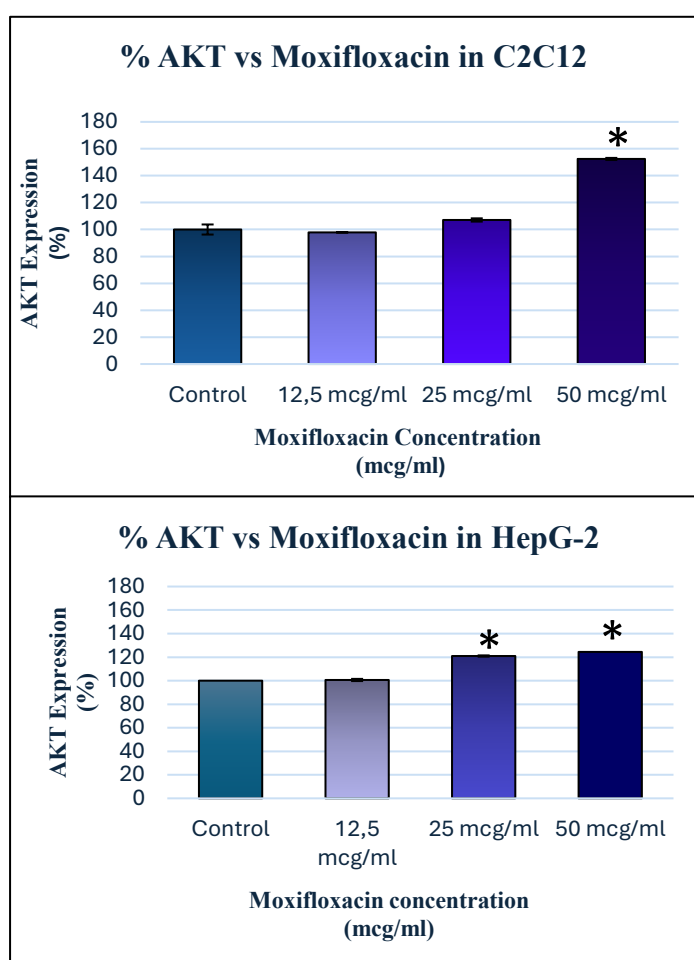


**Figure 3.9:** Relative percentage expression of AKT in C2C12 and HepG-2 cells treated with fluoroquinolones (Moxifloxacin) at different concentrations 12.5, 25, and 50µg/ml. The cells presented as mean ± SD represented with error bars, (n = 3). The asterisk (\*) represents the statistical difference between the test compounds and the control at (p < 0.05).

Ciprofloxacin demonstrated a linear dose-dependent relationship between concentration and the percentage of AKT expression in both C2C12 and HepG2 cell lines. Specifically, in HepG2 cells, a concentration of 50 µg/ml resulted in significantly higher AKT expression compared to the control. In C2C12 cells, ciprofloxacin exhibited a lower percentage of AKT expression relative to the control at a concentration of 12.5 µg/ml; however, at 50 µg/ml, AKT expression increased slightly above that of the control. Notably, the majority of the data points, with the exception of the 50 µg/ml concentration in C2C12 cells, displayed statistically significant differences in mean AKT expression compared to the control. These findings suggest a concentration-dependent modulation of AKT expression by ciprofloxacin, with varying effects across different cell types.

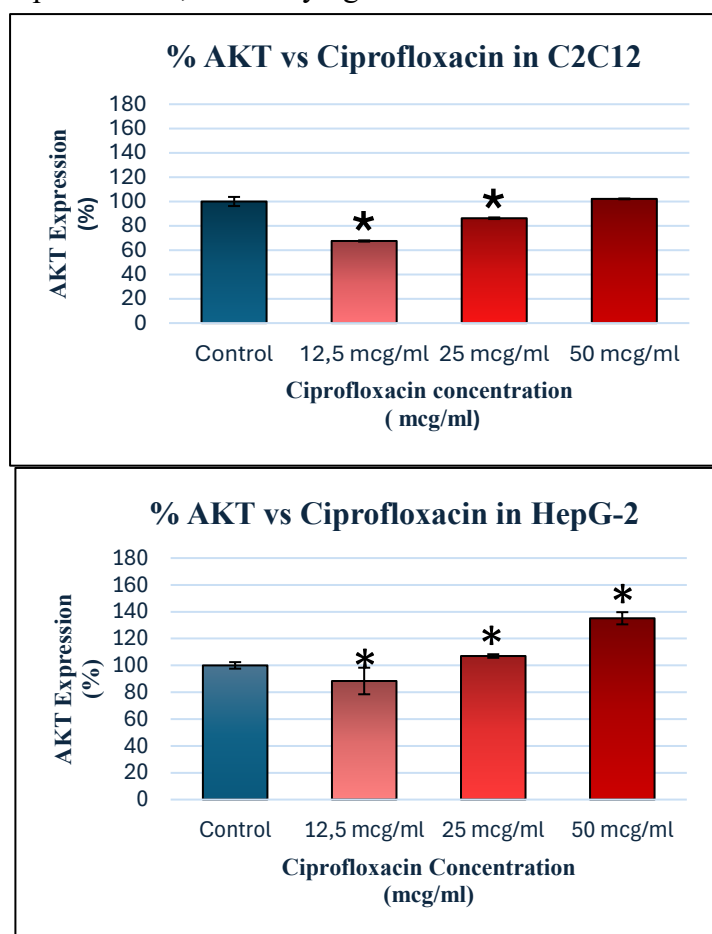


**Figure 3.10:** Relative percentage expression of AKT in C2C12 and HepG-2 cells treated with fluoroquinolones (ciprofloxacin) at different concentrations of 12.5, 25, and 50µg/ml . The cells presented as mean ± SD represented with error bars, (n = 3). The asterisks (\*) represents the statistical difference between the test compounds and the control at (p < 0.05).

---

### 3.4. Non-cell Based Assays

#### 3.4.1. $\alpha$ -Amylase Inhibition Assay

Figure 3.11 demonstrates the evaluation of Fluoroquinolones and Acarbose on  $\alpha$ -Amylase Inhibition Using the DNSA Method. The inhibitory effects of fluoroquinolones (gatifloxacin, moxifloxacin, ciprofloxacin, and lomefloxacin) and acarbose on  $\alpha$ -amylase enzyme activity were evaluated using an *in vitro* assay based on the 3,5-dinitrosalicylic acid (DNSA) method. The assay was conducted at concentrations of 12.5, 25, and 50  $\mu\text{g/ml}$ . The results, presented in Figure 3.11, demonstrate the percentage inhibition of  $\alpha$ -amylase by these compounds. Statistical significance of the differences between the mean percentage inhibitions for all compounds and acarbose, relative to the control (considered as zero percentage inhibition), was assessed ( $p < 0.05$ ). The  $\text{IC}_{50}$  values for all four fluoroquinolones and acarbose are detailed in Table 3.1, with ciprofloxacin exhibiting the highest potency given its lower  $\text{IC}_{50}$  among the fluoroquinolones.

Figure 3.11 shows that all compounds showed significant inhibitory activity comparable to Acarbose, though none exceeded its potency. Higher concentrations of each fluoroquinolone would be required to achieve effects equivalent to acarbose. A strong dose-dependent correlation was observed, with increased concentrations leading to greater  $\alpha$ -amylase inhibition. This was further supported by visual changes in test tube colour intensity, where higher concentrations corresponded to a colour change, suggesting enzyme inhibition. Specifically, gatifloxacin exhibited reduced inhibitory activity compared to Acarbose, while lomefloxacin demonstrated effects closer to the standard drug. However, neither compound surpassed acarbose in potency. Both compounds maintained a clear dose-dependent relationship, with higher concentrations resulting in stronger  $\alpha$ -amylase inhibition.

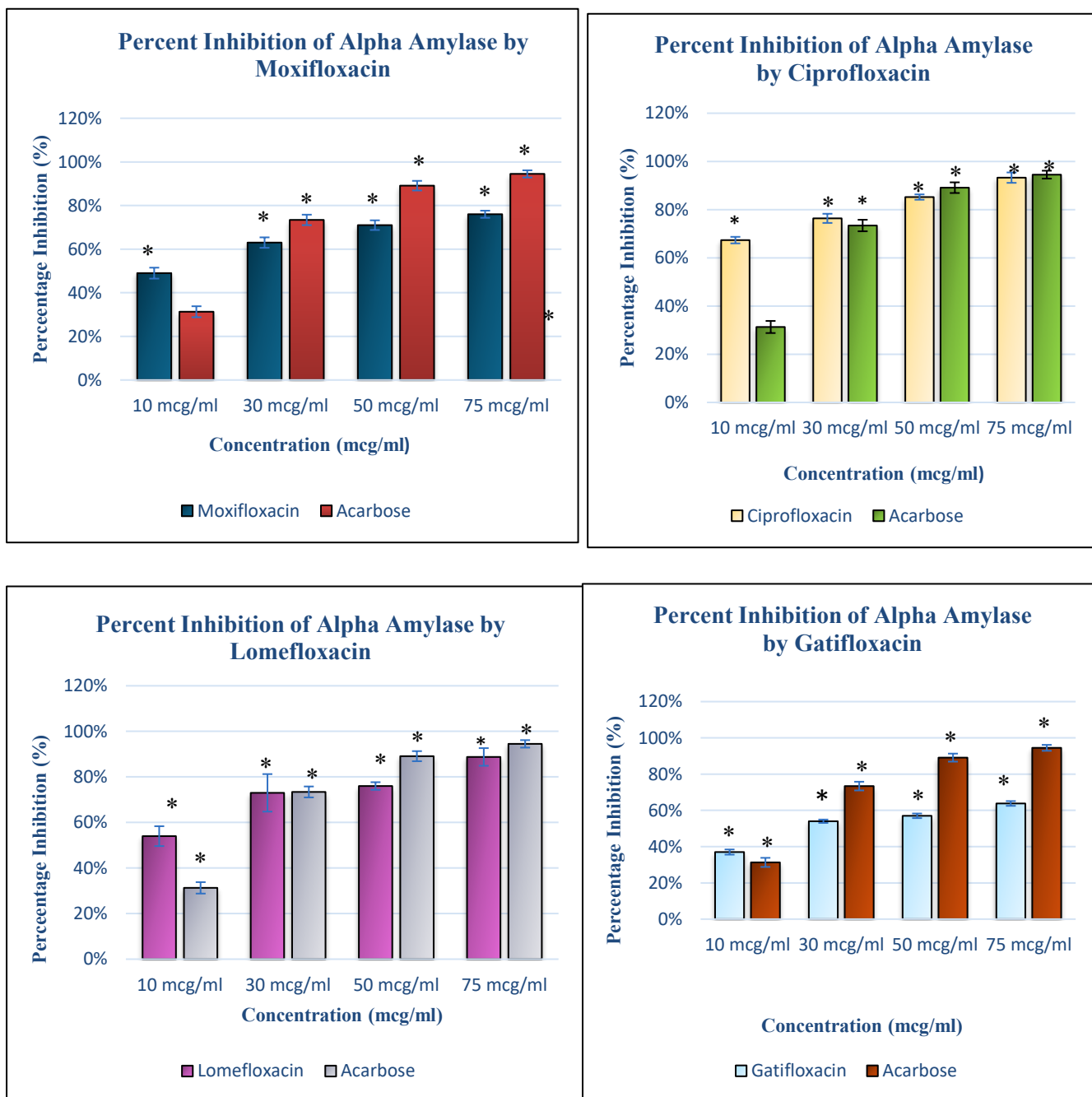


**Figure 3.11:** The inhibition of  $\alpha$ -amylase activity by fluoroquinolones (Ciprofloxacin, moxifloxacin, Lomefloxacin, and Gatifloxacin) at different concentrations 10, 30, 50, and 75 $\mu$ g/ml.  $\mu$ g/ml). The results are represented in a clustered column. The control is set at 0%. Data are presented as mean  $\pm$  standard deviation values. The error bars correspond to the standard errors of the means and asterisks (\*) indicate significant statistical differences relative to the control experiment ( $p$ -value  $\leq 0.05$ ).

---

**Table 3.1:** The IC<sub>50</sub> concentrations for the Fluoroquinolones and acarbose obtained from the alpha-amylase inhibitory assay

<b>Compound</b>	<b>IC-50 for <math>\alpha</math>-amylase</b>
Acarbose	51 $\mu\text{g/ml}$
Lomefloxacin	80 $\mu\text{g/ml}$
Ciprofloxacin	64 $\mu\text{g/ml}$
Gatifloxacin	324 $\mu\text{g/ml}$
Moxifloxacin	175 $\mu\text{g/ml}$

---

### 3.4.2. $\alpha$ -glucosidase Inhibition Assay

The inhibitory effects of fluoroquinolone (moxifloxacin, lomefloxacin, ciprofloxacin, and gatifloxacin) on  $\alpha$ -glucosidase enzyme activity were evaluated using the p-nitrophenyl- $\alpha$ -D-glucopyranoside (PNPG) assay. The assay was conducted in the presence of fluoroquinolones at concentrations of 10, 30, 50, and 75  $\mu\text{g/ml}$ , and the results are presented in Figure 3.12. Mean percentage inhibition values for all compounds were corrected for background effects caused by solvents and solutes, with the negative control set at zero percentage inhibition. The  $\text{IC}_{50}$  values for the fluoroquinolones and acarbose are summarised in Table 3.1.

Moxifloxacin exhibits the lowest  $\text{IC}_{50}$  among the fluoroquinolone derivatives, indicating its relatively higher potency. Moxifloxacin showed lower inhibitory activity compared to Acarbose, while lomefloxacin exhibited activity more closely resembling the reference compound. However, neither compound surpassed the potency of acarbose, suggesting that higher doses would be required to achieve comparable inhibition. Both compounds displayed a clear dose-dependent relationship, with increased concentrations correlating strongly with enhanced  $\alpha$ -glucosidase inhibition. Notably, the percentage inhibition between 10  $\mu\text{g/ml}$  and 30  $\mu\text{g/ml}$  showed negligible differences for both compounds, indicating that these concentrations may be below the threshold required for observable linear enzyme inhibition. Similarly, ciprofloxacin and gatifloxacin were evaluated for their inhibitory effects.

Ciprofloxacin exhibited marginally better activity than Acarbose at lower concentrations (10–30  $\mu\text{g/ml}$ ), while gatifloxacin showed significantly lower inhibition compared to the standard drug. Both compounds demonstrated a dose-dependent correlation, though the improvement in percentage inhibition was minimal: ciprofloxacin yielded 44% inhibition at 10  $\mu\text{g/ml}$  and 51% at 75  $\mu\text{g/ml}$ , while gatifloxacin showed 29% inhibition at 10  $\mu\text{g/ml}$  and 37% at 75  $\mu\text{g/ml}$ . These results indicate that, although both compounds possess some inhibitory capacity, their efficacy remains limited compared to acarbose. In summary, moxifloxacin demonstrated the highest potency among the fluoroquinolones, though none of the compounds exceeded the inhibitory efficacy of acarbose. All compounds exhibited a dose-dependent relationship, with higher concentrations leading to increased  $\alpha$ -glucosidase

inhibition. However, the overall inhibitory capacity of the fluoroquinolones was limited compared to the reference compound acarbose.

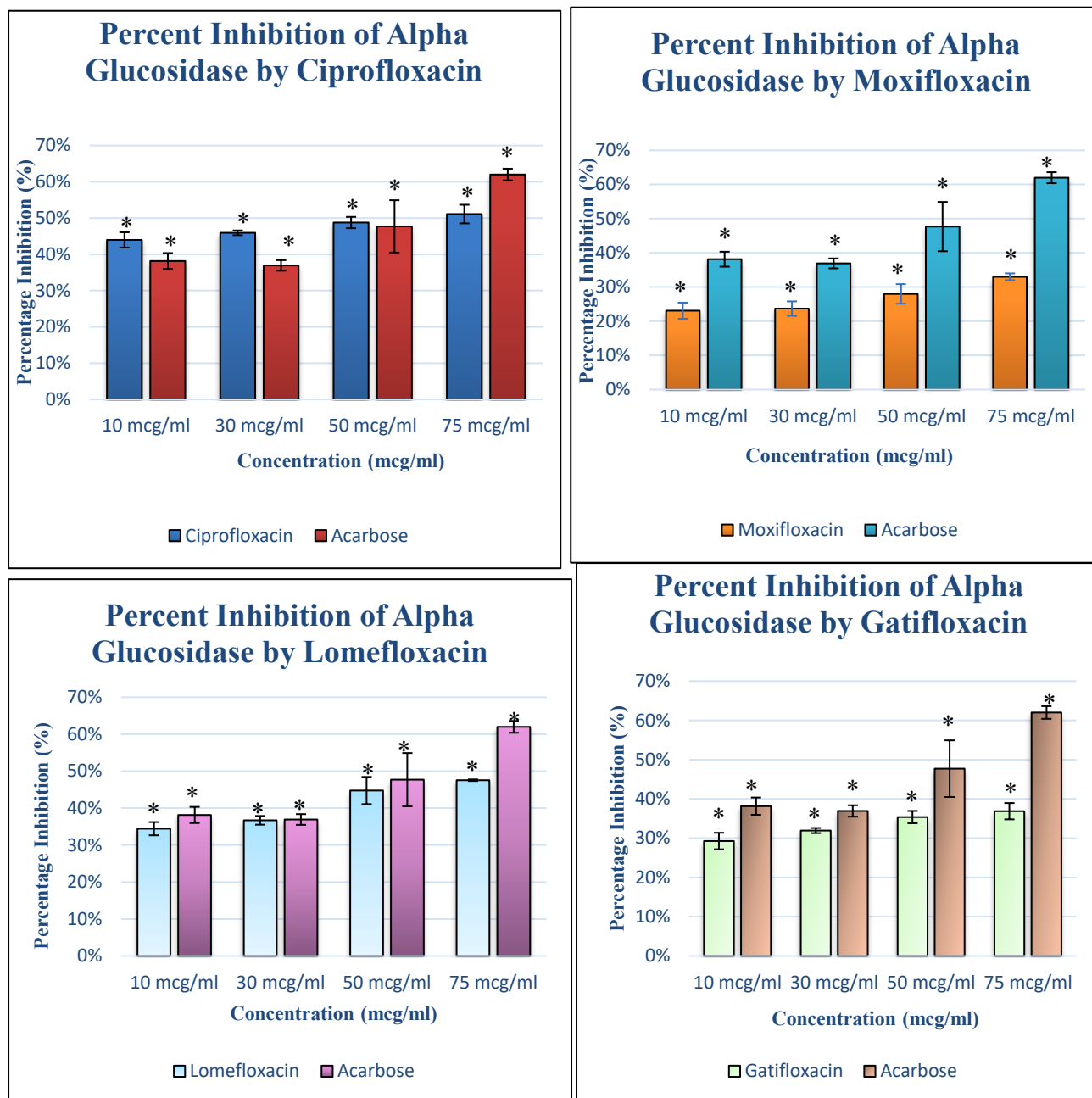


**Figure 3.12:** The inhibition of  $\alpha$ -glucosidase activity by fluoroquinolones (Ciprofloxacin and Moxifloxacin, Lomefloxacin, and Gatifloxacin) at different concentrations, 10, 30, 50, and 75  $\mu\text{g/ml}$ .  $\mu\text{g/ml}$ ). The results are represented in a clustered column. The Control is set at 0%. Data are presented as mean  $\pm$  standard deviation values. The error bars correspond to the standard errors of the means and asterisks (\*) indicate significant statistical differences relative to the control experiment.

---

**Table 3.2:** The IC<sub>50</sub> concentrations for the Fluoroquinolones and acarbose obtained from the alpha-glucosidase inhibitory assay.

<b>Compound</b>	<b>IC-50 for <math>\alpha</math>-Glucosidase</b>
Acarbose	18 $\mu$ g/ml
Lomefloxacin	54 $\mu$ g/ml
Ciprofloxacin	45 $\mu$ g/ml
Gatifloxacin	37 $\mu$ g/ml
Moxifloxacin	20 $\mu$ g/ml

---

### 3.5. In Silico Docking

In silico modelling aimed to predict, analyse, and simulate drug-receptor interactive processes using the computational tool AutoDockTools, aiming to corroborate with or contrast against laboratory experimental findings. This approach proved invaluable for predicting molecular interactions and binding affinities, elucidating the structure-activity relationships (SARs) between fluoroquinolones and glycaemic targets, and providing greater mechanistic insights.

Docking results for Moxifloxacin and Ciprofloxacin on various enzymes and receptors revealed detailed binding conformations and thermodynamic favourability, offering a deeper understanding of their inhibitory or inductive capacities and potential therapeutic applications. Overall, in silico modelling provided detailed insights into the binding mechanisms and inhibitory capacities of Moxifloxacin and Ciprofloxacin across multiple targets.

These findings highlighted the potential therapeutic applications of fluoroquinolones. The results include the ligand-receptor complexes generated from the docking software and the properties behind the binding geometries. Ciprofloxacin and Moxifloxacin formed complexes against various glycaemic targets, which were stabilised by strong non-covalent interactions, namely H-bonds and electrostatic attraction.

### 3.5.1. $\alpha$ -amylase

Figure 3.13 and Table 3.3 show the docking profile of Ciprofloxacin and Moxifloxacin against  $\alpha$ -amylase. Moxifloxacin failed to form a stable docking complex, while Ciprofloxacin exhibited a binding conformation stabilised by non-covalent interactions. Specifically, an H-bond formed between the cationic amine of Lys201A and the carboxyl anion of Ciprofloxacin, supported by electrostatic attraction and Van der Waals forces involving the quinolone backbone and piperazine ring against Tyr199A and Phe159A. The binding energy ( $<0$ ) indicated thermodynamic favourability, and the inhibition constant of 24.38  $\mu\text{M}$  suggested significant inhibitory capacity. The low RMSD value further confirmed minimal variability between predicted and actual cluster simulations, underscoring the reliability of the docking results.

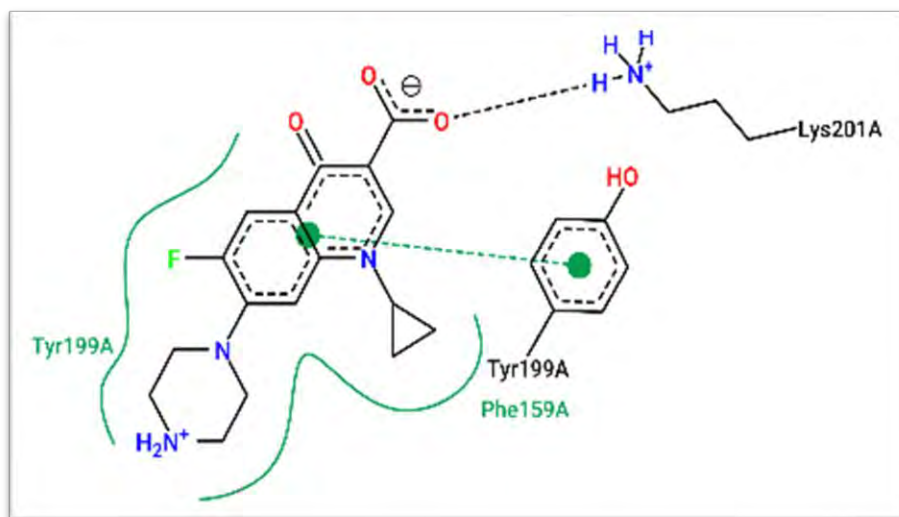


**Figure 3.13:** Ligand-Receptor complex between Ciprofloxacin and Alpha-amylase

**Table 3.3:** Docking profile of fluoroquinolones against alpha-amylase

Compound	RMSD (Ångström.)	Binding Energy (kcal/mol)	Inhibition Constant ( $\mu\text{M}$ )	Active Site Residues
Ciprofloxacin	1,02	-6,29	24,38	Lys201A, Tyr199A, Phe159A

Moxifloxacin	N/A	N/A	N/A	N/A
--------------	-----	-----	-----	-----

### 3.5.2. Phosphoinositide-3-Kinase

Figures 3.14, 3.15 and Table 3.4 show the docking profile of Ciprofloxacin and Moxifloxacin against PI3K. Both compounds formed thermodynamically favourable complexes. Moxifloxacin was stabilised by an H-bond between the cationic amine of Gln629A and its carboxyl anion, while Ciprofloxacin formed two H-bonds: one between the cationic secondary nitrogen and the carboxyl group of Glu880A, and another between the carboxyl anion and the cationic amine of Arg849A. The electron-deficient quinolone backbone of Ciprofloxacin also attracted the electron-dense aromatic group of Phe694A. Ciprofloxacin demonstrated superior binding activity, as evidenced by its lower RMSD, free binding energy, and inhibition constant, suggesting it is a more potent inhibitor of PI3K. Targeting PI3K with activators or modulators can enhance insulin sensitivity and improve glycaemic control.

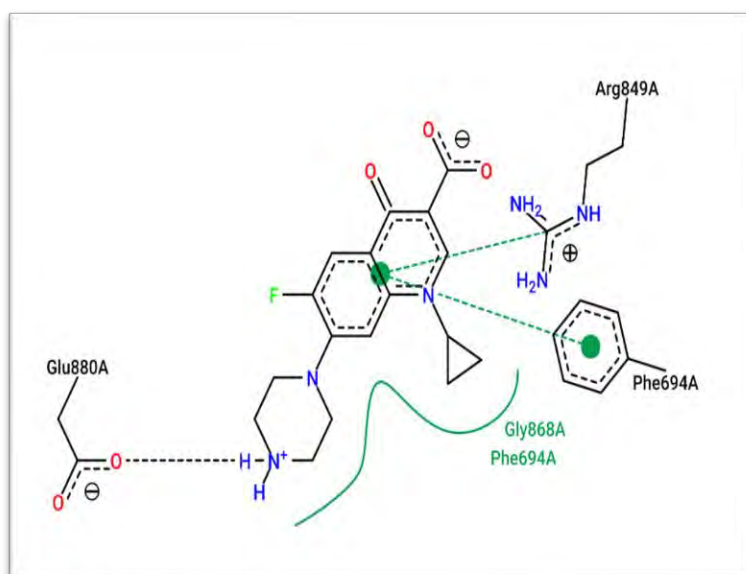


**Figure 3.14:** Ligand-Receptor Complex between Ciprofloxacin and PI3K

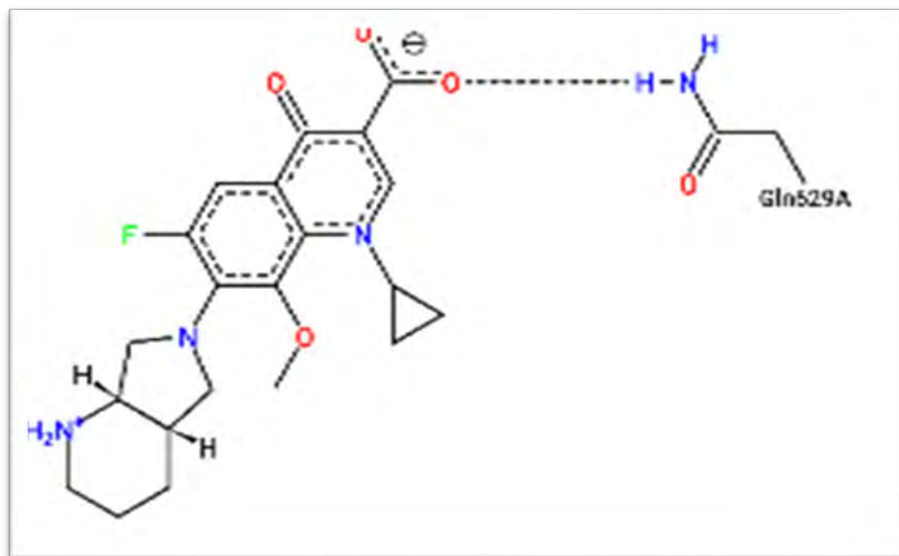


**Figure 3.15:** Ligand-Receptor Complex between Moxifloxacin and PI3K

**Table 3.4:** Docking profile of fluoroquinolones against PI3K

Compound	RMSD (Ångström)	Binding Energy (kcal/mol)	Inhibition Constant ( $\mu$ M)	Active Site Residues
Ciprofloxacin	0,81	-17,32	4,34	Phe694A, Arg849A, Glu880A, Gly868A
Moxifloxacin	2,3	-10,16	35,46	Gln629A

---

### 3.5.3. $\alpha$ -glucosidase

Figure 3.16 and Table 3.5 show the docking profile of Ciprofloxacin and Moxifloxacin against  $\alpha$ -glucosidase. Ciprofloxacin failed to form a stable complex, whereas Moxifloxacin exhibited a binding conformation stabilised by H-bonds between the cationic amines of Leu287A and Asn258A and its carboxyl anion. The octahydro-6H-pyrrolo[3,4-b]pyridin-6-yl group of Moxifloxacin formed an additional H-bond with Pro223A, while the electron-deficient quinolone backbone attracted Phe225A. The binding energy ( $<0$ ) and inhibition constant ( $31.58 \mu\text{M}$ ) indicated significant inhibitory capacity, with a low RMSD confirming minimal variability between predicted and actual simulations. This suggested that Moxifloxacin could effectively inhibit  $\alpha$ -glucosidase activity.

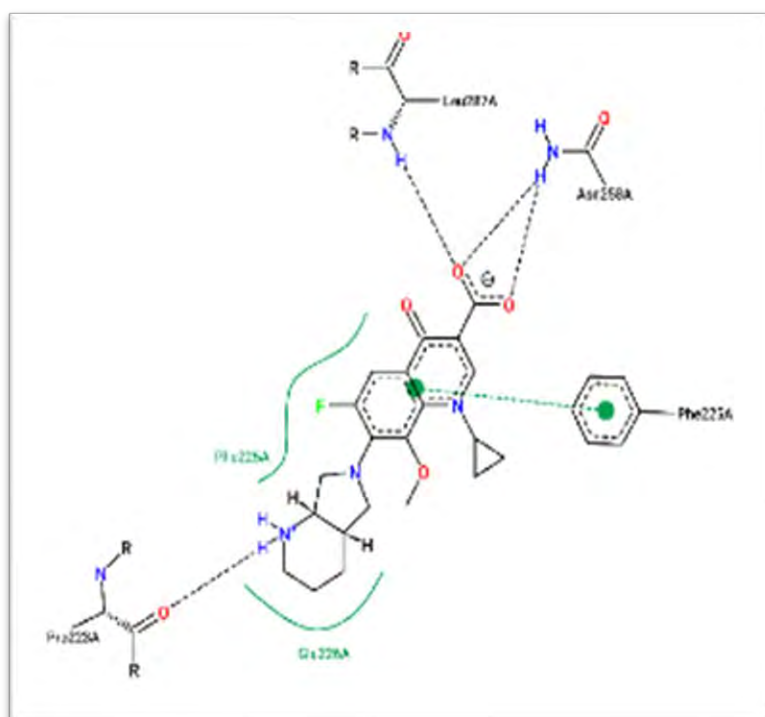


**Figure 3.16:** Ligand-Receptor Complex between Moxifloxacin and Alpha-glucosidase

---

**Table 3.5:** Docking profile of fluoroquinolones against alpha-glucosidase

<b>Compound</b>	<b>RMSD (Ångström.)</b>	<b>Binding Energy (Kcal/mol)</b>	<b>Inhibition Constant (<math>\mu</math>M)</b>	<b>Active Site Residues</b>
Ciprofloxacin	N/A	N/A	N/A	N/A
Moxifloxacin	9.1	-10.23	31.58	Glu226A, Leu287A, Pro223A, Phe225A, Asn258A

---

### 3.5.4. Insulin Receptor

Figure 3.17 and Table 3.6 show the docking profile of Ciprofloxacin and Moxifloxacin against the insulin receptor. These docking studies with the insulin receptor revealed that both compounds formed thermodynamically favourable complexes. Ciprofloxacin was stabilised by an H-bond between the hydroxyl group of Tyr1087A and its carboxyl anion, along with Van der Waals interactions involving the cyclopropyl moiety and piperazine ring. Moxifloxacin, on the other hand, formed an H-bond between its ketone oxygen and the amine nitrogen of Met1079A, with additional Van der Waals interactions involving the cyclopropyl moiety and quinolone backbone. Moxifloxacin demonstrated superior binding activity, as evidenced by its lower RMSD, free binding energy, and inhibition

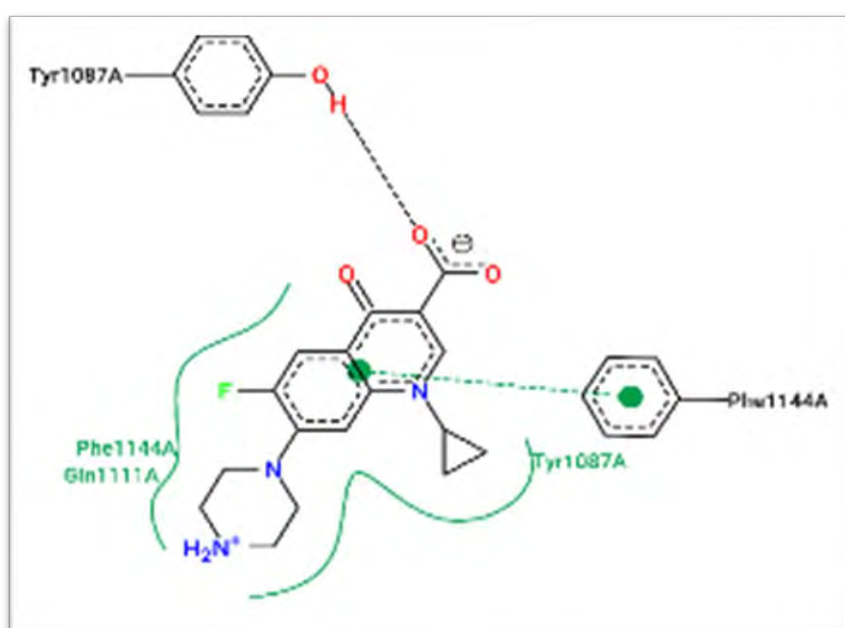


**Figure 3.17:** Ligand-receptor complex between Ciprofloxacin and Insulin Receptor

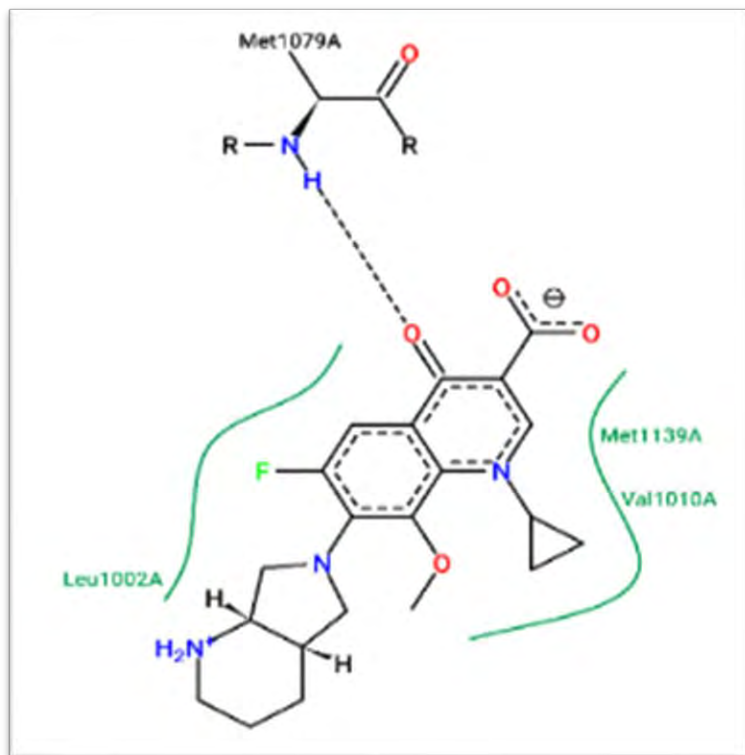


**Figure 3.18:** Ligand-receptor complex between Moxifloxacin and Insulin Receptor

**Table 3.6:** Docking profile of fluoroquinolones against Insulin Receptor

Compound	RMSD (Ångström.)	Binding Energy (Kcal/mol)	Inhibition Constant (μM)	Active Site Residues
Ciprofloxacin	8.1	-6.19	28.96	Phe1144A, Gln1111A, Tyr1087A
Moxifloxacin	0.80	-9.81	19.24	Leu1002A, Val1010A, Met1139A, Met1079A

---

## Chapter 4: Discussion

The central goal of the study was to investigate the role fluoroquinolones play in glucose metabolism. Given the widespread literature regarding how these drugs induce glycaemic aberrations in a clinical setting, it is of vital importance to provide additional data that supplements our understanding regarding the precise mechanisms by which these glycaemic effects arise.

Glycaemic effects are downstream from a change along various pathways through which glucose is metabolised, ranging from the start where polysaccharides are broken down into monosaccharides, to the end where glucose is excreted renally. Each step, including the intermediates, represented areas of drug intervention aimed at treating glucose-related conditions such as diabetes mellitus type 2. The first step for this investigation was the beginning stage, where glucose is absorbed, and its polymeric forms are digested. Alpha-glucosidase and  $\alpha$ -amylase both facilitate the early steps of glucose entry, and therefore, their inhibition was a significant target candidate for fluoroquinolones. Pancreatic amylase cleaves  $\alpha$ -1,4 bonds of starch, subsequently releasing maltose. And alpha-glucosidase, a brush border enzyme, further hydrolyses maltose to glucose. While both enzymes share a  $(\beta/\alpha)_8$  barrel catalytic domain and hydrolyse  $\alpha$ -glycosidic bonds, their functional roles, substrate preferences, and reaction mechanisms differ significantly. Alpha-amylase breaks large polysaccharides into smaller units, whereas alpha-glucosidase works at the ends of these molecules to release free glucose. Both *in vitro* and *in silico* tests were conducted to establish experimental and theoretical bases to rule out or validate the inhibitory action of fluoroquinolones against these pharmacological targets. Convergence in the data would demonstrate a high probability of a real connection between the drug and the target.

The methods for evaluating fluoroquinolones' glycaemic effects were chosen for their reproducibility, sensitivity, and validation. AutoDockTools (ADT) 1.5.7 was used for precise molecular docking, supported by customizable parameters and extensive benchmarking. Enzyme inhibition assays, including Sigma Aldrich's  $\alpha$ -glucosidase (pnpG substrate) and DNSA for  $\alpha$ -amylase, provided quantifiable measures of inhibitory activity. For the results in Figures 3.11 and 3.12, fluoroquinolones were tested against  $\alpha$ -amylase and  $\alpha$ -glucosidase. Gatifloxacin, ciprofloxacin and moxifloxacin had distinct effects regarding their inhibitory capacity. Gatifloxacin demonstrated significant inhibitory activity for both  $\alpha$ -amylase and  $\alpha$ -glucosidase, similar to Moxifloxacin. Lomefloxacin, additionally, resembled ciprofloxacin in that it did not bear unique characteristics for comparison. This similarity in activity was expected, given the clinical, structural and classification data for both compounds. Both

---

---

compounds are 2nd-generation fluoroquinolones with nominal differences in their physicochemical properties.

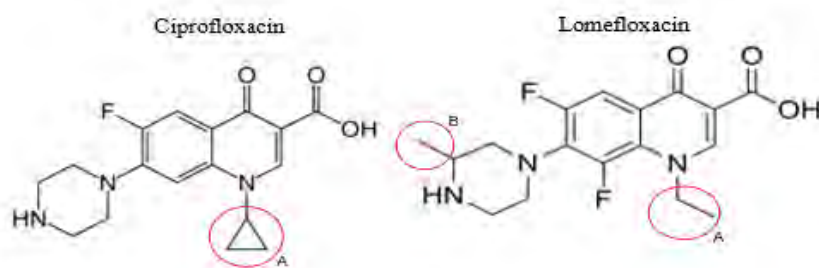


**Figure 4.1:** Structural similarity of Ciprofloxacin and lomefloxacin

Figure 4.1 shows the 2 minor differences in structure between Ciprofloxacin and Moxifloxacin. In circle A, there is a cyclopropyl group in position 1 for Ciprofloxacin vs an Ethyl Group in position 1 for Lomefloxacin. In Circle B, Lomefloxacin has a methyl group on the 3<sup>rd</sup> carbon of the piperazine ring, whereas there are no additional substituents on the piperazine ring on Ciprofloxacin. While most of these compounds were less potent than acarbose, with the exception being moxifloxacin in alpha-glucosidase, their volume of distribution (Vd) is higher, and therefore the duration of action upon administration at a clinical level may be more favourable [193]. Moreover, acarbose has an overall lower systemic bioavailability than fluoroquinolones. A higher Vd generally corresponds to safer dosage frequencies, where a patient takes one dose a day in comparison to three oral doses of acarbose [152]. The inhibitory capacity of ciprofloxacin and moxifloxacin was also proven to be statistically significant ( $P < 0.05$ ) in comparison to the negative control. Ciprofloxacin possessed inconclusive inhibitory capacity against alpha-glucosidase in silico but achieved a successful docking complex against alpha-amylase. Moxifloxacin, contrarily, yielded the opposite outcomes, with the compound failing against alpha-amylase but succeeding against alpha-glucosidase. Whilst the performance on simulated docking software did not produce a one-to-one match, there are significant correlations between the inhibition data and the strengths of the drug-receptor interaction. Moxifloxacin, which had an impressive IC-50 of 20  $\mu\text{g/ml}$  – comparable potency to standard acarbose – on alpha-glucosidase, similarly yielded an optimal docking profile. The zwitterionic forms of the molecule had strong electrostatic attractive forces and H bonds on three different sites on the ligand's structure, namely H-bonds between the cationic amines of Leu287A, Asn258A and Moxifloxacin's carboxyl anion on position 3. The octahydro-6h-pyrrolo [3,4-b]-pyridine-6-yl group bonded to the 7<sup>th</sup> carbon of

Moxifloxacin has its secondary amine similarly H-bonded to the aldehyde oxygen of Pro223A. Importantly, the functional groups involved are also implicated in the general bactericidal activity of moxifloxacin. Therefore, chemical derivatisation of moxifloxacin to mask antimicrobial moieties may counterproductively risk nullifying the anti-diabetic properties [153]. Ciprofloxacin, similarly to moxifloxacin, had its carboxyl anion on position 3 attracted through H-bonds to the cationic amine of the Lys201A residue of alpha-amylase. The carboxylic group in position 3 is the biologically active group contributing to enzyme inhibition for both compounds. The diagram below shows the basic structural similarities between moxifloxacin and Ciprofloxacin.

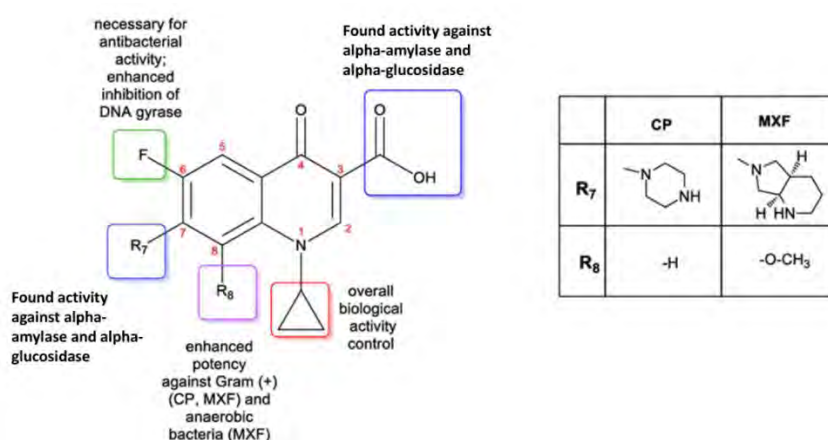


**Figure 4.2:** Moxifloxacin and Ciprofloxacin structure-activity relationship [154]

What we have established so far is that fluoroquinolones can influence the beginning stage of glucose control, namely, the hydrolytic pathways by which complex polysaccharides and disaccharides are broken down into glucose. In comparison to standard inhibitors of carbohydrate hydrolases such as miglitol and acarbose, fluoroquinolones possess superior pharmacokinetic profiles in several key areas. They demonstrate rapid and nearly complete absorption from the gastrointestinal tract, with high bioavailability (e.g., ciprofloxacin: ~70%, moxifloxacin: ~90%), whereas acarbose and miglitol have poor systemic absorption and primarily act locally in the GI tract, accounting for the prevalence adverse GIT effects such as flatulence, bloating, diarrhoea, and abdominal pain. Fluoroquinolones also have a higher volume of distribution, enabling extensive tissue penetration and effective targeting of cellular compartments, while acarbose and miglitol are confined to the GI tract with minimal systemic effects. Additionally, fluoroquinolones have moderate to long half-lives (e.g., ciprofloxacin: ~4 hours, moxifloxacin: ~12 hours), allowing for less frequent dosing compared to the short half-lives of

---

acarbose and miglitol (~2 hours), which require administration with each meal. Furthermore, fluoroquinolones are partially metabolised in the liver and excreted renally or via bile, whereas acarbose and miglitol undergo minimal metabolism and are excreted primarily in faeces or urine. These pharmacokinetic advantages make fluoroquinolones more effective for systemic and localised diabetes management [168].

Additional laboratory studies were performed to investigate further effects on the intermediate stages of glucose control. The primary stages here concern the uptake and utilisation of glucose in the skeletal muscle and liver. Glucose uptake takes place through facilitated diffusion mediated by GLUT transporters. Facilitated diffusion is the most common process used by most body tissues, including the liver, muscle, and adipose tissue, not requiring ATP and allows glucose to pass through the cell membrane down a concentration gradient. Utilisation refers to the subsequent processes by which glucose is transformed and recruited to perform various intracellular functions, such as the provision of nutrients and metabolic intermediates. The glucose uptake assay was therefore conducted to investigate the effect that moxifloxacin and ciprofloxacin had on mediating glucose entry into target cells. The mammalian cell culturing protocol, adapted from Abcam's standardised protocol, ensured stable cell growth with optimal viability, using high-quality media, sterile techniques, and controlled conditions, which facilitated the glucose utilisation assay of fluoroquinolones against skeletal and liver cells. Skeletal muscle is responsible for approximately 75-80% of glucose uptake, while adipose and liver cells contribute significantly less [155]. This insulin-driven glucose uptake is crucial for maintaining normal blood glucose concentrations, and its impairment due to insulin resistance is a key characteristic of diabetes mellitus. The effect fluoroquinolones have on glucose uptake can account for how they elicit dysglycaemia.

In figures 3.2 and 3.3, the tested compounds exhibited glucose-lowering effects exceeding the baseline media glucose concentrations in both cell types. The majority of the compounds, however, did not exceed the glucose-lowering effect of insulin (only gatifloxacin 50µg/ml as the exception). 6 mmol/L of insulin showed a near triple-fold reduction in media glucose. Gatifloxacin showed the highest glucose-lowering effect, corroborating clinical data of hypoglycaemia in patients on that regimen [169]. Whilst this effect was promising, it was countered by its cytotoxicity. Non-toxicity is generally understood as a minimum cell viability of 80%, and all concentrations of gatifloxacin from 12,5 to 100 µg/ml failed to meet that threshold [157]. Lower doses of Ciprofloxacin and Moxifloxacin, however,

---

do meet the threshold. Importantly, given that these low concentrations are sufficient to induce glucose uptake, the compounds increasingly fit the required biological activity as potential anti-diabetic candidates. Therefore, for subsequent assays, we focused only on Ciprofloxacin and gatifloxacin.

An intracellular surge in glucose concentration triggers insulin secretion. Insulin enhances glucose uptake in skeletal muscle, adipose tissue, and liver cells by activating PI3K, the downstream effects of which facilitate the translocation of the GLUT4 transporter to the cell surface. PI3K is an intermediary enzyme that links insulin signal transduction and the series of phosphorylation cascades that ultimately promote glucose regulation. Blocking PI3K, therefore, should block the insulin signalling pathway. Wortmannin irreversibly inhibits PI3K by binding to its catalytic subunit, preventing PIP3 production. PIP3 is essential for recruiting and activating AKT (protein kinase B) in the cell membrane [158]. By blocking PI3K, Wortmannin prevents AKT activation, a critical step for many insulin-mediated metabolic effects, including glucose uptake and glycogen synthesis.

The observation of glucose uptake occurring alongside PI3K inhibition suggests the presence of an alternative pathway mediating GLUT-4 expression. PI3K activity was evaluated through two methods: first, by using the known inhibitor Wortmannin on C2C12 and HepG-2 cells, and second, via direct docking interactions with moxifloxacin and ciprofloxacin. Results from Figures 3.4 and 3.5 demonstrate media glucose utilisation in cells pretreated with Wortmannin. Notably, media glucose utilisation decreased following the administration of moxifloxacin and ciprofloxacin, as indicated by higher glucose concentrations in the media compared to the control. This implies that moxifloxacin and ciprofloxacin may compound PI3K inhibition. This effect was, however, reversed as the concentration of both compounds increased in C2C12 cells. Put another way, these findings indicated that at lower concentrations, fluoroquinolones enhanced the inhibitory effects of wortmannin on glucose uptake in skeletal cells. However, beyond a specific threshold concentration, fluoroquinolones appeared to counteract the PI3K-inhibitory action of wortmannin, thereby promoting glucose uptake.

This biphasic response demonstrated a concentration-dependent interplay between fluoroquinolones and wortmannin in modulating glucose metabolism in the studied cell lines. In addition, the hypothesis of a biphasic metabolic effect is supported by literature that reports hypoglycaemia and hyperglycaemia in various patients [170]. While these effects superficially appear contradictory, it is well-documented that fluoroquinolones interact with other drugs and depending upon the unique properties of the drug-drug interaction, glucose metabolism is altered to yield an overall lower or

---

---

higher serum glucose concentration [171]. What has not been investigated in prior literature, however, was the attribution of the precise concentrations at which each of these effects changes from being glucose-increasing to glucose-lowering. Additional support for this purported biphasic pharmacodynamic hypothesis is enzyme competition, allosterically and then directly: i.e. the transition from allosteric activation to enzyme inhibition with increasing substrate concentration is a regulatory mechanism in which binding at an allosteric site initially enhances enzymatic activity but, at higher concentrations, induces inhibition. This dual behaviour arises from conformational changes in the enzyme's structure, which modulate substrate affinity or catalytic efficiency [172]. At low concentrations, allosteric activators stabilise the enzyme in a high-activity state, promoting catalysis. However, excessive binding at higher concentrations triggers inhibitory conformational shifts, serving as a feedback mechanism to prevent metabolic overactivity [173].

A well-documented example is phosphofructokinase-1 (PFK-1), a critical enzyme in glycolysis. PFK-1 is activated by low concentrations of fructose-6-phosphate and adenosine monophosphate (AMP), signalling low cellular energy. However, high concentrations of its product, fructose-1,6-bisphosphate, or elevated adenosine triphosphate (ATP) levels induce inhibitory conformational changes, ensuring glycolysis is regulated according to energy demands [174]. This mechanism highlights the precise control enzymes exert over metabolic pathways. In the context of Ciprofloxacin and Moxifloxacin, these compounds may act as substrates or modulators for certain enzymes, potentially influencing allosteric regulation. For instance, these fluoroquinolones could bind to allosteric sites on PI3K, initially enhancing activity at low concentrations but inhibiting it at higher concentrations.

These compounds in lower doses therefore act in the opposite way they do in the absence of wortmannin (i.e. figures 3.2 and 3.3). In other words, wortmannin reduces the efficacy of fluoroquinolones in part by interfering with glucose uptake that is downstream from PI3K/Akt signalling. Furthermore, docking results of moxifloxacin and ciprofloxacin demonstrated significant independent binding activity with PI3K. The moxifloxacin-PI3K complex formed a stable binding conformation supported by hydrogen bonds between the carboxyl anion at position 3 and the cationic amine of Gln629A. In the ciprofloxacin-PI3K complex, two hydrogen bonds were observed: one between the cationic secondary nitrogen and the carboxyl group of Glu880A, and another between the anionic carboxyl group at position 3 and the cationic amine groups of Arg849A. The covalent bond formed between wortmannin and PI3K, however, is stronger than these H-bonds because wortmannin

contains a highly reactive electrophilic group in its structure that allows it to form an irreversible bond with a specific nucleophilic residue in the PI3K enzyme, typically a lysine 802A residue in the catalytic domain [159]. The takeaway, therefore, from the cell-based and in silico data for PI3K is that moxifloxacin and ciprofloxacin require unbound PI3K to exert their glucose-controlling effects. This could be an additional mechanism by which diabetes type 2 symptoms can be controlled, along with its hypothesised stimulation of insulin secretion via beta cell potassium channel stimulation. Importantly, directly activating PI3K may bypass a key challenge in insulin-resistant patients: the decreased expression and activation of IRS proteins, which are required to stimulate PI3K before GLUT-4 translocation can commence. The diagram below shows the combined hypothesised mechanisms by which fluoroquinolones regulate glucose concentrations in beta cells and target cells.

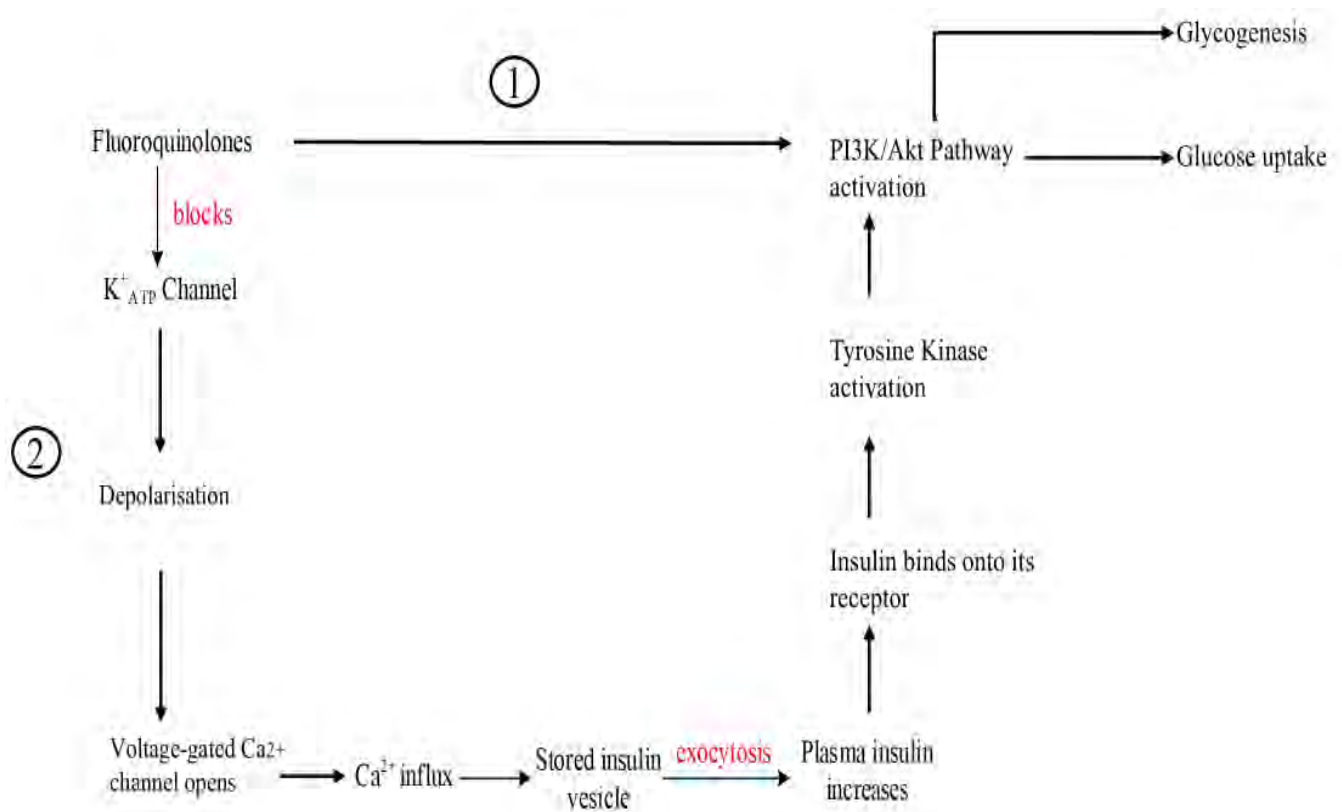


**Figure 4.3:** Pathway 1 illustrates the mechanism of action of fluoroquinolones on target cells. Fluoroquinolone binds to PI3K, activating the PI3K/Akt pathway. Pathway 2 illustrates the mechanism of action of fluoroquinolones in the pancreatic beta-cell. Fluoroquinolones first block the ATP-sensitive potassium channel. The closure of ATP-sensitive channels results in a subsequent opening of

---

the L-type voltage-gated calcium channel, resulting in the influx of calcium ions into the islet cells. Calcium ion triggers exocytosis of insulin [160].

An additional support for the hypothesis of PI3K activation could be observed in the In-Cell Elisa data. Figures 3.6 to 3.10 show the expression of AKT, GLUT-4, and IL-6 for moxifloxacin and ciprofloxacin for C2C12 and HepG-2 cells. AKT promotes the translocation of GLUT4 to the cell membrane, facilitating glucose uptake into skeletal muscle and fat cells. It also stimulates glycogen synthase kinase-3 (GSK-3), promoting glycogen synthesis. Expression of AKT and GLUT-4, therefore, is associated with these downstream glucose-regulatory mechanisms [175]. The results broadly showed diminished activity between 12,5 ug/ml and 25 ug/ml, indicating that low doses of these compounds reduced protein expression. Interestingly, 50 µg/ml of ciprofloxacin in skeletal muscle cells, however, began to show protein expression (AKT and GLUT-4), which began to exceed the control. Whilst most of the data may not have passed the Bonferroni T test for statistical significance, the protein expression linearly increased as the compound concentration increased. For GLUT-4 expression, ciprofloxacin and moxifloxacin passed the Bonferroni T test for statistical significance in skeletal cells. This statistical method controlled the risk of Type I errors (false positives) when performing multiple comparisons. The data, therefore, were statistically significant even after adjusting for the increased likelihood of errors due to multiple testing. The Bonferroni correction achieves this by dividing the original significance level (e.g.,  $\alpha = 0.05$ ) by the number of comparisons, creating a stricter threshold. What this indicated overall was increased Akt and Glut 4 expression at 50 ug/ml and likely above (by graphical extrapolation from observing the linear increases from 12,5 to 50 ug/ml).

Increased expression of AKT and GLUT-4 in skeletal muscle cells would offer significant clinical benefits for diabetic patients by enhancing glucose uptake and improving insulin sensitivity. This mechanism effectively lowers blood glucose concentrations and reduces insulin resistance, addressing core pathophysiological defects in T2DM. Such improvements would lead to better glycaemic control, reduced risk of long-term complications (e.g., neuropathy and retinopathy), and improved overall diabetes management. Additionally, this approach could reduce reliance on exogenous insulin, thereby lowering the risk of hypoglycaemia.

Finally, the traditional mechanism of PI3K/AKT activation is through insulin receptor activation. Moxifloxacin and Ciprofloxacin, therefore, docked against the insulin receptor to determine the potential binding geometries that would likely emerge in a biological system. The docking results for

---

---

these compounds on the insulin receptor showed formed stable complexes; Ciprofloxacin bound via hydrogen bonds (Tyr1087A) and Van der Waals forces (cyclopropyl and piperazine groups); Moxifloxacin stabilised the interaction through hydrogen bonds (Met1079A) and Van der Waals interactions (cyclopropyl). Both drugs exhibited negative binding energies, indicating spontaneous binding and demonstrated significant inhibitory capacity. However, Moxifloxacin showed stronger binding activity, evidenced by a lower RMSD, free binding energy, and inhibition constant, making it more effective in interacting with the insulin receptor compared to Ciprofloxacin. Whilst data indicating successful conformations may seem promising, the insulin receptors were not simulated under an insulin-resistant state. In such a state, the receptor's conformation is altered by abnormal post-translational modifications, such as excessive serine/threonine phosphorylation and glycation, which reduce its affinity for insulin and kinase activity [163]. Dimerisation, essential for receptor activation, is often impaired, preventing proper signalling. The insulin-binding site and allosteric regulatory sites may also be disrupted by oxidative stress, inflammation, or lipid accumulation, further reducing insulin binding. Additionally, oxidative stress and lipid-induced damage modify key residues, impairing receptor structure and function [164]. Therefore, the binding onto PI3K was a comparably better hypothesis for how fluoroquinolones elicit glucose-lowering effects under insulin-resistant states. Nevertheless, the direct binding onto the insulin receptor may still explain the incidence of glycaemic aberrations in patients who are prediabetic or do not yet have insulin resistance.

Fluoroquinolones could emerge as favourable antidiabetic drug candidates with a high volume of distribution and multiple mechanisms of action, such as improving insulin release, enhancing glucose uptake, and reducing glucose digestion and absorption. Through their ability to target multiple pharmacological sites, they are therefore envisaged to provide comprehensive glycaemic control. Their widespread distribution ensures effective targeting of key tissues, while the multi-mechanistic approach simplifies treatment regimens, improving patient adherence and reducing the risk of missed doses or errors. This strategy also minimises side effects and drug interactions compared to polypharmacy often observed in diabetes management. Furthermore, the synergistic effects of multiple mechanisms enhance therapeutic outcomes, and the single-drug approach is more cost-effective, improving patient quality of life by reducing the complexity of diabetes management [176].

Patients with T2DM on polypharmaceutical regimens often present with complex or advanced disease, requiring multiple pharmacologic agents to achieve glycaemic control and manage comorbidities. This

---

---

includes individuals with inadequate glycaemic control (e.g., regimens combining metformin, SGLT2 inhibitors, GLP-1 receptor agonists, and insulin) and elderly patients with multiple comorbidities, severe insulin resistance, or heightened hypoglycaemia risk [177]. While polypharmacy effectively targets hyperglycaemia and mitigates complications, it carries significant risks, including drug-drug interactions, adverse effects, hypoglycaemia, medication non-adherence, cognitive burden, and dosing errors [178]. Additionally, it may exacerbate renal and hepatic stress, obscure clinical symptoms, and elevate healthcare costs. Optimal management requires rigorous medication review, deprescribing where appropriate, and a pivot to simpler treatment regimens.

Diabetes Mellitus is intimately linked with inflammation. Interleukin-6 (IL-6), a multifunctional cytokine, plays a central role in inflammation and is closely linked to the development and progression of T2DM. IL-6 is produced by immune cells like macrophages and T cells, as well as non-immune cells such as adipocytes and muscle cells, in response to infection, injury, or stress. In the context of diabetes, IL-6 contributes to insulin resistance, a defining feature of T2DM. The cytokine impairs insulin signalling in the liver, skeletal muscle, and adipose tissue [161]. In obesity, adipose tissue releases excess IL-6, exacerbating systemic inflammation and metabolic dysfunction. While acute exposure to IL-6 supports beta-cell function, chronic exposure leads to beta-cell dysfunction and apoptosis, reducing insulin production. Additionally, IL-6 influences liver metabolism by promoting gluconeogenesis and impairing glycogen synthesis, further contributing to hyperglycaemia. Elevated IL-6 concentrations, therefore, are associated with an increased risk of developing T2DM and its complications [162]. The ideal effect, therefore, for fluoroquinolones, unlike for Akt and Glut-4 expression, is the reduction in percentage expression of IL-6 to avoid inadvertently worsening diabetic complications.

While apparent differences in the percentage of IL-6 expression were observed in HepG-2 cells, pairwise comparisons between group means and the control did not reach statistical significance after adjusting for multiple comparisons, except for moxifloxacin, which increased IL-6 expression above the control level. This indicates that, although ANOVA identified some variability between groups, the differences were not sufficiently robust to exclude the possibility of random variation. Consequently, the data regarding the effect of fluoroquinolones on IL-6 expression in HepG-2 cells remains inconclusive. In contrast, in C2C12 cells, pairwise comparisons between group means and the control demonstrated statistically significant reductions in IL-6 expression after adjusting for multiple

---

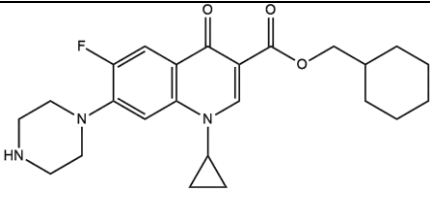
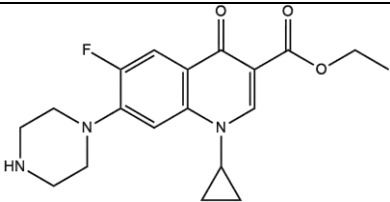
comparisons ( $p < 0.05$ ). Lower concentrations of fluoroquinolones significantly decreased IL-6 expression, suggesting potential anti-inflammatory properties. However, as concentrations increased, the inhibitory effect on IL-6 diminished, with expression levels gradually approximating those of the control. This pattern implies that lower concentrations of fluoroquinolones may exert anti-inflammatory effects, while higher concentrations could initiate cytotoxic responses, reducing their efficacy in suppressing inflammation.

These findings align with broader research on fluoroquinolones, which have been reported to exhibit anti-inflammatory properties in various contexts. For instance, studies have demonstrated that fluoroquinolones can modulate inflammatory signalling pathways, such as the suppression of pro-inflammatory cytokines like IL-6 and TNF- $\alpha$ , in models of infection and inflammation [179]. However, the concentration-dependent effects observed in this study highlight the dual nature of fluoroquinolones, where therapeutic benefits at lower concentrations may be counteracted by adverse effects at higher doses [180]. Further investigation is warranted to elucidate the mechanisms underlying these concentration-dependent responses and to optimise the therapeutic use of fluoroquinolones in inflammatory conditions. Fluoroquinolones are associated with a well-documented side effect profile, including severe adverse effects such as tendon rupture (Achilles tendon most common), peripheral neuropathy (potentially irreversible), QT interval prolongation (risk of arrhythmias like torsades de pointes), and dysglycaemia [181]. Their favourable pharmacokinetic properties, such as high tissue penetration, contribute to their saturation in tenocytes, chondrocytes, neuronal cells, and cardiac cells, leading to these toxicities. Chemical derivatisation of fluoroquinolones could offer a potential solution by modifying properties like lipophilicity, protein binding, molecular size, and ionisation state, which can alter the volume of distribution (Vd).

Increasing lipophilicity through structural derivatization – typically through adding alkyl chains, aromatic rings, esters, ethers, and removing polar groups – may reduce penetration into lean specialised cells with limited lipid content, preventing or reducing binding to intracellular proteins and enzymes critical for tendons and cardiac function, such as matrix metalloproteinases (MMPs) and cardiac ion channels respectively [182]. The chemically altered compounds would resultantly partition preferentially into more lipid-dense cells such as adipocytes. However, this raises the question of whether such modifications might nullify the anti-diabetic properties of these compounds. Esterification of the carboxyl moiety in position 3 of the fluoroquinolone backbone may reduce

polarity and increase the lipophilicity of the resultant product. The table below shows examples of potential derivatives which could have fewer side effects.

**Table 4.1:** Suggested chemical derivatisation of ciprofloxacin envisaged to minimise toxicity

Ciprofloxacin derivative	Substituted Group
	Cyclohexyl methanol bonded to carboxyl group on 3 <sup>rd</sup> Carbon
	Ethanol bonded to carboxyl group on 3 <sup>rd</sup> Carbon

Conventional fluoroquinolones exhibit moderate activity against cell-based and non-cell-based targets, attributed to their amphiphilic nature—hydrophilic components (e.g., carboxyl, ketone, and amine groups) enhance water solubility, while hydrophobic features (e.g., quinolone core and fluorine atoms) facilitate membrane permeability. This dual property enables effective cellular traversal and interactions with intracellular enzymes, contributing to their therapeutic efficacy [183]. Moreover, the preferred binding positions of fluoroquinolones against glycaemic targets (alpha-glucosidase, insulin receptor, PI3K, and alpha-amylase) were elucidated and evaluated for correlations between inhibitory or activating properties and structural moieties to identify anti-diabetic pharmacophoric units. Fluoroquinolones, with their moderate to high Vd (1–4 L/kg), exhibit extensive tissue penetration, facilitated by polar and non-polar components that enable deep dissolution into cellular compartments and interactions with intracellular proteins, receptors, and enzymes. Structural features, such as the carboxylate group at position 3 and substituents at position 7, contribute to strong drug-receptor binding stabilised by hydrogen bonds.

---

Further characterisation of their relationship with intracellular kinases involved in insulin signalling could provide a comprehensive understanding of their influence on insulin signal transduction. Although the study supports the antidiabetic properties of fluoroquinolones, a careful approach would need to be considered, where repurposing of fluoroquinolones towards diabetes is sought. Considering that these are antibiotics in nature, this therefore suggests they cannot be repurposed for diabetes in their current state, as this could be a fertile ground for antimicrobial resistance development. However, through comprehensive structural activity relationship and pharmacophoric units' identification, fluoroquinolone derivatives desirable for diabetes management may be developed.

---

## Conclusion

Diabetes mellitus (T2DM) is a significant global public health challenge, with over 537 million adults living with the condition as of 2021, a number projected to rise to 643 million by 2030. The increasing prevalence of T2DM and its associated complications has contributed to 6.7 million deaths annually, driving researchers to explore novel treatments and preventive strategies. Among the compounds under investigation, fluoroquinolones have garnered attention due to their reported hypoglycaemic side effects, though limited studies have examined their potential as antidiabetic agents. Recent research suggests that fluoroquinolones demonstrate favourable drug-receptor binding and gastrointestinal (GIT) absorption properties, making them suitable for oral formulation. These findings position fluoroquinolones as promising candidates for managing T2DM and its complications, offering a potential avenue for more effective therapies.

These compounds exhibited significant inhibition of  $\alpha$ -amylase,  $\alpha$ -glucosidase and moderate inhibition of other targets, attributed to structural features such as piperazine rings, aromatic rings, and carboxylate groups. A moderate inhibitory profile is advantageous, as excessive inhibition could lead to severe hypoglycaemia. In cell-based assays, fluoroquinolones significantly enhanced glucose uptake compared to controls, indicating improved glucose utilisation. Moxifloxacin and ciprofloxacin were identified as safe at concentrations of 12.5 to 50  $\mu\text{g/ml}$ , meeting the 80% cell viability threshold.

The glucose uptake mechanism was found to depend on PI3K activation, as blocking PI3K significantly reduced media glucose utilisation. This finding was supported by docking studies and In-cell ELISA data, which showed a correlation between fluoroquinolone concentration and increased enzyme activity/expression. These results suggest that fluoroquinolones, particularly moxifloxacin and ciprofloxacin, have potential as antidiabetic agents by enhancing glucose uptake through PI3K-dependent pathways. Further research is warranted to optimise their therapeutic potential and safety profile.

---

## Study Limitations and Future Studies

Cell-based assays are prone to infections, which can impact their reliability. To ensure accuracy, *in vitro* studies should be conducted in replicates and repeated over time to identify consistent trends. However, in this study, resource constraints, including the high cost of screening kits and enzymes, limited the ability to repeat assays. Each experiment was performed once and replicated to obtain results, but future studies should prioritise multiple replicates under standardised conditions to strengthen confidence in the findings.

To enhance the clinical relevance of this research, fluoroquinolone doses utilised in subsequent experiments should be compared to the biologically active doses that fall within the therapeutic window. This would help ensure that the effective concentrations on glycaemic targets do not exceed the minimum toxic concentration documented in the literature. Additional targets such as adipocytes, pancreatic cells also offer promising avenues for investigating ancillary glycaemic effects. Finally, the chemical derivatisation of fluoroquinolones as a means of masking the antimicrobial effects or side effect attenuation may offer a unique area of research, optimising the safety, druggability of novel fluoroquinolone derivatives.

---

## References

1. Giugliano D, Ceriello A, Esposito K. Glucose metabolism and hyperglycaemia. *The American journal of clinical nutrition*. 2008 Jan 1;87(1):217S-22S.
2. Röder PV, Wu B, Liu Y, Han W. Pancreatic regulation of glucose homeostasis. *Experimental & molecular medicine*. 2016 Mar;48(3):e219-
3. Güemes M, Rahman SA, Hussain K. What is a normal blood glucose?. *Archives of disease in childhood*. 2016 Jun 1;101(6):569-74.
4. Da Silva Xavier G. The cells of the islets of Langerhans. *Journal of Clinical Medicine*. 2018 Mar 12;7(3):54.
5. Holst JJ, Holland W, Gromada J, Lee Y, Unger RH, Yan H, Sloop KW, Kieffer TJ, Damond N, Herrera PL. Insulin and glucagon: partners for life. *Endocrinology*. 2017 Apr 1;158(4):696-701.
6. Thorens B, Mueckler M. Glucose transporters in the 21st Century. *American Journal of Physiology-Endocrinology and Metabolism*. 2010 Feb;298(2):E141-5.
7. Wright EM, Loo DD, Hirayama BA. Biology of human sodium glucose transporters. *Physiological reviews*. 2011 Apr;91(2):733-94.
8. Wood IS, Trayhurn P. Glucose transporters (GLUT and SGLT): expanded families of sugar transport proteins. *British journal of nutrition*. 2003 Jan;89(1):3-9.
9. Schuit FC. Is GLUT2 required for glucose sensing?. *Diabetologia*. 1997 Jan;40:104-11.
10. Huang S, Czech MP. The GLUT4 glucose transporter. *Cell metabolism*. 2007 Apr 4;5(4):237-52.
11. Boyer PD. Energy, life, and ATP (Nobel lecture). *Angewandte Chemie International Edition*. 1998 Sep 18;37(17):2296-307.
12. Neupane P, Bhujju S, Thapa N, Bhattarai HK. ATP synthase: structure, function and inhibition. *Biomolecular concepts*. 2019 Jan 1;10(1):1-0.
13. Khakh BS, Burnstock G. The double life of ATP. *Scientific American*. 2009 Dec;301(6):84.

- 
14. Kader AA, Saltveit ME. Respiration and gas exchange. Postharvest physiology and pathology of vegetables. 2002 Dec 4:31-56.
  15. Chandel NS. Glycolysis. Cold Spring Harbor Perspectives in Biology. 2021 May 1;13(5):a040535.
  16. Ahmad M, Wolberg A, Kahwaji CI. Biochemistry, electron transport chain.
  17. Horecker BL. The pentose phosphate pathway. Journal of Biological Chemistry. 2002 Dec 13;277(50):47965-71.
  18. Mulichak AM, Wilson JE, Padmanabhan K, Garavito RM. The structure of mammalian hexokinase-1. Nature structural biology. 1998 Jul;5(7):555-60.
  19. Radziuk J, Pye S. Hepatic glucose uptake, gluconeogenesis and the regulation of glycogen synthesis. Diabetes/metabolism research and reviews. 2001 Jul;17(4):250-72.
  20. Srivastava AK, Pandey SK. Potential mechanism (s) involved in the regulation of glycogen synthesis by insulin. Molecular and cellular biochemistry. 1998 May;182:135-41.
  21. Kleczkowski LA, Kunz S, Wilczynska M. Mechanisms of UDP-glucose synthesis in plants. Critical reviews in plant sciences. 2010 Jul 14;29(4):191-203.
  22. Biermann CJ. Hydrolysis and other cleavage of glycosidic linkages. Analysis of Carbohydrates by GLC and MS 2021 Dec 16 (pp. 27-41). CRC Press.
  23. Cohen PT. Protein phosphatase 1—targeted in many directions. Journal of cell science. 2002 Jan 15;115(2):241-56.
  24. Tengholm A, Gylfe E. cAMP signalling in insulin and glucagon secretion. Diabetes, obesity and metabolism. 2017 Sep;19:42-53.
  25. Edwards AS, Scott JD. A-kinase anchoring proteins: protein kinase A and beyond. Current opinion in cell biology. 2000 Apr 1;12(2):217-21.
  26. Agius L. Role of glycogen phosphorylase in liver glycogen metabolism. Molecular aspects of medicine. 2015 Dec 1;46:34-45.
-

- 
27. Newgard CB, Hwang PK, Fletterick RJ. The family of glycogen phosphorylases: structure and function. *Critical reviews in biochemistry and molecular biology*. 1989 Jan 1;24(1):69-99.
  28. Chasiotis D. The regulation of glycogen phosphorylase and glycogen breakdown in human skeletal muscle. *Acta Physiologica Scandinavica. Supplementum*. 1983 Jan 1;518:1-68.
  29. Gray LR, Tompkins SC, Taylor EB. Regulation of pyruvate metabolism and human disease. *Cellular and molecular life sciences*. 2014 Jul;71:2577-604.
  30. Miyamoto T, Amrein H. Gluconeogenesis: An ancient biochemical pathway with a new twist. *Fly*. 2017 Jul 3;11(3):218-23.
  31. Yang J, Kalhan SC, Hanson RW. What is the metabolic role of phosphoenolpyruvate carboxykinase?. *Journal of Biological Chemistry*. 2009 Oct 2;284(40):27025-9.
  32. Yu S, Meng S, Xiang M, Ma H. Phosphoenolpyruvate carboxykinase in cell metabolism: Roles and mechanisms beyond gluconeogenesis. *Molecular metabolism*. 2021 Nov 1;53:101257.
  33. Thorens B. GLUT2, glucose sensing and glucose homeostasis. *Diabetologia*. 2015 Feb;58(2):221-32.
  34. Lewis GF, Carpentier AC, Pereira S, Hahn M, Giacca A. Direct and indirect control of hepatic glucose production by insulin. *Cell metabolism*. 2021 Apr 6;33(4):709-20.
  35. Jain R, Lammert E. Cell–cell interactions in the endocrine pancreas. *Diabetes, Obesity and Metabolism*. 2009 Nov;11:159-67.
  36. Mainz DL, Black O, Webster PD. Hormonal control of pancreatic growth. *The Journal of Clinical Investigation*. 1973 Sep 1;52(9):2300-4.
  37. Giugliano D, Ceriello A, Esposito K. Glucose metabolism and hyperglycemia. *The American journal of clinical nutrition*. 2008 Jan 1;87(1):217S-22S.
  38. Saudek CD, Eder HA. Lipid metabolism in diabetes mellitus. *The American Journal of Medicine*. 1979 May 1;66(5):843-52.

- 
39. Bismut H, Caron M, Coudray-Lucas C, Capeau J. Glucose contribution to nucleic acid base synthesis in proliferating hepatoma cells: a glycine-biosynthesis-mediated pathway. *Biochemical Journal*. 1995 Jun 15;308(3):761-7.
  40. Mayer JP, Zhang F, DiMarchi RD. Insulin structure and function. *Peptide Science: Original Research on Biomolecules*. 2007;88(5):687-713.
  41. Steiner DF, Park SY, Støy J, Philipson LH, Bell GI. A brief perspective on insulin production. *Diabetes, Obesity and Metabolism*. 2009 Nov;11:189-96.
  42. Kitabchi AE. Proinsulin and C-peptide: a review. *Metabolism*. 1977 May 1;26(5):547-87.
  43. Komatsu M, Takei M, Ishii H, Sato Y. Glucose-stimulated insulin secretion: A newer perspective. *Journal of diabetes investigation*. 2013 Nov;4(6):511-6.
  44. Jensen MV, Joseph JW, Ronnebaum SM, Burgess SC, Sherry AD, Newgard CB. Metabolic cycling in control of glucose-stimulated insulin secretion. *American Journal of Physiology-Endocrinology and Metabolism*. 2008 Dec;295(6):E1287-97.
  45. Straub SG, Sharp GW. Glucose-stimulated signalling pathways in biphasic insulin secretion. *Diabetes/metabolism research and reviews*. 2002 Nov;18(6):451-63.
  46. Rasmussen H, Zawalich KC, Ganesan S, Calle R, Zawalich WS. Physiology and pathophysiology of insulin secretion. *Diabetes Care*. 1990 Jun 1;13(6):655-66.
  47. Draznin B. Intracellular calcium, insulin secretion, and action. *The American journal of medicine*. 1988 Nov 28;85(5):44-58.
  48. Henquin JC. Triggering and amplifying pathways of regulation of insulin secretion by glucose. *Diabetes*. 2000 Nov 1;49(11):1751-60.
  49. Kalwat MA, Cobb MH. Mechanisms of the amplifying pathway of insulin secretion in the  $\beta$  cell. *Pharmacology & therapeutics*. 2017 Nov 1;179:17-30.
  50. Bisht S, Singh MF. The triggering pathway, the metabolic amplifying pathway, and cellular transduction in the regulation of glucose-dependent biphasic insulin secretion. *Archives of Physiology and Biochemistry*. 2024 Jan 9:1-2.
-

- 
51. Rutter GA. Regulating glucagon secretion: somatostatin in the spotlight. *Diabetes*. 2009 Feb;58(2):299.
52. Balsan GA, Vieira JL, Oliveira AM, Portal VL. Relationship between adiponectin, obesity and insulin resistance. *Revista da Associação Médica Brasileira*. 2015 Feb;61(1):72-80.
53. Kahn CR, White M. The insulin receptor and the molecular mechanism of insulin action. *The Journal of Clinical Investigation*. 1988 Oct 1;82(4):1151-6.
54. Boucher J, Kleinridders A, Kahn CR. Insulin receptor signalling in normal and insulin-resistant states. *Cold Spring Harbor perspectives in biology*. 2014 Jan 1;6(1):a009191.
55. Topp B, Promislow K, Devries G, Miura RM, T FINEGOOD DI. A model of  $\beta$ -cell mass, insulin, and glucose kinetics: pathways to diabetes. *Journal of theoretical biology*. 2000 Oct 21;206(4):605-19.
56. Holst JJ. The physiology of glucagon-like peptide 1. *Physiological reviews*. 2007 Oct;87(4):1409-39.
57. White MF, Kahn CR. The insulin signalling system. *Journal of Biological Chemistry*. 1994 Jan 7;269(1):1-4.
58. Lee YH, White MF. Insulin receptor substrate proteins and diabetes. *Archives of pharmacal research*. 2004 Apr;27:361-70.
59. Laketa V, Zarbakhsh S, Traynor-Kaplan A, MacNamara A, Subramanian D, Putyrski M, Mueller R, Nadler A, Mentel M, Saez-Rodriguez J, Pepperkok R. PIP3 induces the recycling of receptor tyrosine kinases. *Science signalling*. 2014 Jan 14;7(308):ra5-.
60. Storz P, Toker A. 3'-phosphoinositide-dependent kinase-1 (PDK-1) in PI 3-kinase signaling. *Front Biosci*. 2002 Apr 1;7:d886-902.
61. White MF. Insulin signalling in health and disease. *Science*. 2003 Dec 5;302(5651):1710-1.
62. Created in BioRender. Katshaza, O. (2025) <https://BioRender.com/p60v248>
63. Wilcox G. Insulin and insulin resistance. *Clinical biochemist reviews*. 2005 May;26(2):19.
-

- 
64. Wallace TM, Matthews DR. The assessment of insulin resistance in man. *Diabetic medicine*. 2002 Jul;19(7):527-34.
65. Bahiru E, Hsiao R, Phillipson D, Watson KE. Mechanisms and treatment of dyslipidemia in diabetes. *Current cardiology reports*. 2021 Apr;23:1-6.
66. Mooradian AD. Dyslipidemia in T2DM mellitus. *Nature Reviews Endocrinology*. 2009 Mar;5(3):150-9.
67. Gatewood S.S., & R. (2017). DIABETES mellitus: existing disease: establishing optimal control level. In & R. Gatewood S.S., *Pharmacotherapy Casebook: A Patient-Focused Approach*, 10e. McGraw Hill. Schwinghammer T.L., & Koehler J.M., & Borchert J.S., & Slain D, & Park S.K.(Eds.).
68. Mudaliar S, Edelman SV. Insulin therapy in T2DM. *Endocrinology and Metabolism Clinics*. 2001 Dec 1;30(4):935-82.
69. Guthrie RA, G. D. (2004). Pathophysiology of diabetes mellitus. *Critical care nursing quarterly*., 27(2):113-25.
70. Barbot, M., Ceccato, F., & Scaroni, C. (2018). Diabetes mellitus secondary to Cushing's disease. *Frontiers in endocrinology*, 9, 284.
71. Diagnosis and classification of autoimmune diabetes mellitus. *Autoimmunity reviews*, 13(4-5):403-7.
72. Mohler ML, He Y, Wu Z, Hwang DJ, Miller DD. Recent and emerging anti-diabetes targets. *Medicinal research reviews*. 2009 Jan;29(1):125-95. 13(4-5):403-7.
73. Forouhi NG, Wareham NJ. Epidemiology of diabetes. *Medicine*. 2019 Jan 1;47(1):22-7.
74. Deshpande AD, Harris-Hayes M, Schootman M. Epidemiology of diabetes and diabetes-related complications. *Physical therapy*. 2008 Nov 1;88(11):1254-64.
75. Gloyn AL. The search for T2DM genes. *Ageing research reviews*. 2003 Apr 1;2(2):111-27.
-

- 
76. Ciarambino T, Crispino P, Leto G, Mastrolorenzo E, Para O, Giordano M. Influence of gender in diabetes mellitus and its complication. *International journal of molecular sciences*. 2022 Aug 9;23(16):8850.
77. Feingold KR, Grunfeld C. The effect of inflammation and infection on lipids and lipoproteins. *Endotext* [internet]. 2022 Mar 7.
78. Caricilli AM, Saad MJ. The role of gut microbiota on insulin resistance. *Nutrients*. 2013 Mar 12;5(3):829-51.
79. Boizel R, Benhamou PY, Lardy B, Laporte F, Foulon TH, Halimi SE. The ratio of triglycerides to HDL cholesterol is an indicator of LDL particle size in patients with T2DM and normal HDL cholesterol levels. *Diabetes care*. 2000 Nov 1;23(11):1679-85.
80. Redza-Dutordoir M, Averill-Bates DA. Activation of apoptosis signalling pathways by reactive oxygen species. *Biochimica et Biophysica Acta (BBA)-Molecular Cell Research*. 2016 Dec 1;1863(12):2977-92.
81. Fakhruddin S, Alanazi W, Jackson KE. Diabetes-induced reactive oxygen species: mechanism of their generation and role in renal injury. *Journal of diabetes research*. 2017;2017(1):8379327.
82. Han CY. Roles of reactive oxygen species on insulin resistance in adipose tissue. *Diabetes & metabolism journal*. 2016 Aug 1;40(4):272-9.
83. Knapp S. Diabetes and infection: Is there a link?-A mini-review. *Gerontology*. 2013 Nov 24;59(2):99-104.
84. Pearson-Stuttard J, Blundell S, Harris T, Cook DG, Critchley J. Diabetes and infection: assessing the association with glycaemic control in population-based studies. *The lancet Diabetes & endocrinology*. 2016 Feb 1;4(2):148-58.
85. Kim EJ, Ha KH, Kim DJ, Choi YH. Diabetes and the risk of infection: a national cohort study. *Diabetes & metabolism journal*. 2019 Dec;43(6):804.
-

- 
86. Butler SO, Btaiche IF, Alaniz C. Relationship between hyperglycemia and infection in critically ill patients. *Pharmacotherapy: The Journal of Human Pharmacology and Drug Therapy*. 2005 Jul;25(7):963-76.
87. Luna B, Feinglos MN. Drug-induced hyperglycemia. *Jama*. 2001 Oct 24;286(16):1945-8.
88. Gstraunthaler G, Seppi T, Pfaller W. Impact of culture conditions, culture media volumes, and glucose content on metabolic properties of renal epithelial cell cultures: are renal cells in tissue culture hypoxic?. *Cellular physiology and biochemistry*. 1999 Sep 8;9(3):150-72.
89. Alvim RO, Cheuhen MR, Machado SR, Sousa AG, Santos PC. General aspects of muscle glucose uptake. *Anais da Academia Brasileira de Ciências*. 2015 Mar 6;87:351-68.
90. Saied IH,UDDIN In HepG-22 human liver cancer cell line. *Anticancer Res*. 1998;18:4083-90.
91. Arzumanian VA, Kiseleva OI, Poverennaya EV. The curious case of the HepG-22 cell line: 40 years of expertise. *International journal of molecular sciences*. 2021 Dec 4;22(23):13135.
92. Conejo R, Lorenzo M. Insulin signaling leading to proliferation, survival, and membrane ruffling in C2C12 myoblasts. *Journal of cellular physiology*. 2001 Apr;187(1):96-108.
93. Babiker A, Al Dubayee M. Anti-diabetic medications: How to make a choice?. *Sudanese journal of paediatrics*. 2017;17(2):11.
94. Poon K, King AB. Glargine and detemir: Safety and efficacy profiles of the long-acting basal insulin analogues. *Drug, healthcare and patient safety*. 2010 Oct 28:213-23.
95. LaMoia TE, Shulman GI. Cellular and molecular mechanisms of metformin action. *Endocrine reviews*. 2021 Feb 1;42(1):77-96.
96. Rena G, Hardie DG, Pearson ER. The mechanisms of action of metformin. *Diabetologia*. 2017 Sep;60(9):1577-85.
97. Bosi E. Metformin—the gold standard in T2DM: what does the evidence tell us?. *Diabetes, Obesity and Metabolism*. 2009 May;11:3-8.
98. Gallwitz B. Clinical use of DPP-4 inhibitors. *Frontiers in endocrinology*. 2019 Jun 19;10:389.
-

- 
99. Barnett A. DPP-4 inhibitors and their potential role in the management of T2DM. *International journal of clinical practice*. 2006 Nov;60(11):1454-70.
100. Vanhaesebroeck B, Perry MW, Brown JR, André F, Okkenhaug K. PI3K inhibitors are finally coming of age. *Nature reviews Drug discovery*. 2021 Oct;20(10):741-69.
101. Franke TF. PI3K/Akt: getting it right matters. *Oncogene*. 2008 Oct;27(50):6473-88.
102. Powis G, Bonjouklian R, Berggren MM, Gallegos A, Abraham R, Ashendel C, Zalkow L, Matter WF, Dodge J, Grindey G, Vlahos CJ. Wortmannin is a potent and selective inhibitor of phosphatidylinositol-3-kinase. *Cancer research*. 1994 May 1;54(9):2419-23.
103. MacKinnon R. Potassium channels. *FEBS letters*. 2003 Nov 27;555(1):62-5.
104. Petit P, Loubatières-Mariani MM. Potassium channels of the insulin-secreting B cell. *Fundamental & clinical pharmacology*. 1992 Apr;6(3):123-34.
105. AG HB. Pharmacology of  $\alpha$ -glucosidase inhibition. *European journal of clinical investigation*. 1994 Aug;24(S3):3-10.
106. MacGregor EA, Janeček Š, Svensson B. Relationship of sequence and structure to specificity in the  $\alpha$ -amylase family of enzymes. *Biochimica et Biophysica Acta (BBA)-Protein Structure and Molecular Enzymology*. 2001 Mar 9;1546(1):1-20.
107. Nair SS, Kavrekar V, Mishra A. In vitro studies on alpha-amylase and alpha-glucosidase inhibitory activities of selected plant extracts. *European journal of experimental biology*. 2013;3(1):128-32.
108. Rangwala SM, Lazar MA. Peroxisome proliferator-activated receptor  $\gamma$  in diabetes and metabolism. *Trends in pharmacological sciences*. 2004 Jun 1;25(6):331-6.
109. Sauer S. Ligands for the nuclear peroxisome proliferator-activated receptor gamma. *Trends in Pharmacological Sciences*. 2015 Oct 1;36(10):688-704.
110. Stumvoll M. Thiazolidinediones—some recent developments. *Expert opinion on investigational drugs*. 2003 Jul 1;12(7):1179-87.
-

- 
111. Hooper DC. Mode of action of fluoroquinolones. *Drugs*. 1999 Oct;58(Suppl 2):6-10.
112. Drlica K, Malik M. Fluoroquinolones: action and resistance. *Current topics in medicinal chemistry*. 2003 Jan 1;3(3):249-82.
113. Tillotson GS. Quinolones: structure-activity relationships and future predictions. *Journal of medical microbiology*. 1996 May;44(5):320-4.
114. Mitscher, L.A., Ma, Z. (2003). Structure-activity relationships of quinolones. In: Ronald, A.R., Low, D.E. (eds) *Fluoroquinolone Antibiotics. Milestones in Drug Therapy*. Birkhäuser, Basel. [https://doi.org/10.1007/978-3-0348-8103-6\\_2](https://doi.org/10.1007/978-3-0348-8103-6_2)
115. Saraya A, Y. M. (2004). Effects of fluoroquinolones on insulin secretion and  $\beta$ -cell ATP-sensitive  $K^+$  channels. *European journal of pharmacology*, 497(1):111-7.
116. Althaqafi A, Ali M, Alzahrani Y, Ming LC, Hussain Z. How safe are fluoroquinolones for diabetic patients? A systematic review of dysglycemic and neuropathic effects of fluoroquinolones. *Therapeutics and Clinical Risk Management*. 2021 Oct 13:1083-90.
117. Letourneau G, Morrison H, McMorran M. Gatifloxacin (Tequin): hypoglycemia and hyperglycemia. *Can Adverse Reaction Newsl* 2003;13(3).
118. Park-Wyllie LY, Juurlink DN, Kopp A, et al. Outpatient gatifloxacin therapy and dysglycemia in older adults. *N .Engl J Med* 2006; published 2006 Mar 1 at [www.nejm.org](http://www.nejm.org) (10.1056/NEJMoa055191). [DOI] [PubMed]
119. Henics T, Wheatley DN. Cytoplasmic vacuolation, adaptation and cell death: a view on new perspectives and features. *Biology of the Cell*. 1999 Sep;91(7):485-98.
120. El Ghandour S, Azar ST. Dysglycemia associated with quinolones. *Prim Care Diabetes*. 2015 Jun 1;9(3):168-71."
121. Catero M. Dysglycemia and fluoroquinolones: are you putting patients at risk? Consider an alternative in patients with specific risk factors. *J Fam Practice*. 2007 Feb 1;56(2):101-8."
-

- 
122. Shaheen, A. A. (2021). Design and synthesis of fluoroquinolone derivatives as potent  $\alpha$ -glucosidase inhibitors: in vitro inhibitory screening with in silico docking studies. *ChemistrySelect*, 6(10), 2483-2491.
123. Takahashi N, Sugamori T, Hamaguchi S, Kijima T, Yamagata S, Makiishi T. Tosufloxacin-induced severe hypoglycemia in a non-diabetic patient. *JOURNAL OF HOSPITAL GENERAL MEDICINE*. 2023 Jul 31;5(4):151-4.
124. Gharib HM, Abajy MY, Omaren A. Investigating the effect of some fluoroquinolones on blood glucose and insulin levels in STZ-induced diabetic wistar rats. *Research Journal of Pharmacy and Technology*. 2020;13(12):5993-8.
125. Turnidge J. Pharmacokinetics and pharmacodynamics of fluoroquinolones. *Drugs*. 1999 Oct;58(Suppl 2):29-36.
126. Davenport JM, Covington P, Gotfried M, Medlock M, Watanalumlerd P, McIntyre G, Turner L, Almenoff J. Summary of Pharmacokinetics and Tissue Distribution of a Broad-Spectrum Fluoroquinolone, JNJ-Q2. *Clinical Pharmacology in Drug Development*. 2012 Oct;1(4):121-30.
127. Ademiluyi AO, Oboh G. Soybean phenolic-rich extracts inhibit key enzymes linked to T2DM ( $\alpha$ -amylase and  $\alpha$ -glucosidase) and hypertension (angiotensin I converting enzyme) in vitro. *Experimental and Toxicologic Pathology*. 2013 Mar 1;65(3):305-9.
128. Yonekura, L., Hisada, H. & Intravichakul, J. Human  $\alpha$ -glucosidase inhibition and phytochemical profile of natural and shinzuke treated olives: implications from the processing method. *Food Prod Process and Nutr* 6, 46 (2024). <https://doi.org/10.1186/s43014-024-00227-7>
129. Worthington Biochemical Corp., 1993b. Maltase-a-glucosidase. In: V. Worthington (Eds.), *Worthington Enzyme Manual*. Freehold, 261.
130. Lankatillake, Chintha & Luo, Shiqi & Flavel, Matthew & Lenon, George & Gill, Harsharn & Huynh, Tien & Dias, Daniel. (2021). Screening natural product extracts for potential enzyme inhibitors: protocols, and the standardisation of the usage of blanks in  $\alpha$ -amylase,  $\alpha$ -glucosidase and lipase assays. *Plant Methods*. 17. 10.1186/s13007-020-00702-5.
-

- 
131. Le TS, McCann M, Azarin SM, Hu WS. An introduction to mammalian cell culture. *Chem Eng Prog.* 2016 Apr 1;112(4):34-40.
132. Created in BioRender. Katshaza, O. (2025)  
<https://BioRender.com/illustrations/67895b8969c6dce1570162d2>
133. Bardouille C, Lehmann J, Heimann P, Jockusch H. Growth and differentiation of permanent and secondary mouse myogenic cell lines on microcarriers. *Applied microbiology and biotechnology.* 2001 May;55:556-62.
134. Hernández-Hernández JM, García-González EG, Brun CE, Rudnicki MA. The myogenic regulatory factors, determinants of muscle development, cell identity and regeneration. In *Seminars in cell & developmental biology* 2017 Dec 1 (Vol. 72, pp. 10-18). Academic Press.
135. Helgason CD, Miller CL. *Basic cell culture protocols.* Totowa, NJ.: Humana Press; 2005.
136. Heinemann L, Braune K, Carter A, Zayani A, Krämer LA. Insulin storage: a critical reappraisal. *Journal of diabetes science and technology.* 2021 Jan;15(1):147-59.
137. Kumar P, Nagarajan A, Uchil PD. Analysis of cell viability by the MTT assay. *Cold spring harbor protocols.* 2018 Jun 1;2018(6):pdb-rot095505.
138. Created in BioRender. Katshaza, O. (2025)  
<https://BioRender.com/illustrations/67895646d293fd5385f7496d>
139. Ravi L, Kannabiran K. A handbook on protein-ligand docking tool: AutoDock 4. *Innovare Journal of Medical Sciences.* 2016 Jun 1:28-33.
140. Goodsell DS, Sanner MF, Olson AJ, Forli S. The AutoDock suite at 30. *Protein Science.* 2021 Jan;30(1):31-43.
141. Maiorov VN, Crippen GM. Significance of root-mean-square deviation in comparing three-dimensional structures of globular proteins. *Journal of molecular biology.* 1994 Jan 13;235(2):625-34.
142. Rizvi SM, Shakil S, Haneef M. A simple click by click protocol to perform docking: AutoDock 4.2 made easy for non-bioinformaticians. *EXCLI journal.* 2013;12:831.
-

- 
143. Varela-Salinas G, García-Pérez CA, Peláez R, Rodríguez AJ. A visual clustering approach for docking results from vina and autodock. In Hybrid Artificial Intelligent Systems: 12th International Conference, HAIS 2017, La Rioja, Spain, June 21-23, 2017, Proceedings 12 2017 (pp. 342-353). Springer International Publishing.
144. Ekins S, Mestres J, Testa B. In silico pharmacology for drug discovery: methods for virtual ligand screening and profiling. *British journal of pharmacology*. 2007 Sep;152(1):9-20.
145. Molnár E. Cell-based enzyme-linked immunosorbent assay (Cell-ELISA) analysis of native and recombinant glutamate receptors. *Glutamate Receptors: Methods and Protocols*. 2019:47-54.
146. Created in BioRender. Katshaza, O. (2025)<https://BioRender.com/p62v535>
147. Created in Bio/Render. Katshaza, O. (2025)<https://BioRender.com/illustrations/67893a1fd02c49ee07337875>
148. Powis G, Bonjouklian R, Berggren MM, Gallegos A, Abraham R, Ashendel C, Zalkow L, Matter WF, Dodge J, Grindey G, Vlahos CJ. Wortmannin, is a potent and selective inhibitor of phosphatidylinositol-3-kinase. *Cancer research*. 1994 May 1;54(9):2419-23.
148. Created in Bio/Render. Katshaza, O. (2025)<https://BioRender.com/illustrations/67893ee07337875>
150. Monks S. SigmaPlot 8.0. *Biotech Software & Internet Report: The Computer Software Journal for Scientists*. 2002 Nov 1;3(5-6):141-5.
151. Letourneau G, Morrison H, McMorran M. Gatifloxacin (Tequin): hypoglycemia and hyperglycemia. *Can Adverse Reaction Newsl* 2003;13(3)"
152. Ulldemolins M, Rello J. The relevance of drug volume of distribution in antibiotic dosing. *Current Pharmaceutical Biotechnology*. 2011 Dec 1;12(12):1996-2001.
153. Fedorowicz J, Sączewski J. Modifications of quinolones and fluoroquinolones: hybrid compounds and dual-action molecules. *Monatshefte für Chemie-Chemical Monthly*. 2018 Jul;149:1199-245.
-

- 
154. Peterson, L.R. Quinolone molecular structure-activity relationships: What we have learned about improving antimicrobial activity. *Clin. Infect. Dis.* 2001, 33 (Suppl. 3), S180–S186.
155. Chadt A, Al-Hasani H. Glucose transporters in adipose tissue, liver, and skeletal muscle in metabolic health and disease. *Pflügers Archiv-European Journal of Physiology.* 2020 Sep;472(9):1273-98.
156. Freshney RI. *Culture of animal cells: a manual of basic technique and specialized applications.* John Wiley & Sons; 2015 Dec 23.
157. Johnson S, Nguyen V, Coder D. Assessment of cell viability. *Curr. Protoc. Cytom.* 2013 Apr 26;64(9.2):1-9.
158. Powis G, Bonjouklian R, Berggren MM, Gallegos A, Abraham R, Ashendel C, Zalkow L, Matter WF, Dodge J, Grindey G, Vlahos CJ. Wortmannin, is a potent and selective inhibitor of phosphatidylinositol-3-kinase. *Cancer research.* 1994 May 1;54(9):2419-23.
159. Wymann MP, Bulgarelli-Leva G, Zvelebil MJ, Pirola L, Vanhaesebroeck B, Waterfield MD, Panayotou G. Wortmannin inactivates phosphoinositide 3-kinase by covalent modification of Lys-802, a residue involved in the phosphate transfer reaction. *Molecular and cellular biology.* 1996 Apr 1.
160. Althaqafi A, Ali M, Alzahrani Y, Ming LC, Hussain Z. How safe are fluoroquinolones for diabetic patients? A systematic review of dysglycemic and neuropathic effects of fluoroquinolones. *Therapeutics and Clinical Risk Management.* 2021 Oct 13:1083-90.
161. Jorgensen SB, O'Neill HM, Sylow L, Honeyman J, Hewitt KA, Palanivel R, Fullerton MD, Öberg L, Balendran A, Galic S, van der Poel C. Deletion of skeletal muscle SOCS3 prevents insulin resistance in obesity. *Diabetes.* 2013 Jan 1;62(1):56-64.
162. Akbari M, Hassan-Zadeh V. IL-6 signalling pathways and the development of T2DM. *Inflammopharmacology.* 2018 Jun;26:685-98.
163. Kahn CR. Role of insulin receptors in insulin-resistant states. *Metabolism.* 1980 May 1;29(5):455-66.
-

- 
164. Evans JL, Maddux BA, Goldfine ID. The molecular basis for oxidative stress-induced insulin resistance. *Antioxidants & redox signaling*. 2005 Jul 1;7(7-8):1040-52.
165. Blokhina SV, Sharapova AV, Ol'khovich MV, Volkova TV, Perlovich GL. Solubility, lipophilicity and membrane permeability of some fluoroquinolone antimicrobials. *European Journal of Pharmaceutical Sciences*. 2016 Oct 10;93:29-37.
166. Higgins PG, Fluit AC, Schmitz FJ. Fluoroquinolones: structure and target sites. *Current drug targets*. 2003 Feb 1;4(2):181-90.
167. Salpeter SR, Buckley NS, Kahn JA, Salpeter EE. Meta-analysis: metformin treatment in persons at risk for diabetes mellitus. *The American journal of medicine*. 2008 Feb 1;121(2):149-57.
168. Turnidge J. Pharmacokinetics and pharmacodynamics of fluoroquinolones. *Drugs*. 1999 Oct;58(Suppl 2):29-36.
169. Khovidhunkit W, Sunthornyothin S. Hypoglycemia, hyperglycemia, and gatifloxacin. *Annals of internal medicine*. 2004 Dec 21;141(12):969.
170. Catero M. Dysglycemia and fluoroquinolones: are you putting patients at risk?. *Journal of family practice*. 2007 Feb 1;56(2).
171. Fish DN. Fluoroquinolone adverse effects and drug interactions. *Pharmacotherapy: The Journal of Human Pharmacology and Drug Therapy*. 2001 Oct;21(10P2):253S-72S.
172. Abdel-Magid AF. Allosteric modulators: an emerging concept in drug discovery. *ACS medicinal chemistry letters*. 2015 Feb 12;6(2):104-7.
173. Van Westen GJ, Gaulton A, Overington JP. Chemical, target, and bioactive properties of allosteric modulation. *PLoS Computational Biology*. 2014 Apr 3;10(4):e1003559.
174. Mansour TE. Kinetic and physical properties of phosphofructokinase. *Advances in Enzyme Regulation*. 1970 Jan 1;8:37-51.
175. Mackenzie RW, Elliott BT. Akt/PKB activation and insulin signaling: a novel insulin signaling pathway in the treatment of T2DM. *Diabetes, metabolic syndrome and obesity: targets and therapy*. 2014 Feb 13:55-64.
-

- 
176. Shakib S. Problems of polypharmacy. *Australian family physician*. 2002 Feb;31(2):125-8.
177. Good CB. Polypharmacy in elderly patients with diabetes. *Diabetes Spectrum*. 2002 Oct 1;15(4):240-8.
178. Colley CA, Lucas LM. Polypharmacy: the cure becomes the disease. *Journal of general internal medicine*. 1993 May;8:278-83.
179. Dalhoff A. Immunomodulatory activities of fluoroquinolones. *Infection*. 2005 Dec;33(Suppl 2):55-70.
180. Schentag JJ. Clinical pharmacology of the fluoroquinolones: studies in human dynamic/kinetic models. *Clinical Infectious Diseases*. 2000 Aug 1;31(Supplement\_2):S40-4.
181. Rusu A, Munteanu AC, Arbănași EM, Uivarosi V. Overview of side-effects of antibacterial fluoroquinolones: new drugs versus old drugs, a step forward in the safety profile?. *Pharmaceutics*. 2023 Mar 1;15(3):804.
182. Ahmed SH, Clark LL, Pennington WR, Webb CS, Bonnema DD, Leonardi AH, McClure CD, Spinale FG, Zile MR. Matrix metalloproteinases/tissue inhibitors of metalloproteinases: relationship between changes in proteolytic determinants of matrix composition and structural, functional, and clinical manifestations of hypertensive heart disease. *Circulation*. 2006 May 2;113(17):2089-96.
183. Blokhina SV, Sharapova AV, Ol'khovich MV, Volkova TV, Perlovich GL. Solubility, lipophilicity and membrane permeability of some fluoroquinolone antimicrobials. *European Journal of Pharmaceutical Sciences*. 2016 Oct 10;93:29-37.
184. Rehman K, Akash MS, Liaqat A, Kamal S, Qadir MI, Rasul A. Role of interleukin-6 in development of insulin resistance and type 2 diabetes mellitus. *Critical Reviews™ in Eukaryotic Gene Expression*. 2017;27(3).
185. Shilling AM, Raphael J. Diabetes, hyperglycemia, and infections. *Best Practice & Research Clinical Anaesthesiology*. 2008 Sep 1;22(3):519-35.
186. Saraya A, Yokokura M, Gono T, Seino S. Effects of fluoroquinolones on insulin secretion and  $\beta$ -cell ATP-sensitive  $K^+$  channels. *European journal of pharmacology*. 2004 Aug 16;497(1):111-7.
-

- 
187. Ramachandran A. Know the signs and symptoms of diabetes. *Indian Journal of Medical Research*. 2014 Nov 1;140(5):579-81.
188. Barski L, Nevzorov R, Jotkowitz A, Rabaev E, Zektser M, Zeller L, Shleyfer E, Harman-Boehm I, Almog Y. Comparison of diabetic ketoacidosis in patients with type-1 and type-2 diabetes mellitus. *The American journal of the medical sciences*. 2013 Apr 1;345(4):326-30.
189. Qian Y, Feldman E, Pennathur S, Kretzler M, Brosius III FC. From fibrosis to sclerosis: mechanisms of glomerulosclerosis in diabetic nephropathy. *Diabetes*. 2008 Jun 1;57(6):1439-45.
190. Nentwich MM, Ulbig MW. Diabetic retinopathy-ocular complications of diabetes mellitus. *World journal of diabetes*. 2015 Apr 15;6(3):489.
191. Akbari CM, LoGerfo FW. Diabetes and peripheral vascular disease. *Journal of vascular surgery*. 1999 Aug 1;30(2):373-84.
192. Dahlén AD, Dashi G, Maslov I, Attwood MM, Jonsson J, Trukhan V, Schiöth HB. Trends in antidiabetic drug discovery: FDA approved drugs, new drugs in clinical trials and global sales. *Frontiers in Pharmacology*. 2022 Jan 19;12:807548.
193. Clissold SP, Edwards C. Acarbose: a preliminary review of its pharmacodynamic and pharmacokinetic properties, and therapeutic potential. *Drugs*. 1988 Mar;35:214-43.

---

# APPENDICES

## Appendix 1: Research Ethics Declaration



### RESEARCH ETHICS DECLARATION

To be included in the Appendices of research papers / dissertations / theses submitted for postgraduate examination where research did not involve interaction with human participants, or the use of animal subjects, and therefore did not require research ethics approval.

Candidates whose research did require ethics clearance must include their ethics approval letter in the Appendix of their examination submission.

**Name of Candidate: Oyisa Sisipho  
Hope Katshaza**

**Name of Supervisor: Prof N Sibiya**

**Degree: Master of Science in  
Pharmacy**

**Title of research: AN *IN VITRO*  
INVESTIGATION OF  
FLUOROQUINOLONES ON  
GLYCAEMIC  
PHARMACOLOGICAL TARGETS**

I declare that my research did not require ethical clearance because (tick all that apply):

I did not collect data from human participants or animal subjects	<input checked="" type="checkbox"/>
I used previously collected data that had already received ethics clearance.	<input type="checkbox"/>
I analysed documents / open-access digital texts that are freely available in the public domain.	<input type="checkbox"/>

I did a literature review/analysis of theoretical or secondary material only.	
I used human datasets of non-sensitive information that are either anonymous (identifiers were never collected) or have been de-identified (identifiers have been completely removed).	
I used commercially produced human biological material (e.g. established human cell lines).	x
I observed people in public spaces and natural environments where they had no reasonable expectation of privacy and I did not interact with them or intervene in any way.	
I used non-living animal materials (eg bones of already deceased organisms or fossils) while complying with any custody and/or jurisdiction requirements.	
I did a content analysis of public media (newspapers, advertisements, and social media posts).	
I did a simulation study with no real-world consequences and does not involve disturbing or distressing content.	
I observed flora, fauna, and ecosystems without interfering with or disturbing their natural state while complying with any jurisdiction requirements.	
Other (Please provide details):	

**Signature of Candidate:**



**Date:**

19/02/2025

**Signature of Supervisor:**



**Date:**

19/02/2025

## Appendix 2: Abstract Acceptance for a presentation that was presented during 56<sup>th</sup> ANNUAL CONFERENCE 2023



20 July 2023

To: Mr O Katshaza  
Division of Pharmacology; Faculty of Pharmacy  
Rhodes University  
Makhanda, 6139

### ABSTRACT ACCEPTANCE FOR THE 56<sup>th</sup> ANNUAL CONFERENCE 2023

Dear Mr Katshaza

This letter serves to notify you that the abstract you submitted for the 56<sup>th</sup> Annual SASBCP conference, titled "Fluoroquinolone-induced glucose uptake in skeletal muscle cells in vitro." has been accepted. The abstract has been accepted for **podium** presentation. You will be given 15 minutes (10 minutes plus 5 minutes for questions) for the presentation. Information regarding your specific time slot will be provided closer to the conference date.

Do complete your registration for the conference online. You are kindly advised to book your accommodation at the earliest possible.

If you intend to compete for the Young Pharmacologist Award, send a separate email, with the abstract and the signed declaration form to the scientific committee chairperson, [n.sibiya@ru.ac.za](mailto:n.sibiya@ru.ac.za). The criteria for eligibility and the declaration form are available on the website. Visit the website <http://www.sasbcpcconference2023.co.za/> for additional information.

Do not hesitate to contact the Organising Committee if you have any queries.

Thanking you in anticipation.

Yours sincerely,

Dr N Sibiya  
Chairperson of Scientific Committee  
On behalf of the Local Organising Committee

Page 1 of 1

South African Society for Basic and Clinical Pharmacology - Section 21 Company, registration no. 2006 / 029983 / 08  
Directors: V Steenkamp, G Matsibisa, H Pakar, M Mthibane, P Sinoedi, M Stockman, K Cohen, E Dedebedi, B Hanney, M Lekhoo, L Mathibe  
Registry Office: Alchemy Financial Services Inc., Unit 3, Bush Hill Office Park, Jan Fredericks Ave, Bush Hill, Honey Dew, 2154